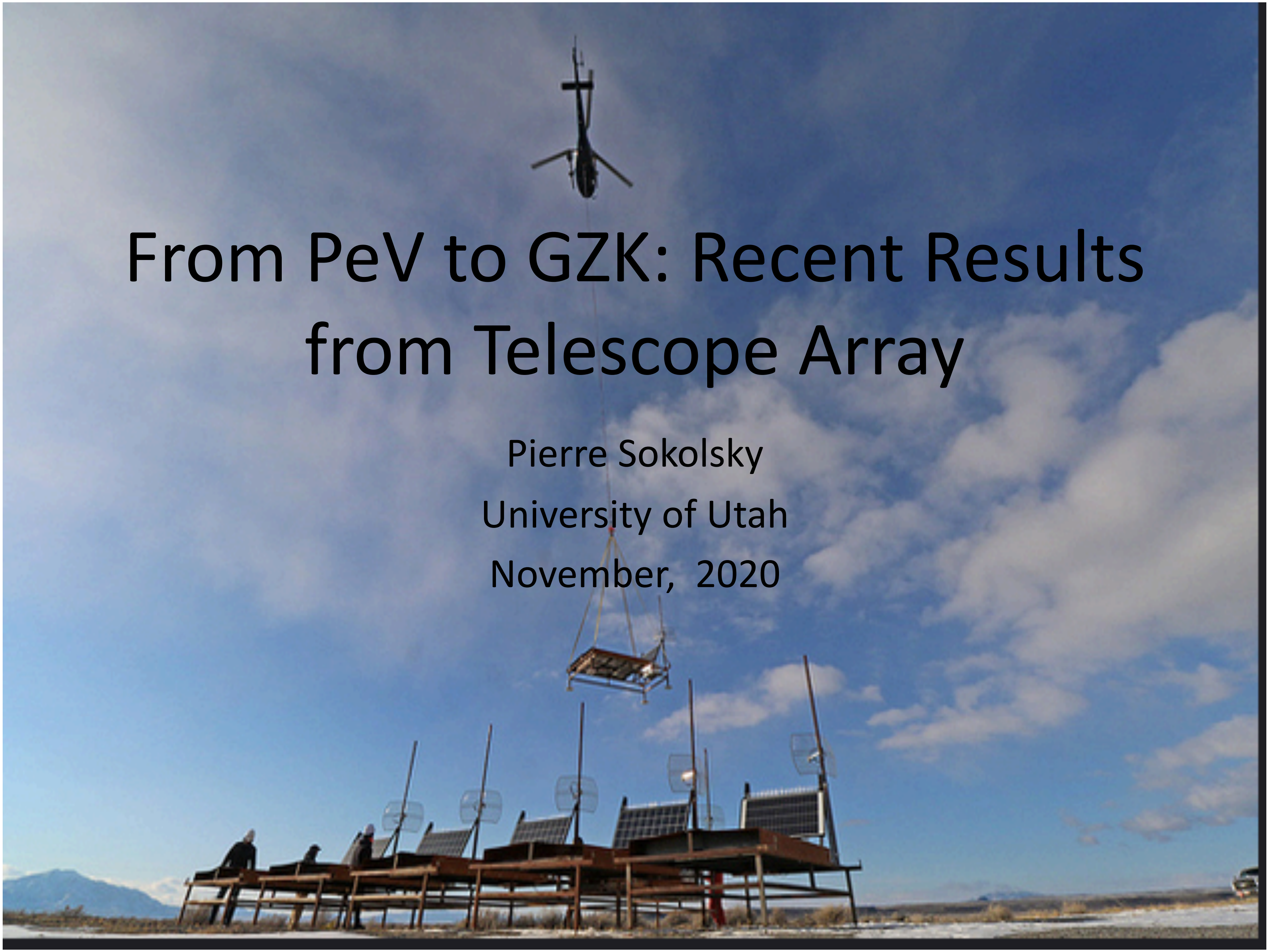

From PeV to GZK: Recent Results from Telescope Array

Pierre Sokolsky
University of Utah

November, 2020

Outline

- Some history
- TA and TALE
- The spectrum above the “knee” ~ 1 PeV to 100 EeV
- Composition – data and interpretation
- Hadronic physics: Proton-air cross section/Muon excess
- Anisotropy – Hot Spot, Energy Spectrum anisotropy, Magnetic effects.
- New projects: TAx4, Radio Astronomy, Lightning Array, Niche.

Textbook Figure of Cosmic Ray Spectrum

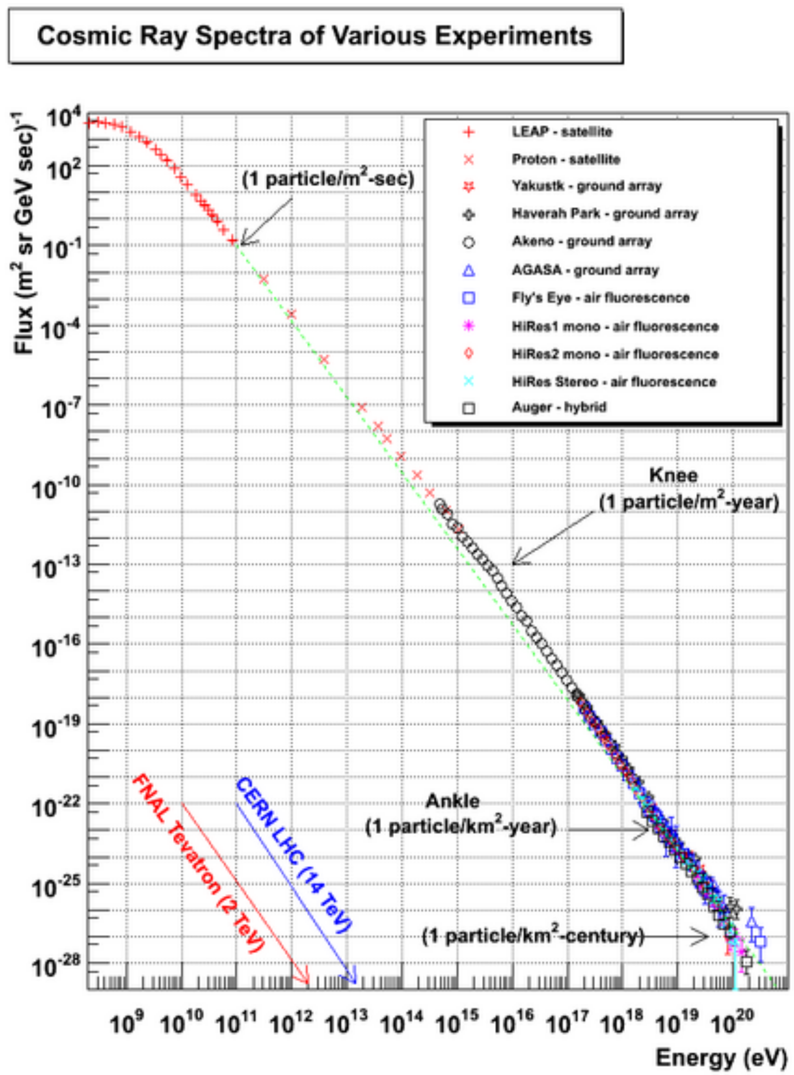

Why study such an apparently featureless flux?

- Discovery of microwave background radiation (1967) → GZK cutoff prediction (1968).
- *Is the lack of structure in the spectrum real or due to poor resolution and primitive energy reconstruction?*
- *Anisotropy must begin to appear at the highest energies unless cosmic rays are ~ Fe nuclei. Composition matters.*
- More fundamentally: they are a puzzle that Nature hands us – but a puzzle that leads to things that matter.
- Extremes in scale often lead to the unexpected. These energies a well beyond accelerator energies.

UHECR nature and origin questions

- As a function of energy, are they galactic or extra-galactic?
- What are the acceleration mechanism?

  (SN, galactic wind, AGN jets, Starburst galaxies, GRB's, decays of super-heavy primordial objects}
- As a function of energy, what is the composition of the cosmic rays?
- As a function of energy, what is the effect of propagation thru space ?

  (Interactions with relic BB radiation, starlight, dust, etc.; effect of magnetic fields on trajectories)

Are things simpler at the highest energies?

- Propagation effects should be striking for distant sources
  - Cut off due to relic BB photons?
  - Simplification of composition to protons and Fe?
  - Effect of magnetic fields is minimized – protons should point back to their sources

A single experiment with overlapping cross-calibrated energy scale can connect GZK cutoff with galactic cosmic ray flux. Need ~ 5 decades in energy. TA/TALE idea (first discussed in 2006 Aspen Workshop)

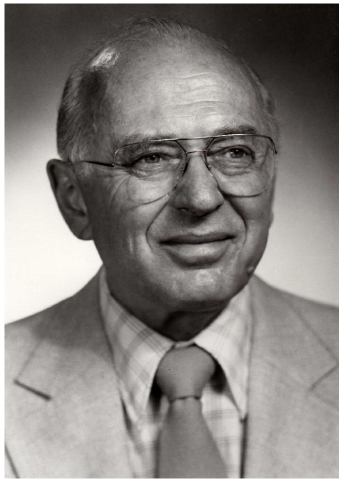

- Cut off predicted in 1966 by K. Greisen, G. Zatsepin, and V. Kuzmin.
- Photons of CMBR interact with cosmic ray protons of extragalactic origin.
- Photoproduction of pions; Δ resonance.
- Pion carries away 20% of proton's energy ➔ strong energy-loss mechanism for protons that travel > 50 Mpc
- Causes a strong break in the spectrum if sources are distant.
- Should occur at about 6×10^{19} eV (10J) if Sources ~ universally distributed

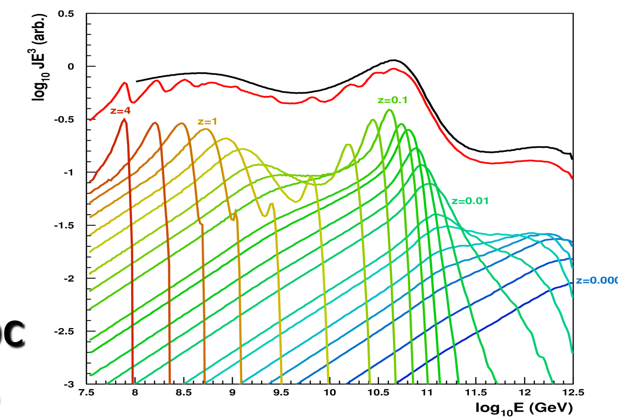

.

Contributions to Extra-galactic spectrum

The extra-galactic cosmic ray **spectrum fractionates with source red shift Additional e+ e- energy loss mechanism produces Ankle**

$p+\gamma_{CMB} \rightarrow \Delta(1232) \rightarrow \pi+N$

$\pi^{\pm} \rightarrow \mu^{\pm} + \nu_{\mu}$

$\mu^{\pm} \rightarrow e^{\pm} + \nu_{e} + \nu_{\mu}$

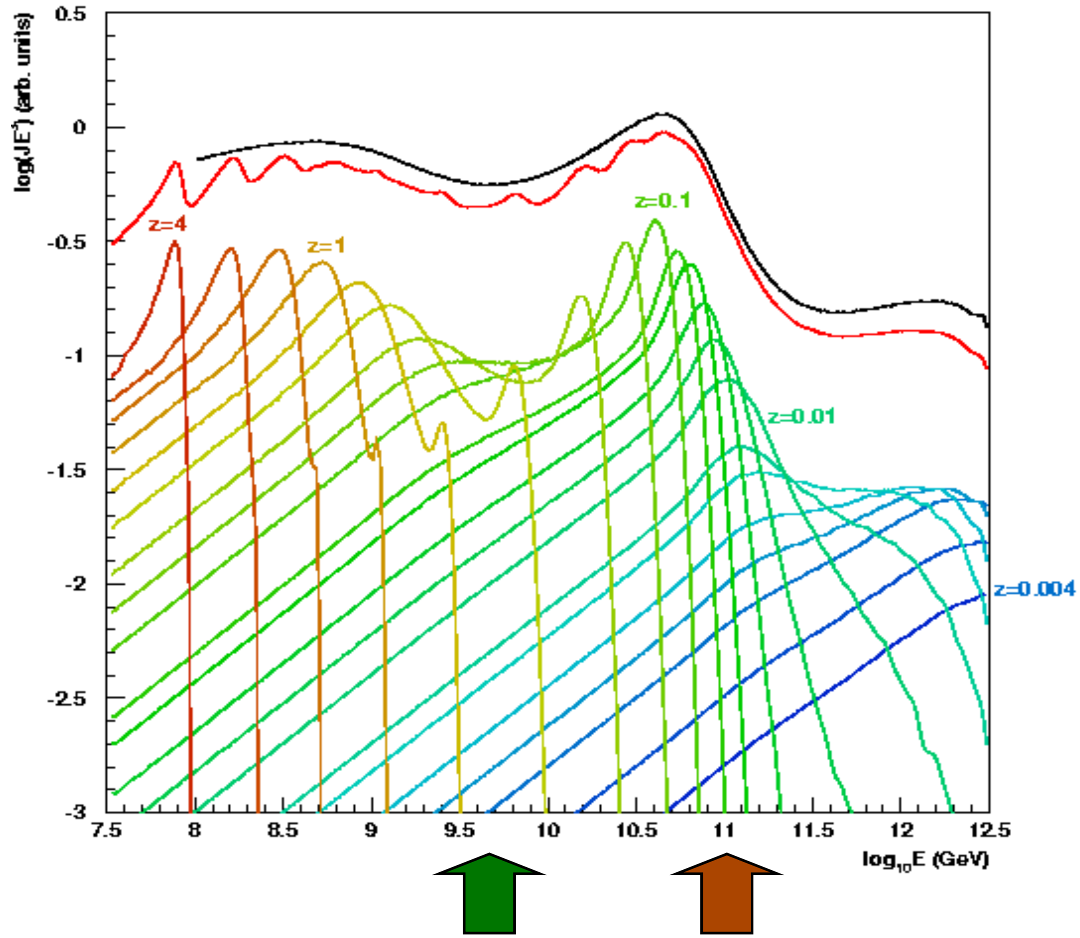

The first air-fluorescence detector prototype (Fly's Eye at Volcano Ranch)

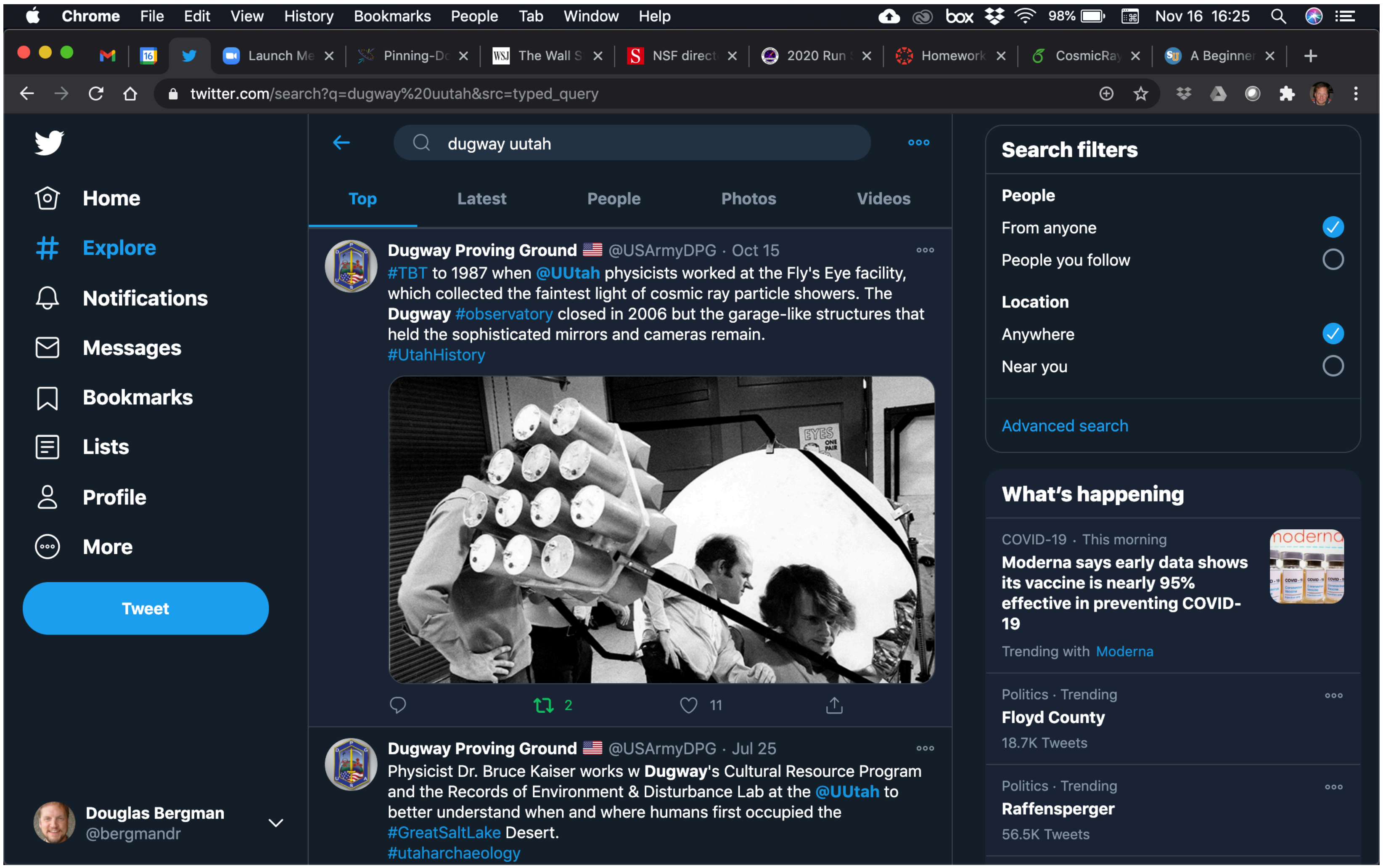

HiRes was located on the U.S. Army's Dugway Proving Ground, ~2 hours south-west of the University of Utah

- HiRes1: @ Five Mile Hill
  (aka Little Granite Mountain)
- 21 mirrors, 1 ring (3^o<altitude<17^o)
- Sample-and-hold electronics
  (pulse height and trigger time)

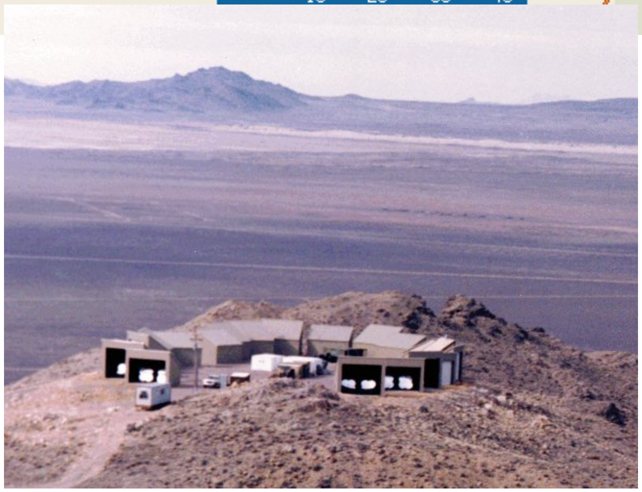

- HiRes2: @ Camel's Back Ridge 12.6 km south-west of HiRes1.
- 42 mirrors, 2 rings (3^o<altitude<31^o)
- FADC electronics (100 ns period)

First Observation of the Greisen-Zatsepin-Kuzmin Suppression

R.U. Abbasi,[1] T. Abu-Zayyad,[1] M. Allen,[1] J.F. Amman,[2] G. Archbold,[1] K. Belov,[1] J.W. Belz,[1] S.Y. Ben Zvi,[3] D.R. Bergman,[4,*] S.A. Blake,[1] O.A. Brusova,[1] G.W. Burt,[1] C. Cannon,[1] Z. Cao,[1] B.C. Connolly,[3] W. Deng,[1] Y. Fedorova,[1] C.B. Finley,[3] R.C. Gray,[1] W.F. Hanlon,[1] C.M. Hoffman,[2] M.H. Holzscheiter,[2] G. Hughes,[4] P. Hüntemeyer,[1] B.F Jones,[1] C.C.H. Jui,[1] K. Kim,[1] M.A. Kirn,[5] E.C. Loh,[1] M.M. Maestas,[1] N. Manago,[6] L.J. Marek,[2] K. Martens,[1] J.A.J. Matthews,[7] J.N. Matthews,[1] S.A. Moore,[1] A. O'Neill,[3] C.A. Painter,[2] L. Perera,[4] K. Reil,[1] R. Riehle,[1] M. Roberts,[7] D. Rodriguez,[1] N. Sasaki,[6] S.R. Schnetzer,[4] L.M. Scott,[4] G. Sinnis,[2] J.D. Smith,[1] P. Sokolsky,[1] C. Song,[3] R.W. Springer,[1] B.T. Stokes,[1] S.B. Thomas,[1] J.R. Thomas,[1] G.B. Thomson,[4] D. Tupa,[2] S. Westerhoff,[3] L.R. Wiencke,[1] X. Zhang,[3] and A. Zech[4]

(The High Resolution Fly's Eye Collaboration)

[1]*University of Utah, Department of Physics, Salt Lake City, UT, USA*
[2]*Los Alamos National Laboratory, Los Alamos, NM, USA*
[3]*Columbia University, Department of Physics and Nevis Laboratory, New York, New York, USA*
[4]*Rutgers University — The State University of New Jersey, Department of Physics and Astronomy, Piscataway, NJ, USA*
[5]*Montana State University, Department of Physics, Bozeman, MT , USA*
[6]*University of Tokyo, Institute for Cosmic Ray Research, Kashiwa, Japan*
[7]*University of New Mexico, Department of Physics and Astronomy, Albuquerque, NM, USA*

The High Resolution Fly's Eye (HiRes) experiment has observed the Greisen-Zatsepin-Kuzmin suppression (called the GZK cutoff) with a statistical significance of five standard deviations. HiRes' measurement of the flux of ultrahigh energy (UHE) cosmic rays shows a sharp suppression at an energy of 6×10^{19} eV, consistent with the expected cutoff energy. We observe the "ankle" of the cosmic-ray energy spectrum as well, at an energy of 4×10^{18} eV. We describe the experiment, data collection, analysis, and estimate the systematic uncertainties. The results are presented and the calculation of the statistical significance of our observation is described.

PACS numbers: 98.70.Sa, 95.85.Ry, 96.50.sb, 96.50.sd

5 Sigma Observation of the GZK Suppression

- *Broken Power Law Fits (independent data)*
  - *No Break Point*
    - *χ^2/DOF = 162/39*
  - *One BP*
    - *χ^2/DOF = 63.0/37*
    - *BP = 18.63*
  - *Two BP's*
    - *χ^2/DOF = 35.1/35*
    - *1st BP = 18.65 +/- .05*
    - *2nd BP = 19.75 +/- .04*
  - *BP with Extension*
    - *Expect 43.2 events*
    - *Observe 13 events*
    - *Poisson prob:P(15;51.1)=7x10^{-8}(5.3σ)*

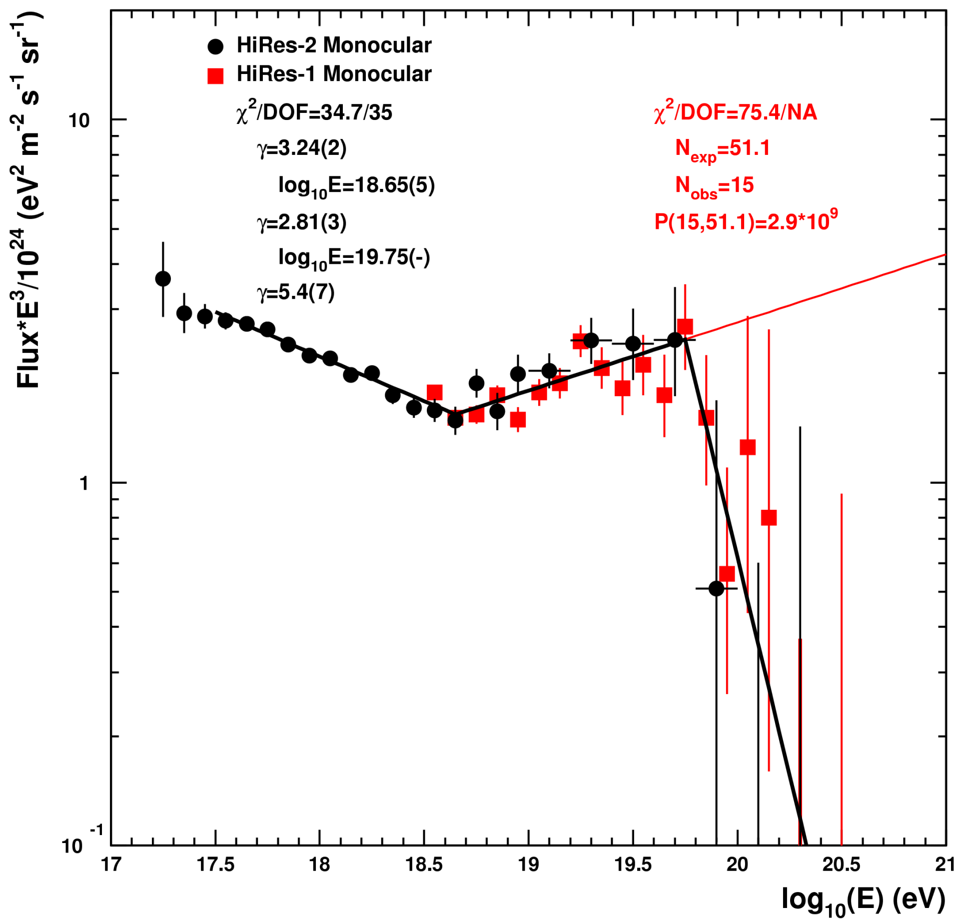

Cutoff observed at correct predicted energy (Berezinsky E1/2), but situation now seems More complicated.

How to detect very rare events? Utilize secondary interations

The Hybrid Concept

Surface Detector Array

lateral distribution, 100% duty cycle

Air Fluorescence Detectors

Longitudinal profile, calorimetric energy measurement, ~15% duty cycle

accurate energy and direction measurement

mass composition studies in a complementary way

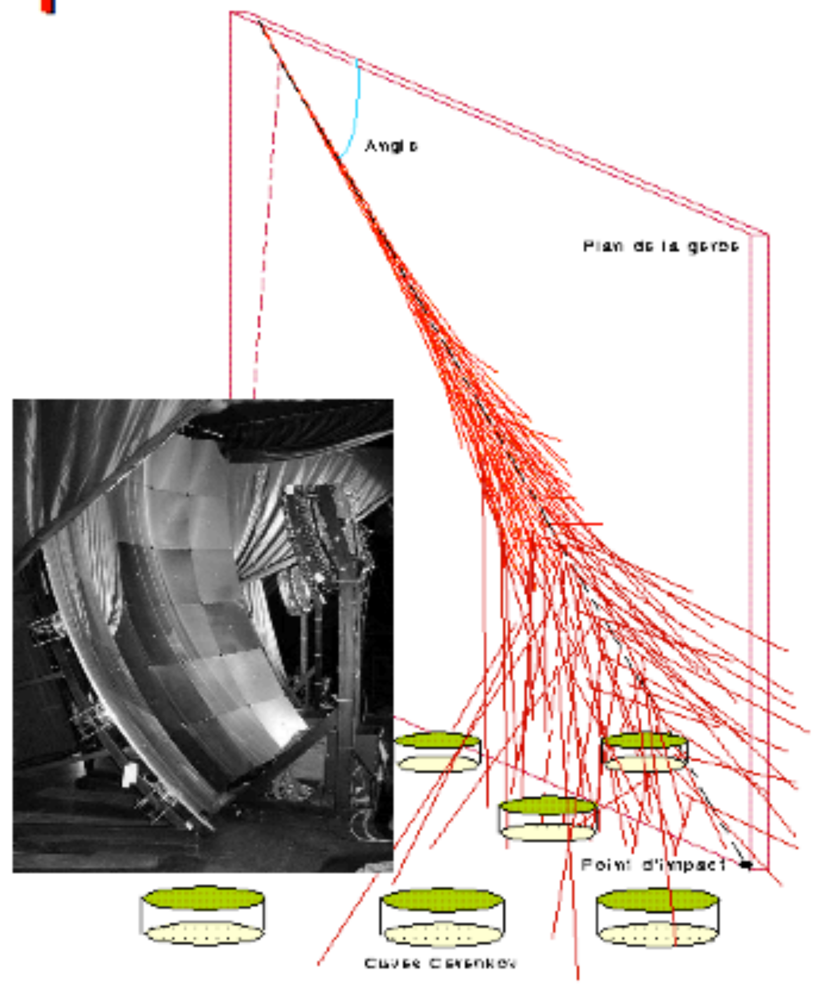

Since HiRes – Moving down in energy

- TA - 1-100 EeV Northern hemisphere
- Auger – 1-100 EeV Southern hemisphere
- TALE – few PeV to 1 EeV Extension
- Auger (HEAT and AMIGA) – 50 PeV to few EeV Extension
- Ice Top – PeV to EeV surface array
- Tunka – PeV to EeV Cherenkov/surface array
- Kascade/Kascade Grande – PeV to EeV surface array
- HAWC and a number of smaller arrays exploring 1-10 PeV region.

TA and Low Energy Extension (TALE)

Galactic to Extra-Galactic Transition

10 new telescopes to look higher in the sky (31-59^{o}) to see shower development to much lower energies

Graded infill surface detector array - more densely packed surface detectors (lower energy threshold)

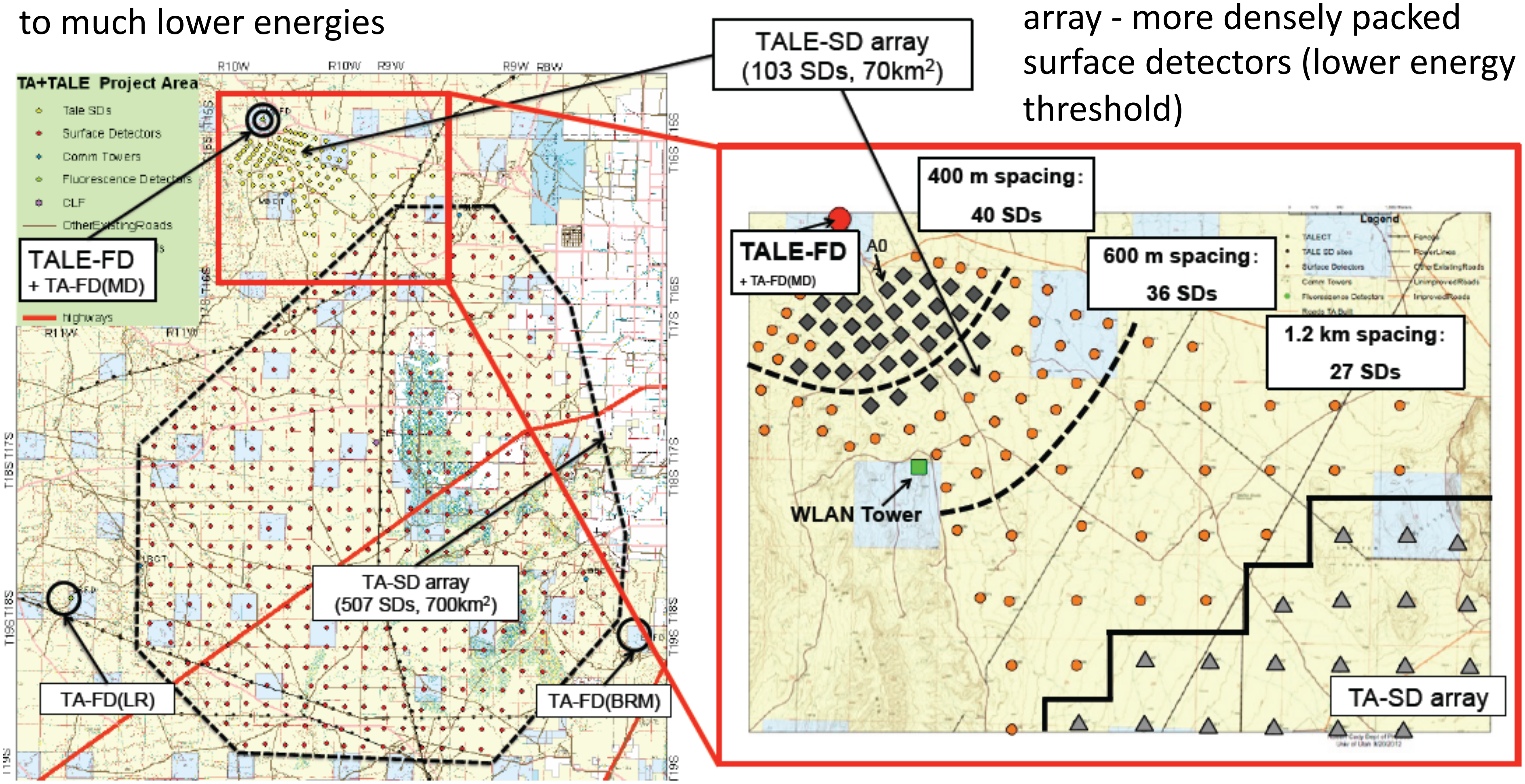


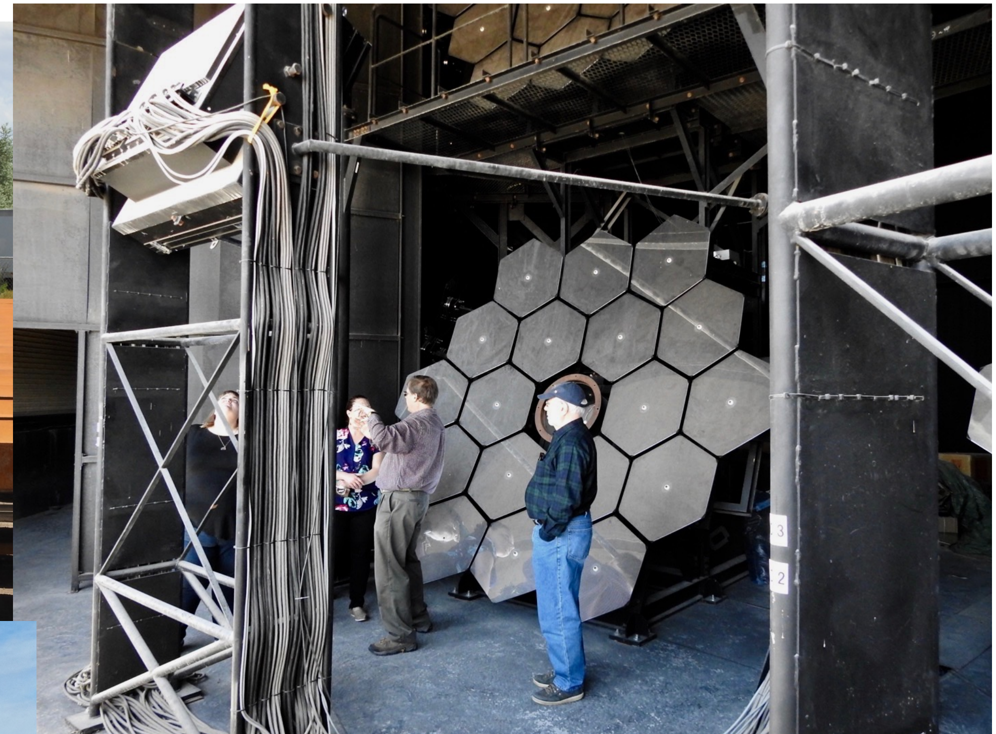

Event reconstruction

Stereo

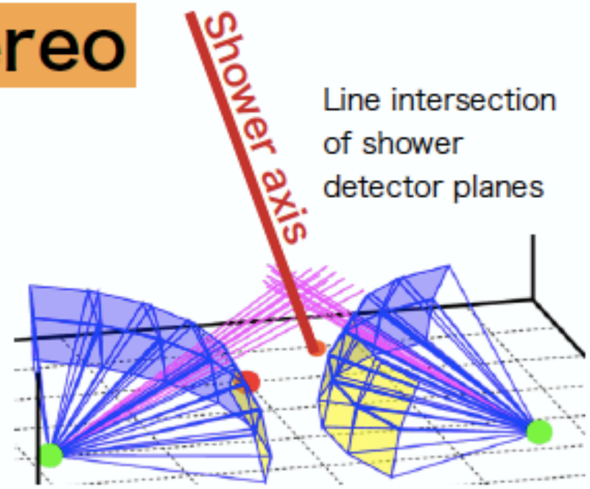

observed images

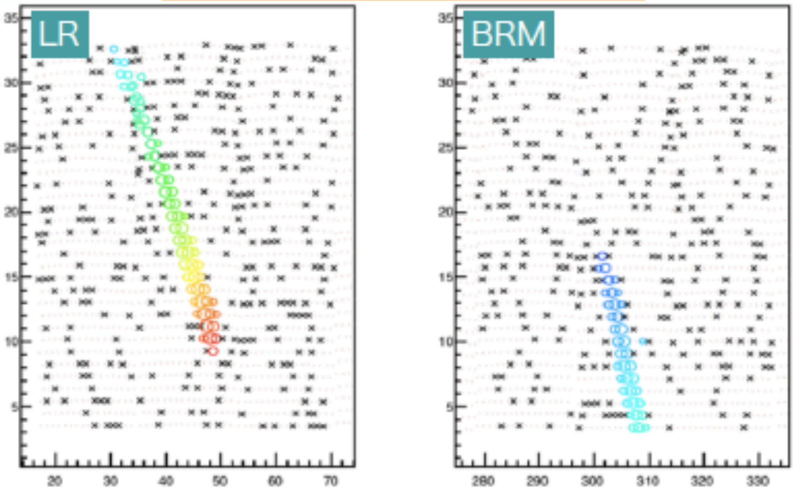

Hybrid

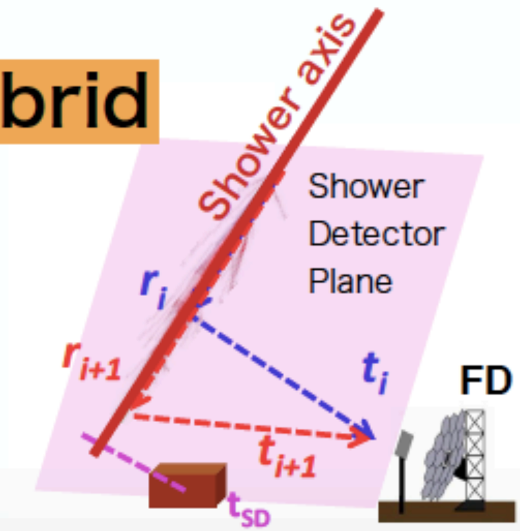

reconstructed shower profiles

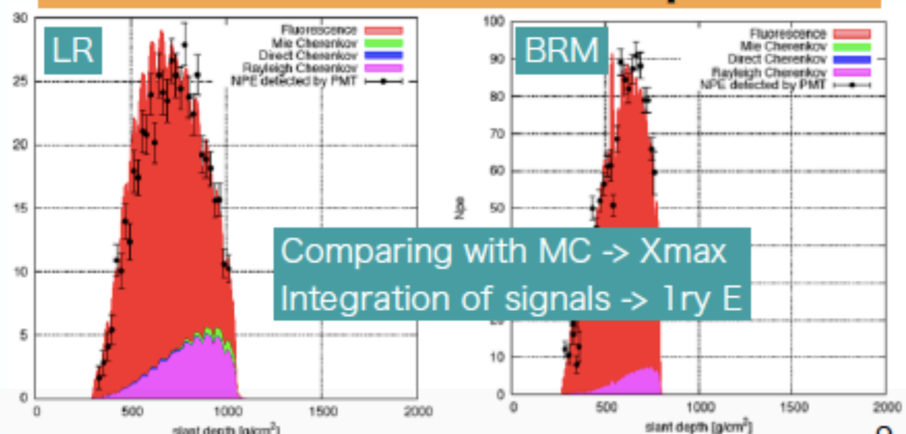

Event sample by SD array

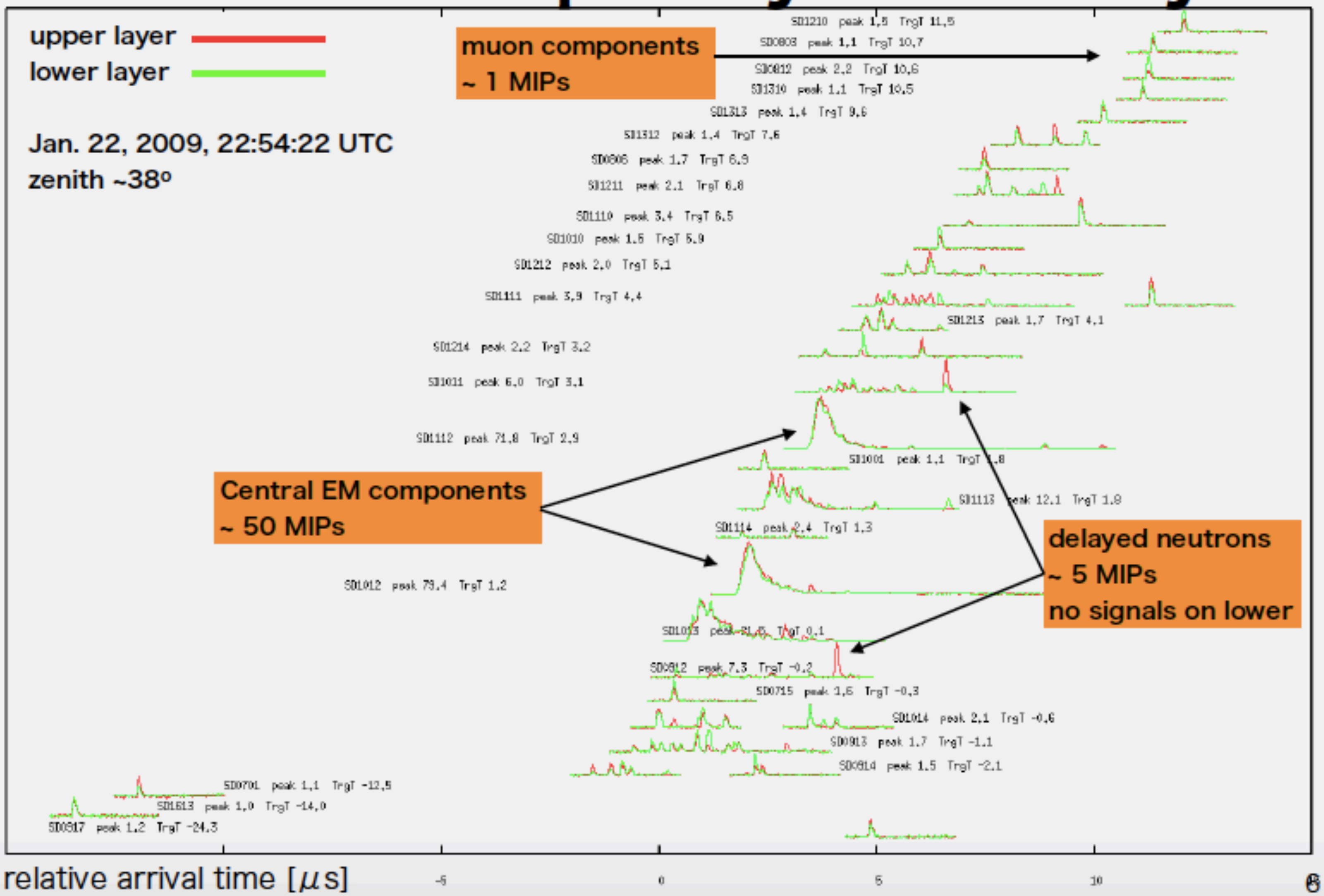

Event reconstruction

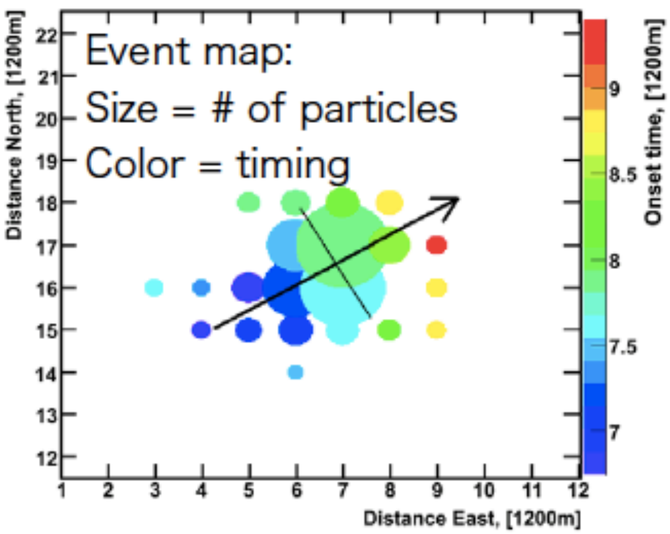

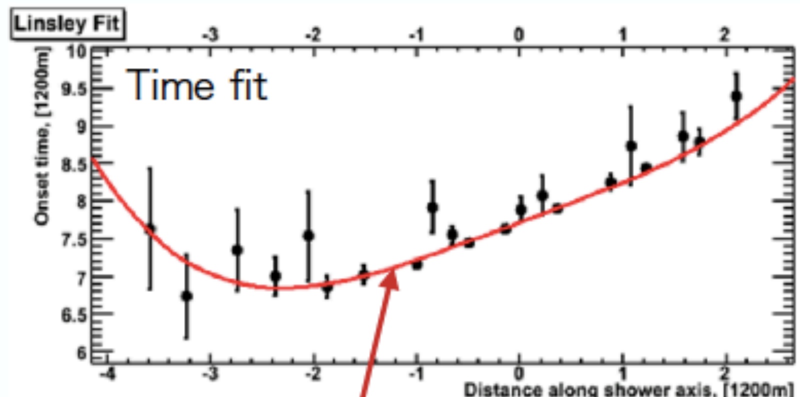

$$\tau = a\left(1 - \frac{l}{12\times10^3\mathrm{m}}\right)^{1.05}\left(1.0 + \frac{s}{30\mathrm{m}}\right)^{1.35}\rho^{-0.5}$$

Modified empirical formula in AGASA

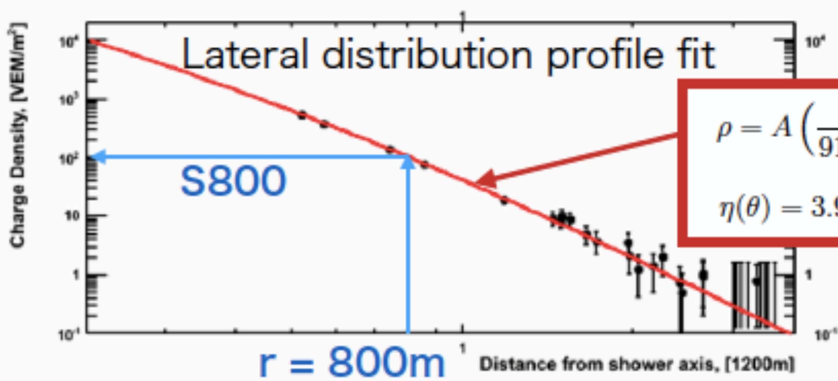

$$\rho = A\left(\frac{s}{91.6\mathrm{m}}\right)^{-1.2}\left(1 + \frac{s}{91.6\mathrm{m}}\right)^{-(\eta(\theta)-1.2)}\left(1 + \left[\frac{s}{1000\mathrm{m}}\right]^2\right)^{-0.6}$$

$$\eta(\theta) = 3.97 - 1.79\,[\sec(\theta) - 1]$$

Empirical formula used by AGASA

S800 -> primary energy

Primary energy determination

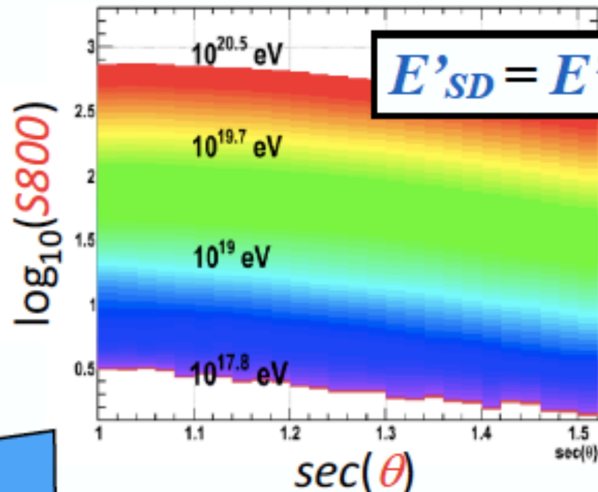

$E'_{SD} = E'_{SD}(S800, \theta)$

Scale to FD energy

$E_{SD} = E'_{SD} / 1.27$

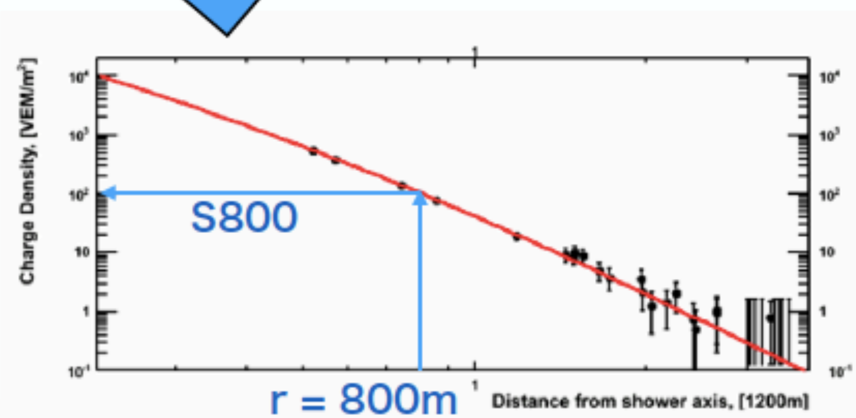

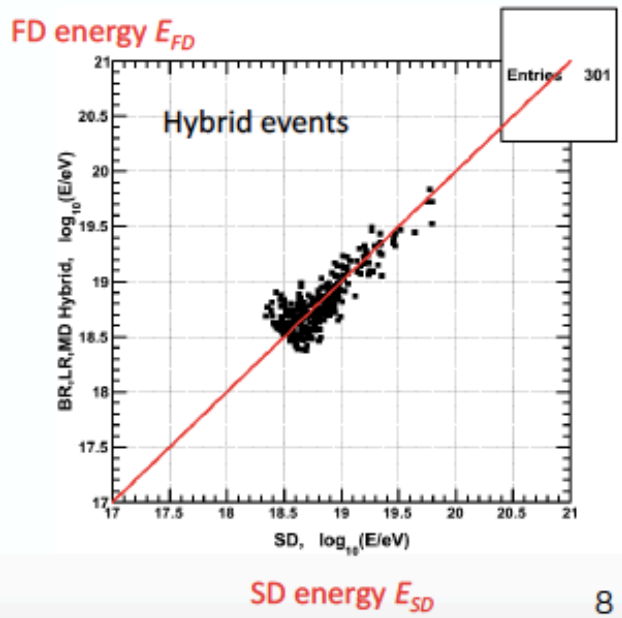

TA SD Spectrum (9 yrs data)

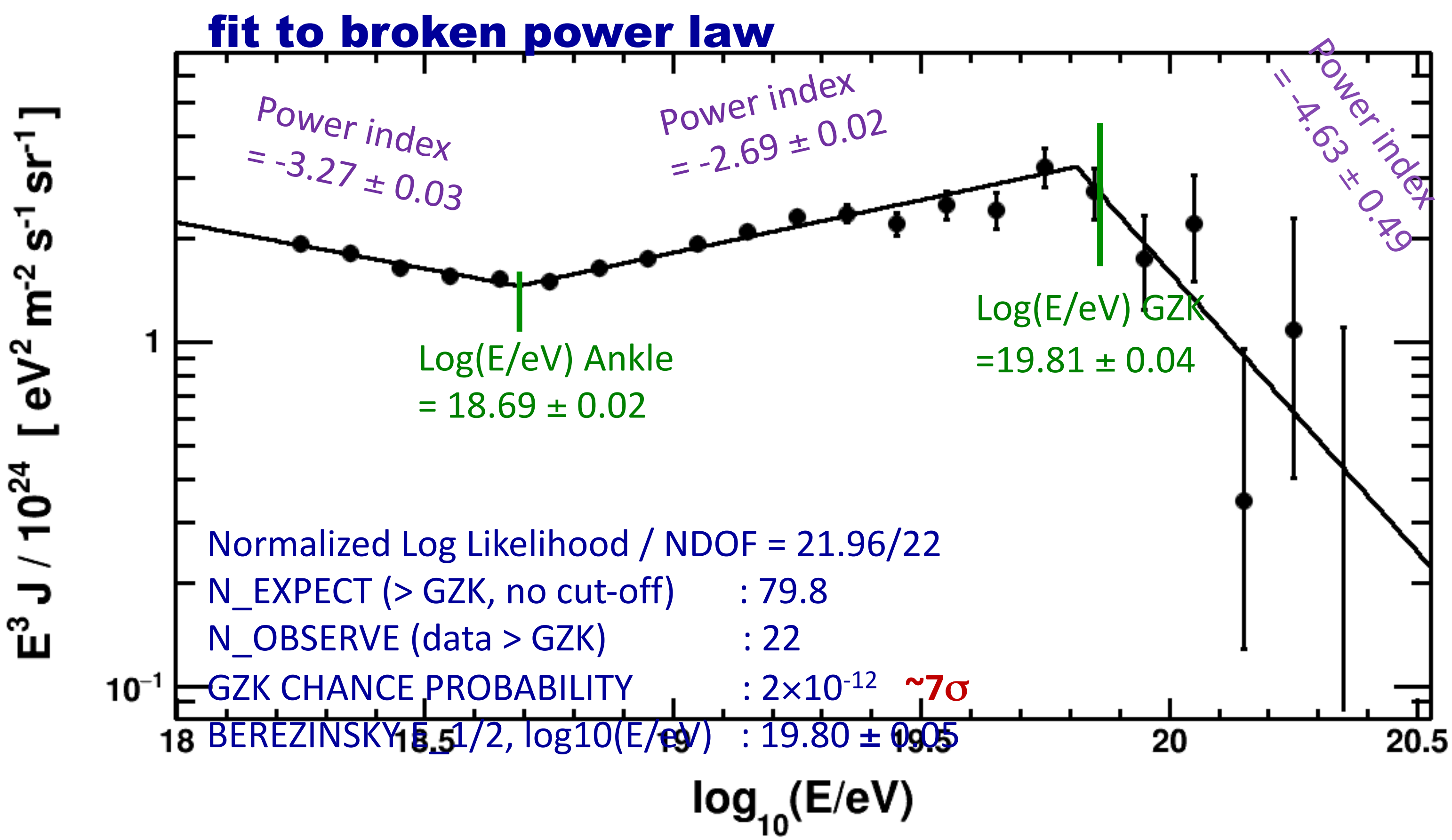

See D.Ivanov CRI 236

Auger Spectrum in Southern Hemisphere

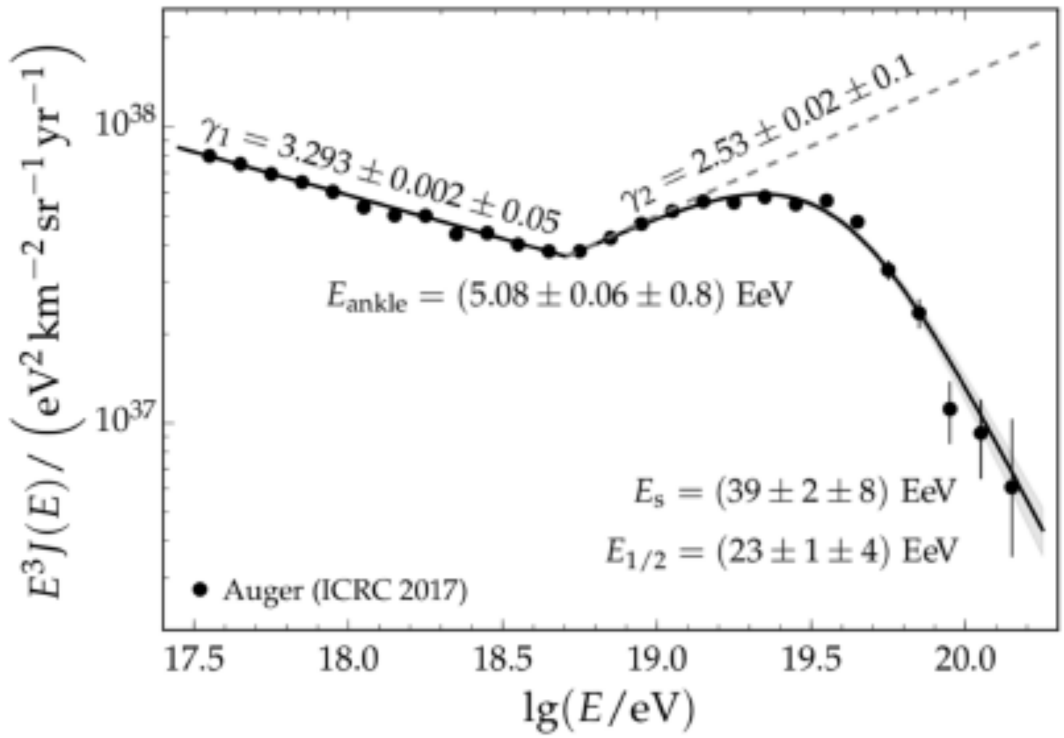

Extending to Lower Energies – TA Low Energy Exension

TALE Fluorescence Detector

- 10 high-elevation telescopes at the Middle Drum site, looking from 31°-59° in elevation.
- Operate in conjunction with the TA Middle Drum FD.

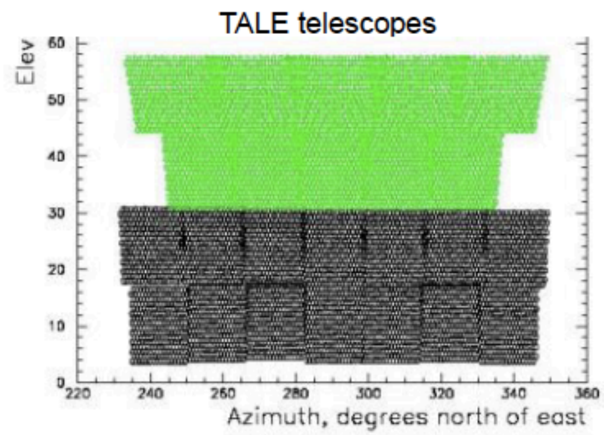

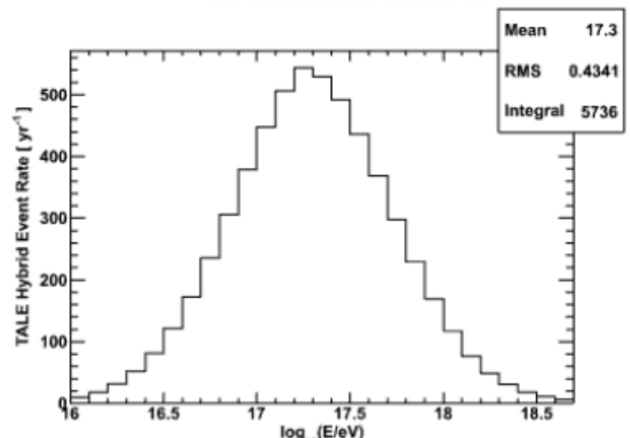

Expected TALE hybrid events per year

All 10 Telescopes installed and in operation since fall 2013

Test array of 16 scintillation surface detectors in operation

TALE Cherenkov Event

PCGF turns out to work very well on
Cherenkov light dominated events

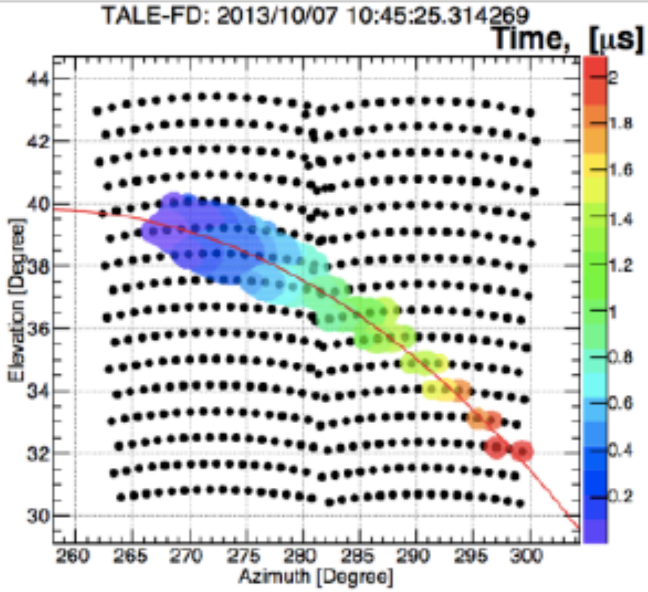

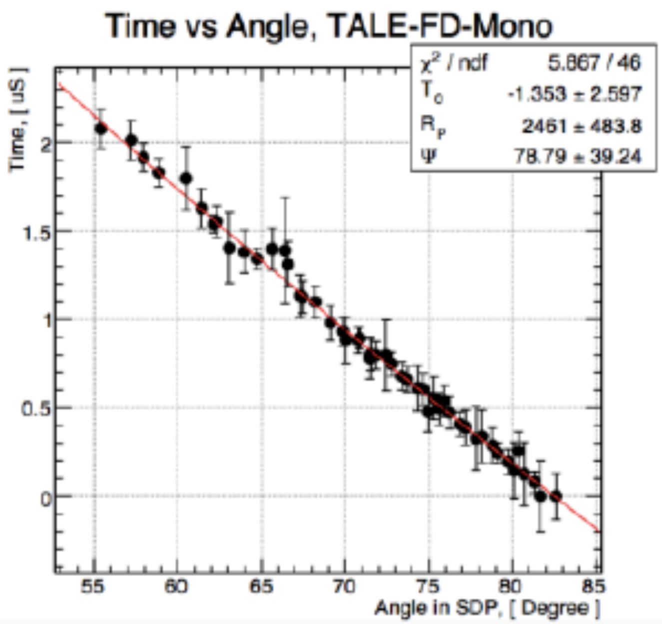

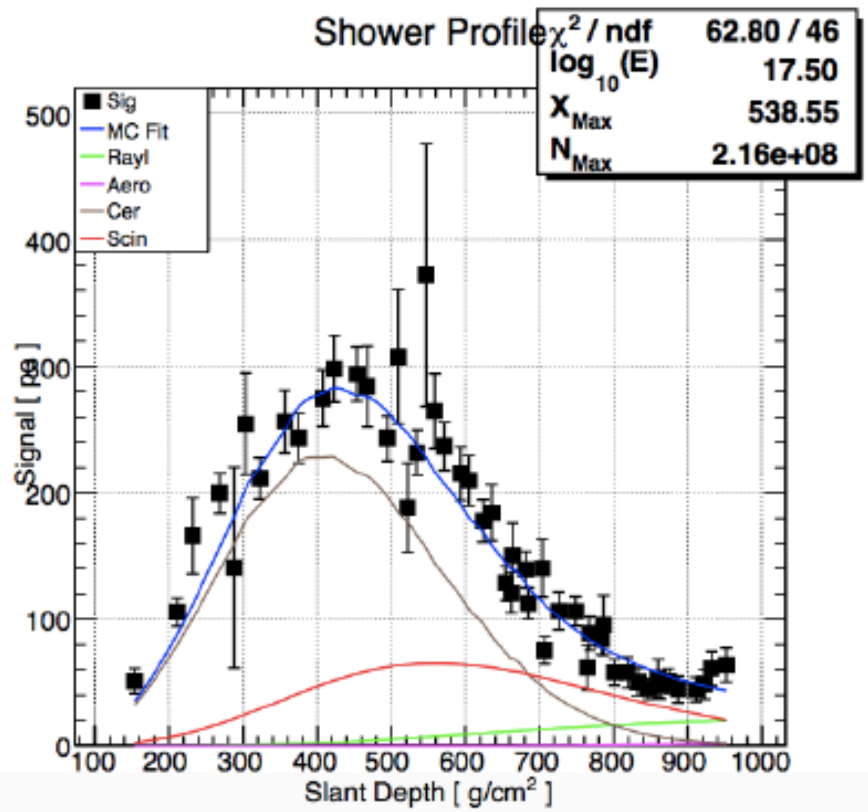

TALE Energy Spectrum

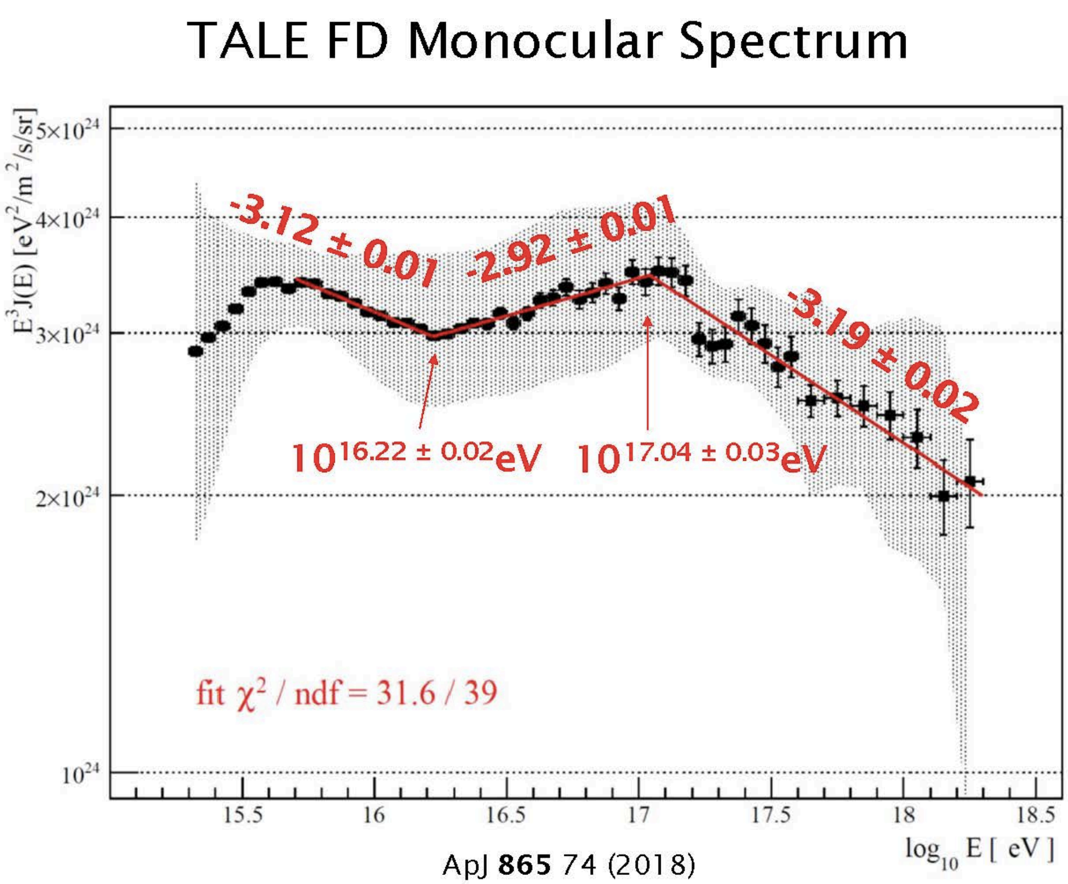

ApJ **865** 74 (2018)

Combined TA Spectrum

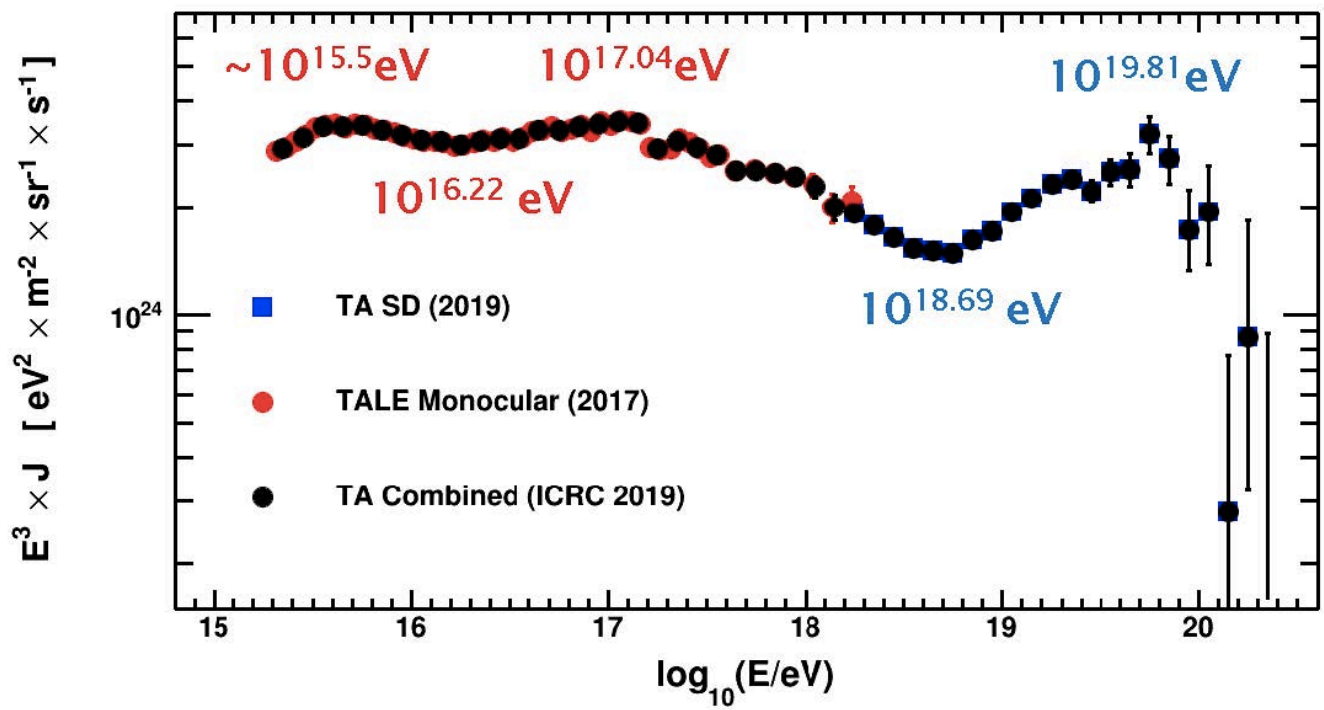

Most recent result (ICRC 2019)

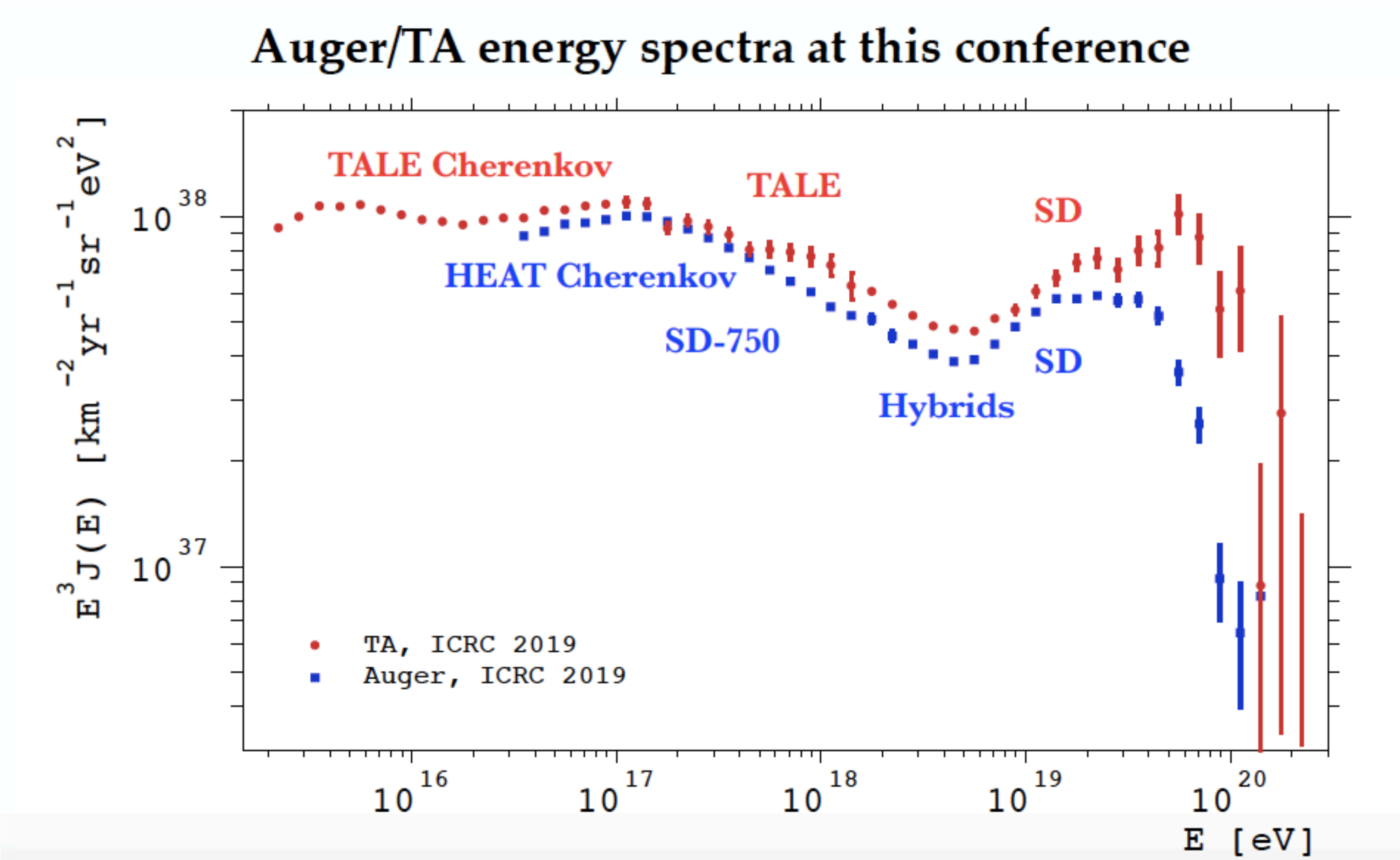

Monocular FD spectrum: combined TA and HiRes

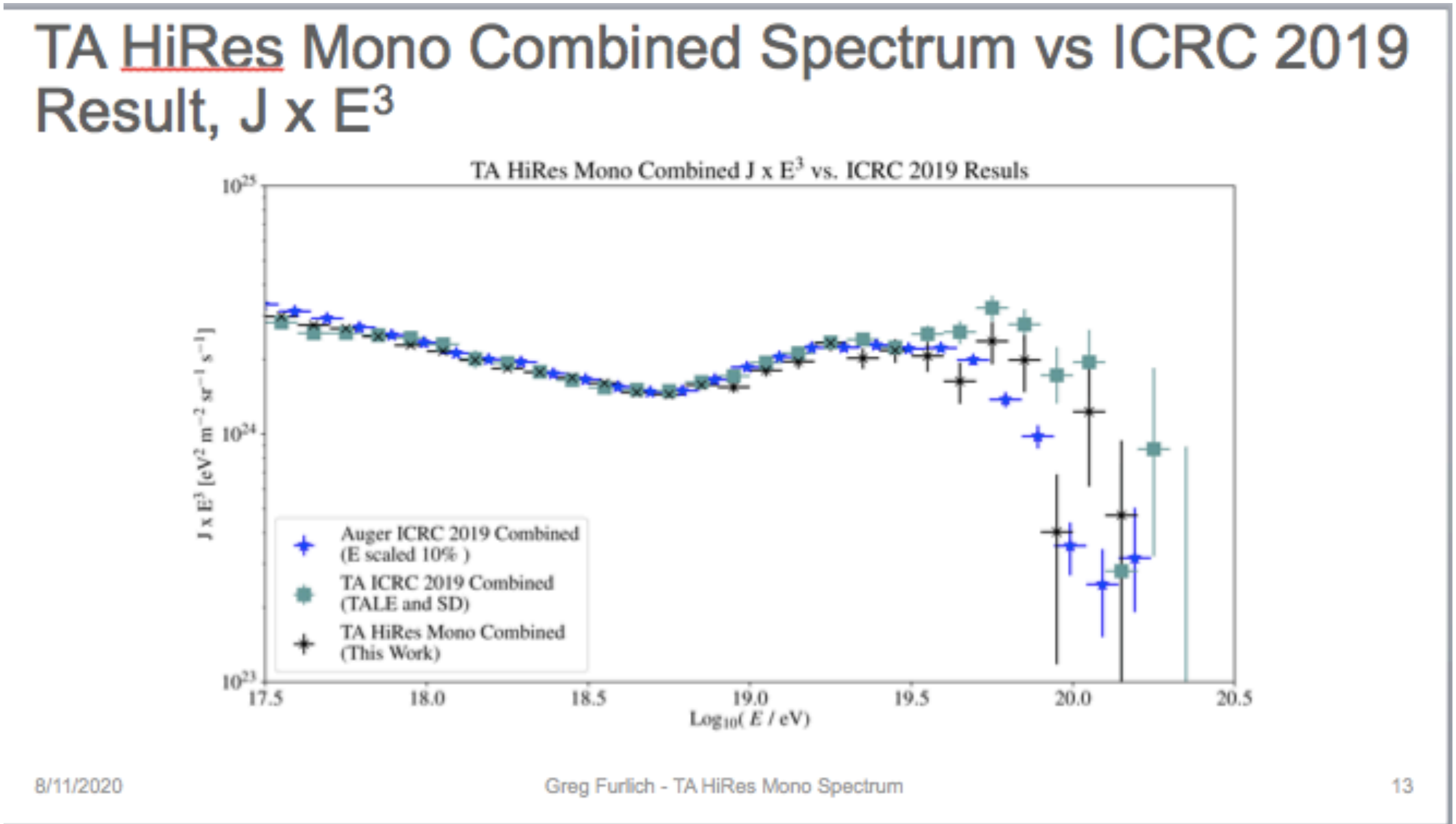

Not a simple power law. Many questions arise.

- Is the cutoff difference in shape due to systematics or a real reflection of source differences N and S? Is this correlated with appearance of Hot Spot in N and Cen A in S?
- If the spectra at highest energies are different, are the composition also different? Is there a composition dependent anisotropy?
- What is the origin of the ankle, second knee, and dip structure between first and second knee.
- Are there corresponding composition changes?

Is the difference in cutoff N/S a real effect?

- Check spectrum in common declination band to look for possible systematic effects.

- Energy thresholds chosen to match the measured integral fluxes in $-12^\circ \le \delta \le +42^\circ$
  - Mismatches of nominal energies within systematic uncertainties ($\pm 14\%_{\mathrm{Auger}} \pm 21\%_{\mathrm{TA}}$)
- **Lower-energy dataset** ≥ 8.86 EeV / ≥ 10 EeV
- Higher-energy dataset ≥ 40 EeV / ≥ 53.2 EeV

Auger data $E_{\mathrm{Auger}} \ge 8.86$ EeV

- 01 Jan 2004 – 31 Aug 2016
- $\theta < 80^\circ$[1] ($\delta < +44.8^\circ$)
- 78 400 km^2 yr sr (27k events)

TA data $E_{\mathrm{TA}} \ge 10$ EeV

- 11 May 2018 – 10 May 2017
- $\theta < 55^\circ$ ($\delta > -15.7^\circ$)
- 11 500 km^2 yr sr (4k events)

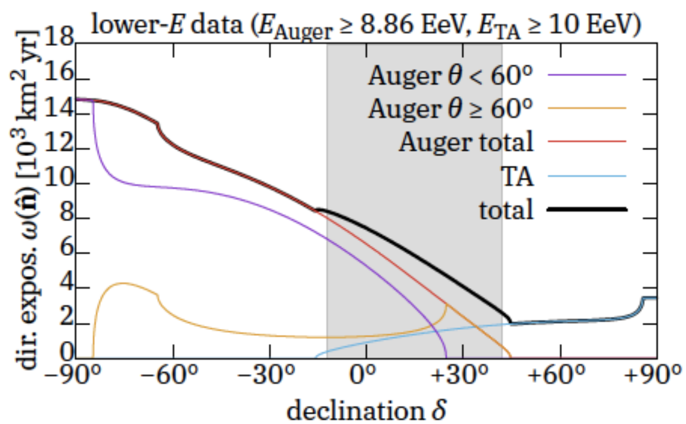

[1] Different quality cuts and reconstruction techniques for $\theta \lessgtr 60^\circ$

Searches for declination dependences in TA and Auger

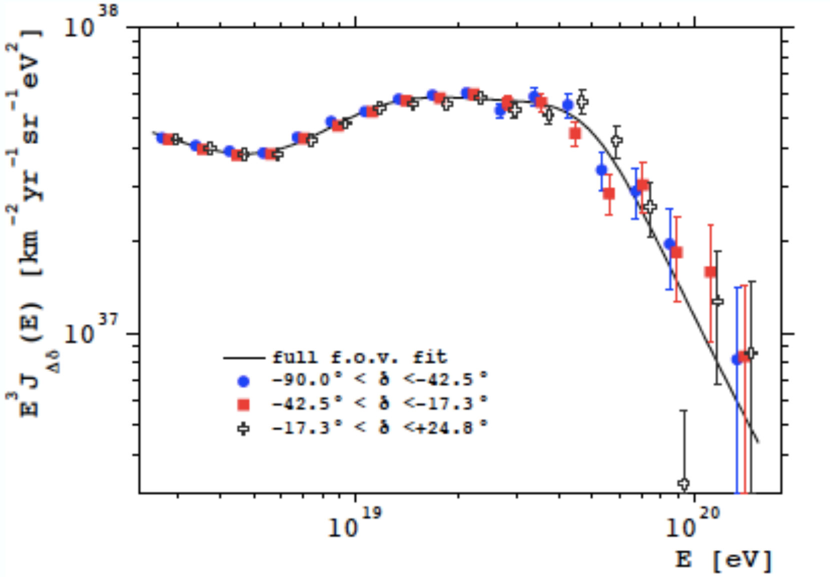

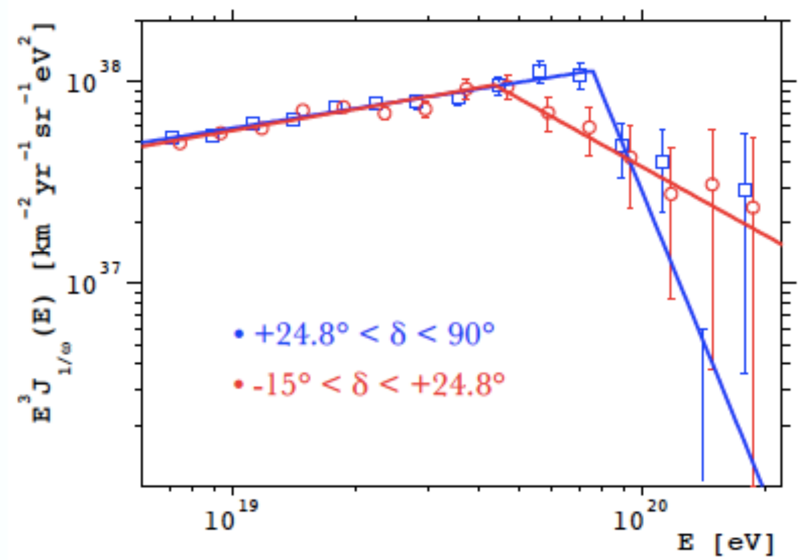

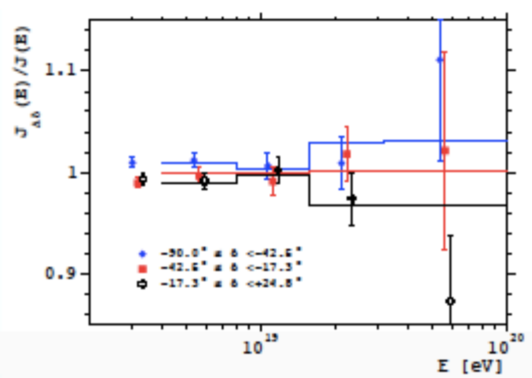

- Auger: Only a trend for a slightly larger intensity in the South (consistent with dipole expectations)
- TA: Differences in the suppression energy, with an excess of intensity in the Northernmost sky

How often would this difference arise from statistical fluctuations?

Using 11 years of SD data

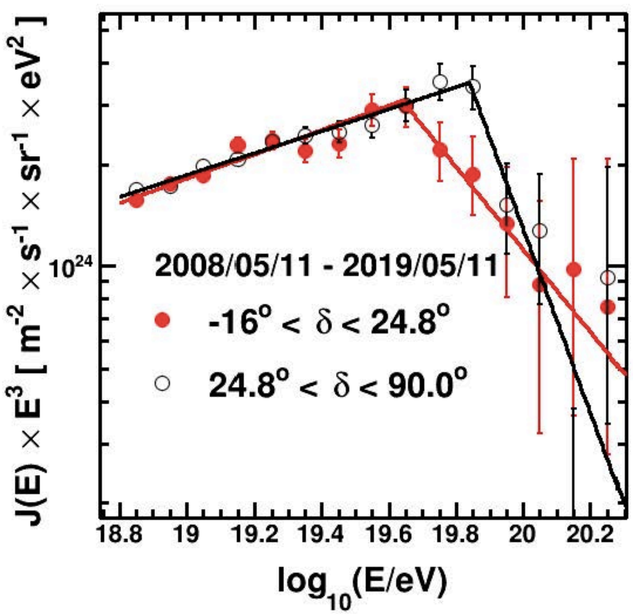

- Cutoff energies in lower and higher declination bands now 4.7 σ different.
  - **4.3 σ global chance probability of the effect**
- **Strong evidence of cosmic ray spectrum declination dependence in the Northern Hemisphere**

Is there a systematic issue between Auger and TA?

Lessons from the common declination band

[D. Ivanov et al., Proc. of UHECR 2018]

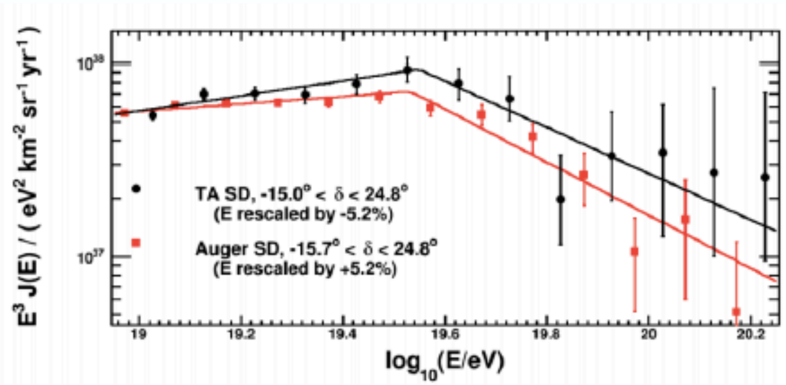

- Better agreement than whole f.o.v. spectra for the suppression energy
- Still, constant rescaling of energies insufficient to get satisfactory agreement
- Non-linearity of ~+(-)10% / decade on top of a +(-)5.2% global rescaling

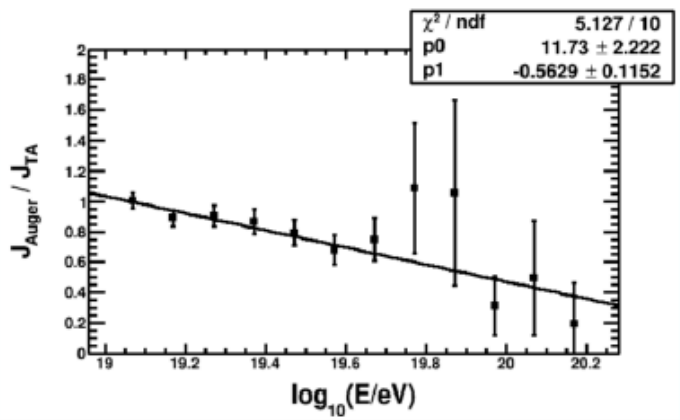

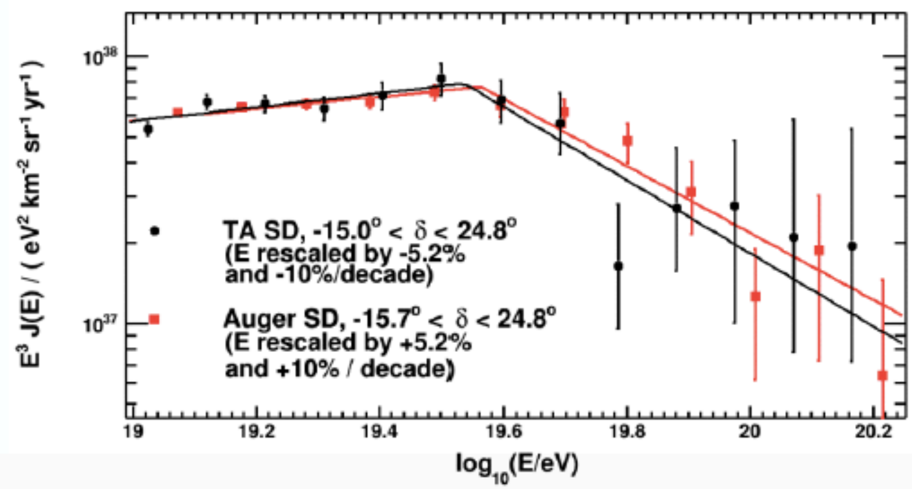

Is the remaining difference in common declination band a statistical effect?
Frequency of Auger/TA flux ratio slope

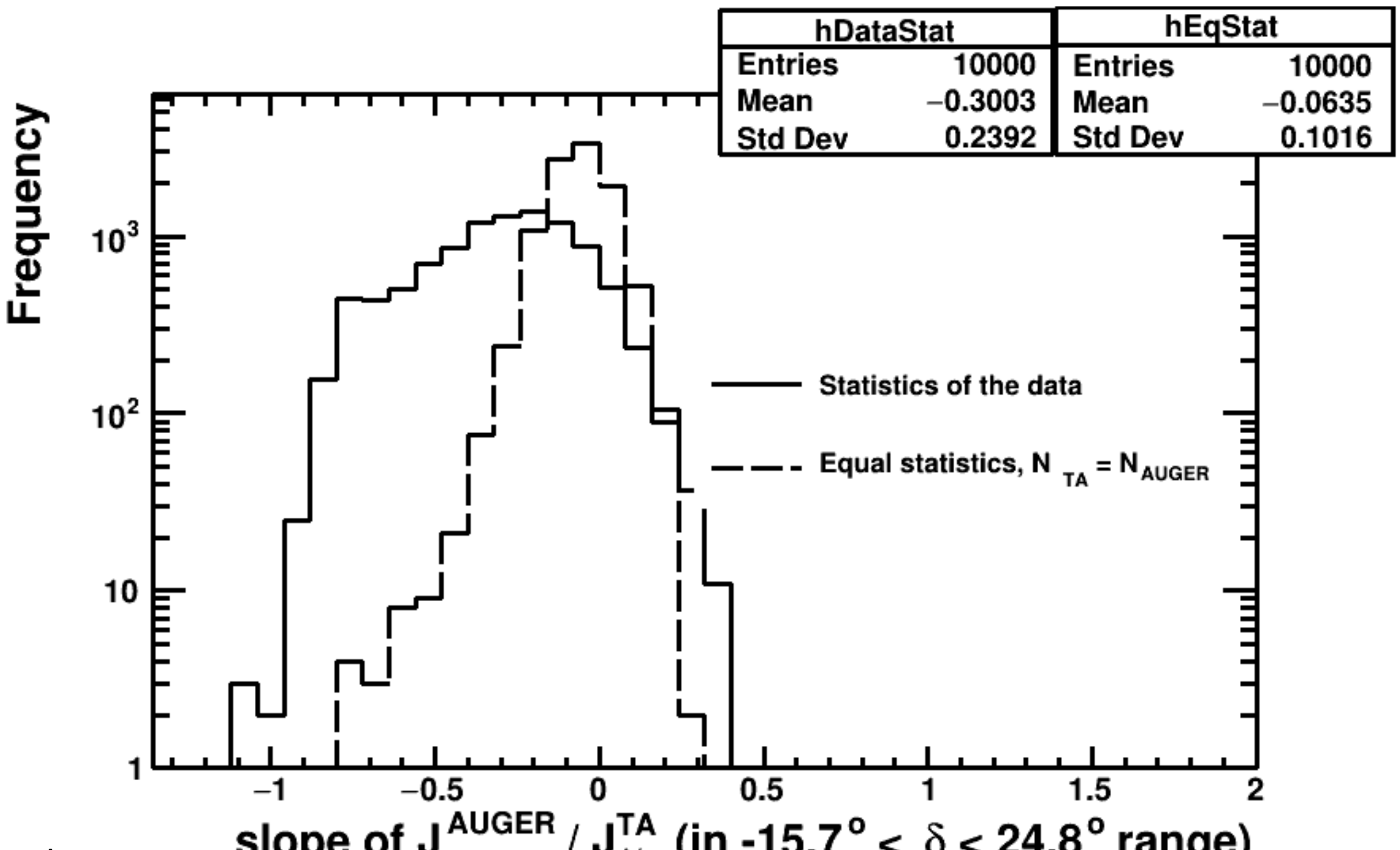

1/omega method: P_{Chance}=22% to get slope < -0.5 and 14% to get slope < -0.6
(for the traditional average exposure method, P_{Chance}=14%
to get slope < -0.5 and 9% to get slope < -0.6.)

Putting all experiments together

Cosmic Ray Spectrum

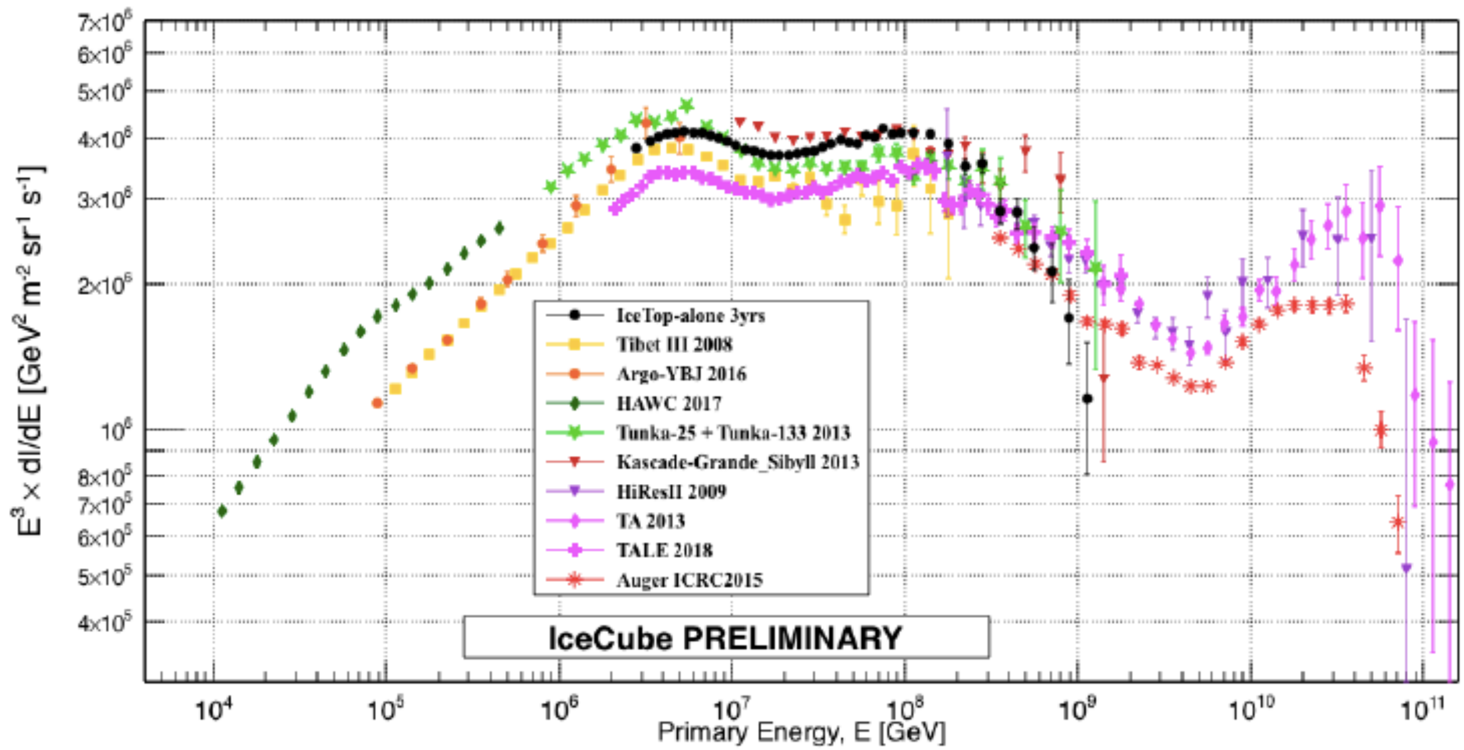

Interpretations of Structure

1. First knee: (proton knee)- galactic “leaky box” –rigidity dependent proton leakage
2. Second knee: (Fe knee) galactic Fe Emax: roughly 26 x proton knee.
3. Ankle: Extragalactic protons- spectrum excavated by proton energy loss by e+e- production OR dominance of extra-galactic flux with harder spectrum
4. Cut-off: GZK cutoff for protons/Fe – energy loss by pion photoproduction OR Emax of dominant CR source(s).
5. Does composition follow this? – Central question to resolve origins of structure.
6. Anisotropy can give important clues. Galactic proton anisotropy should be very strong at 10^{18} eV

Spectrum

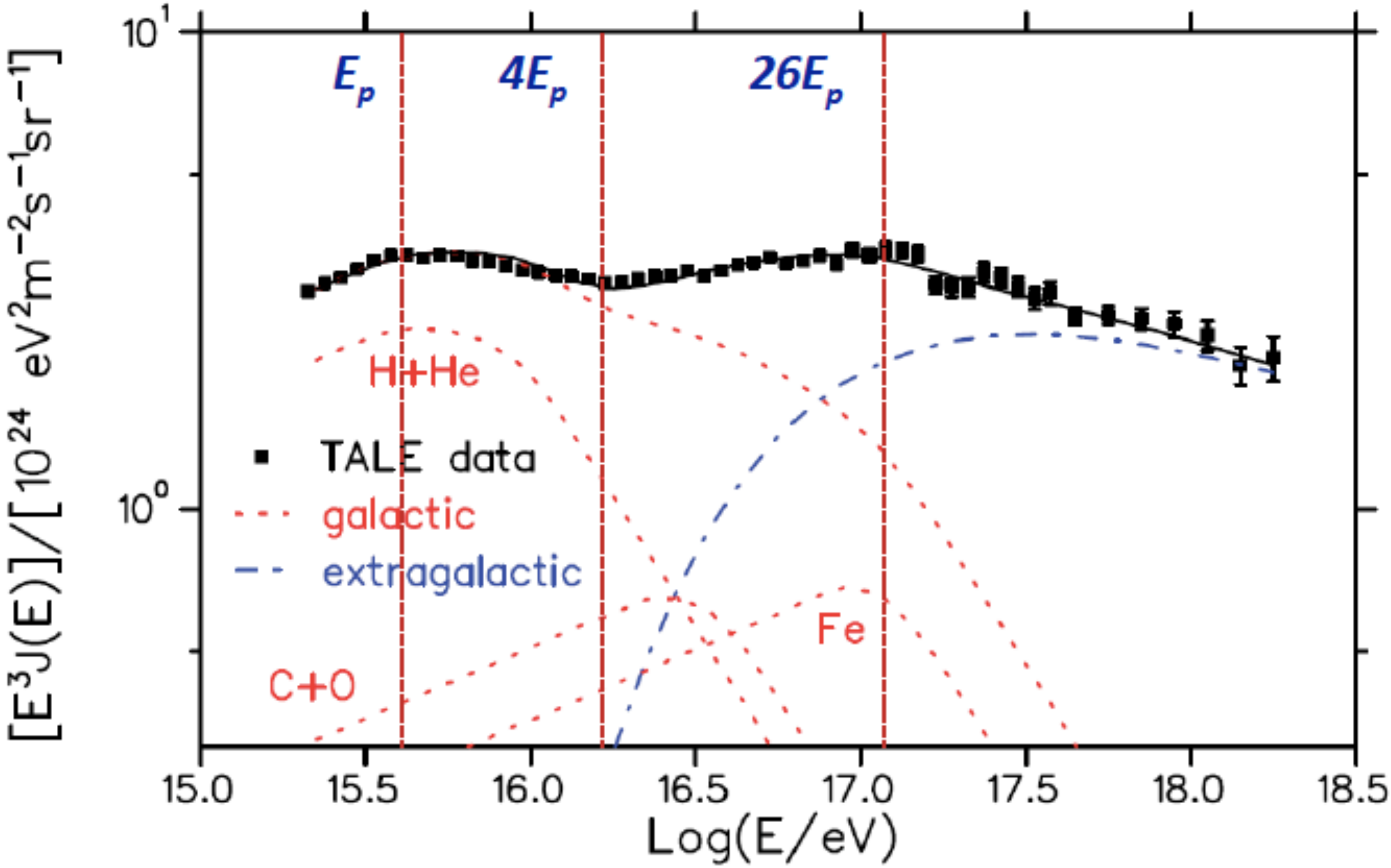

E_p
$4E_p$
$26E_p$
H+He
C+O
Fe
TALE data
galactic
extragalactic
$[E^3J(E)]/[10^{24}\ eV^2m^{-2}s^{-1}sr^{-1}]$
10^1
10^0
15.0
15.5
16.0
16.5
17.0
17.5
18.0
18.5
Log(E/eV)

What about below the knee? Direct precision measurement is possible

- ISS based experiments – AMS, CALET, ISS-CREAM
- Primary cosmic rays – p, He, C, O, Fe all show unexpected deviation from simple power law behavior at ~ few 100 GeV energies.
- Proton spectrum is different from He and other nuclei.
- Challenge to “standard” picture

AMS Results

Structure in the latest proton spectrum

Proton spectrum measured by AMS shows a deviation from a single law above few hundred GV.

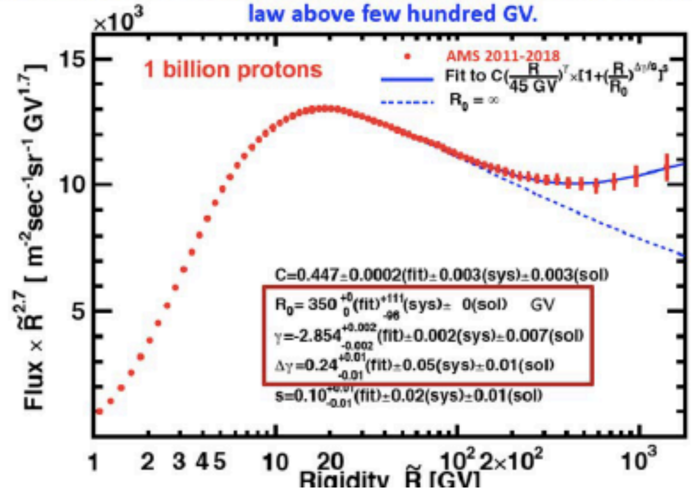

Origin of Structure in the latest helium spectrum

The structure in He (P) spectrum requires modification of cosmic ray transportation model or inclusion of local sources.

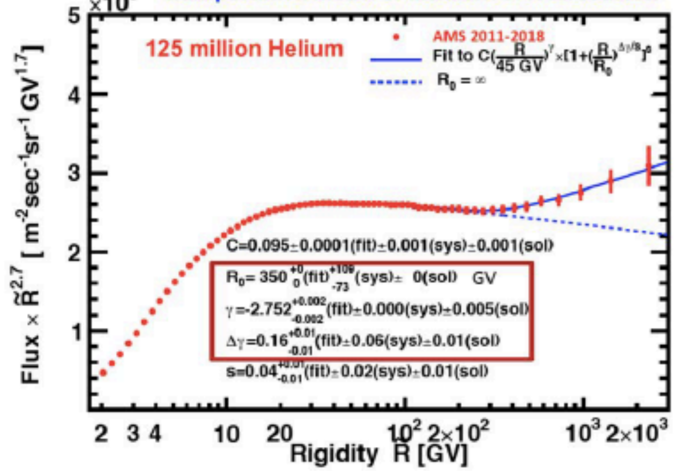

Latest AMS Measurements of He, C and O spectra

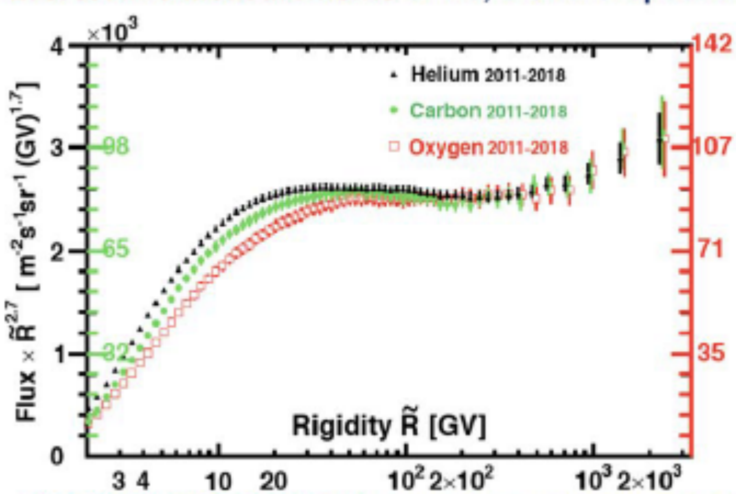

The latest AMS Results on the He/O and C/O Flux Ratios

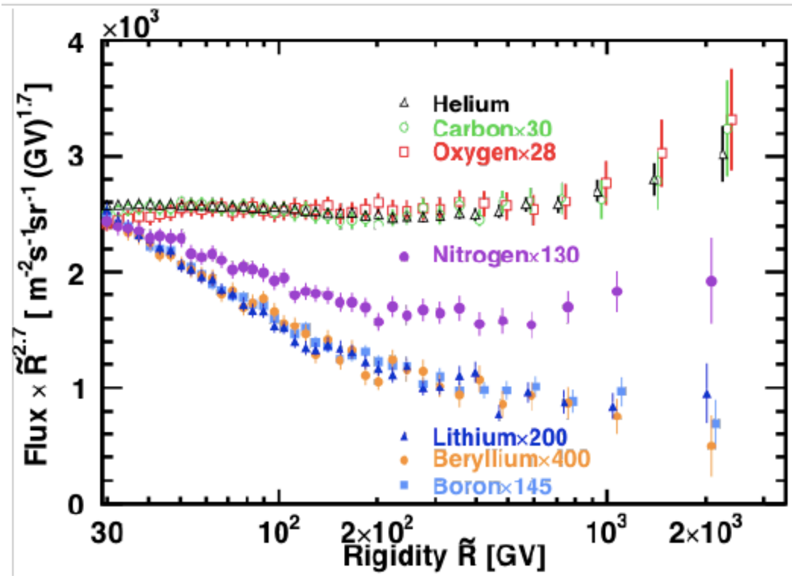

CALET Results

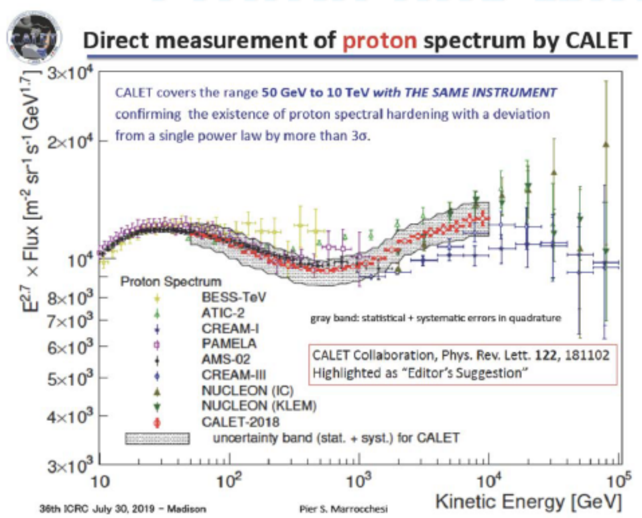

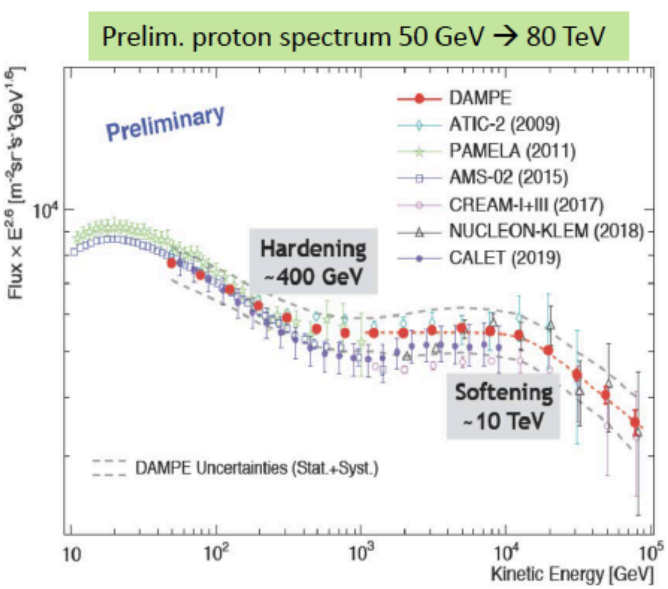

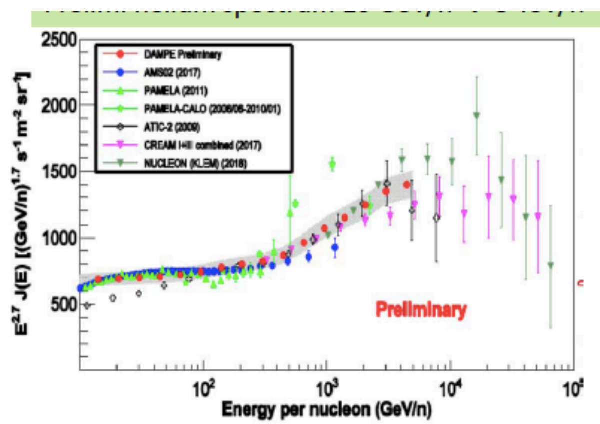

Important features for protons:
- confirmation of spectral hardening but at 400 GeV
- Softening above at 10 TeV

What the energy spectrum tells us

- There is significant structure and variation in spectral index over the entire range of cosmic rays.
- This is a significant challenge to theoretical understanding.
- Source origin versus propagation effects.
- Composition of cosmic rays plays an important role.

Composition: What to expect? p/He by far most abundant at low energies

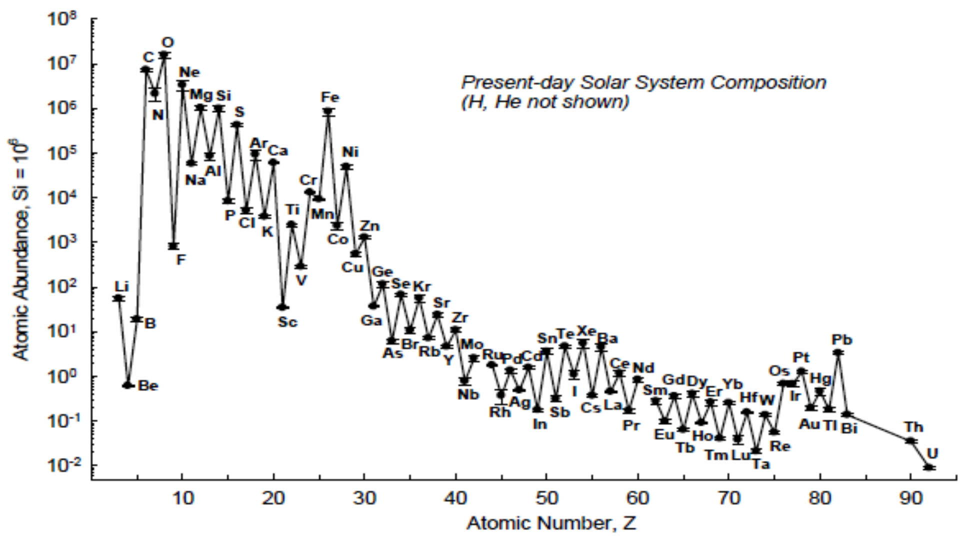

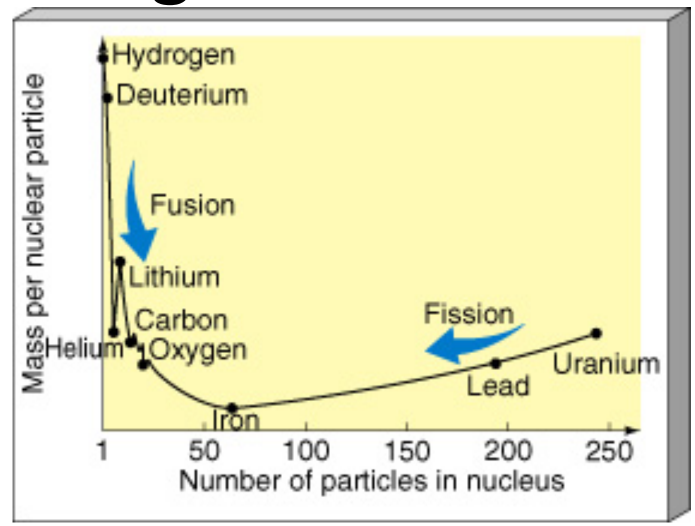

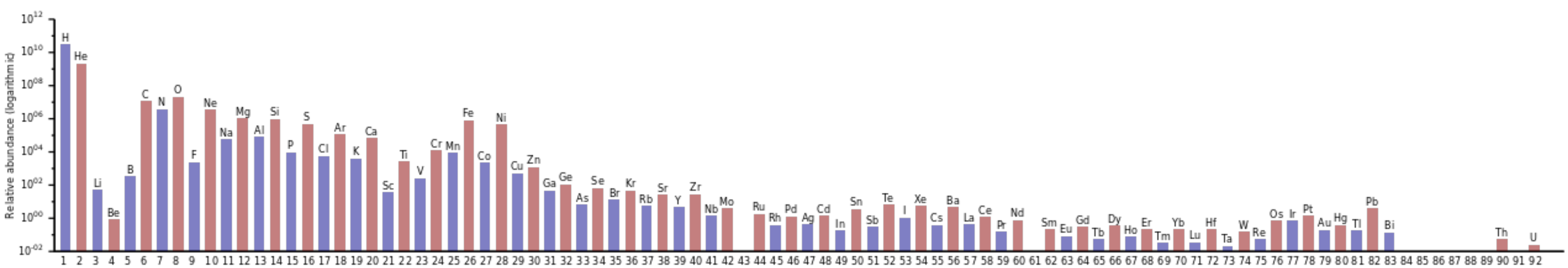

Interaction lengths of p,He,O and Fe Propagation important at high energy

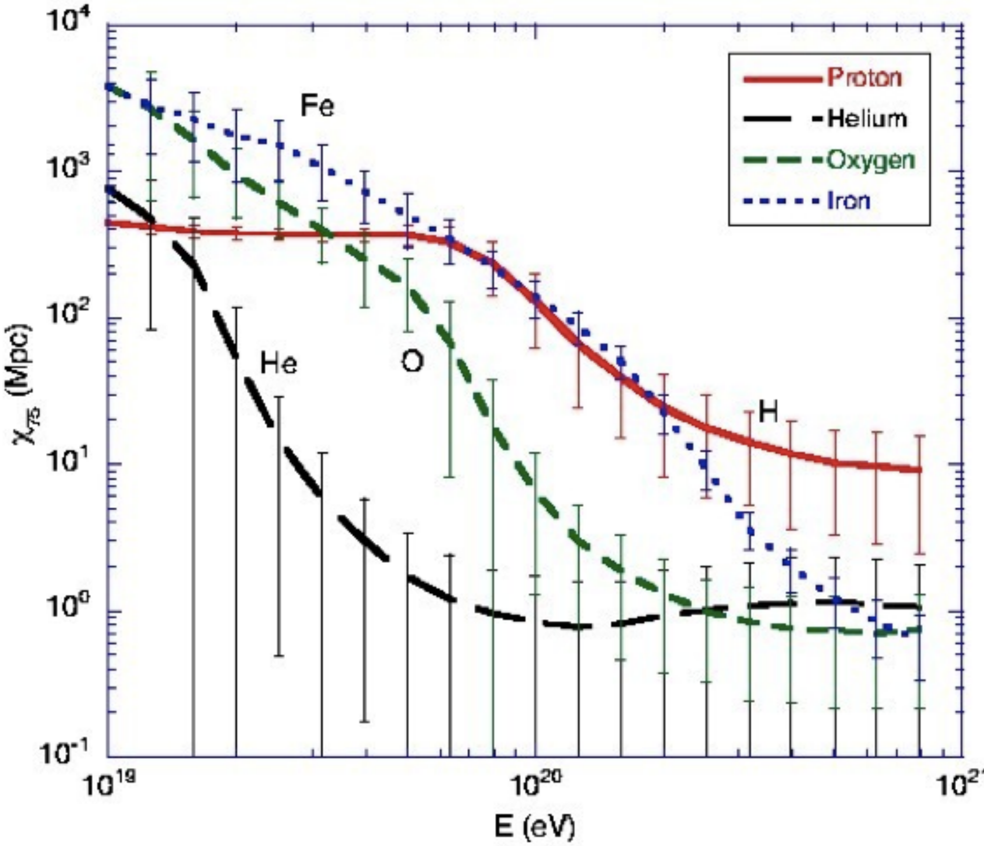

Fluorescence Analysis-Xmax distribution as measure of compostion

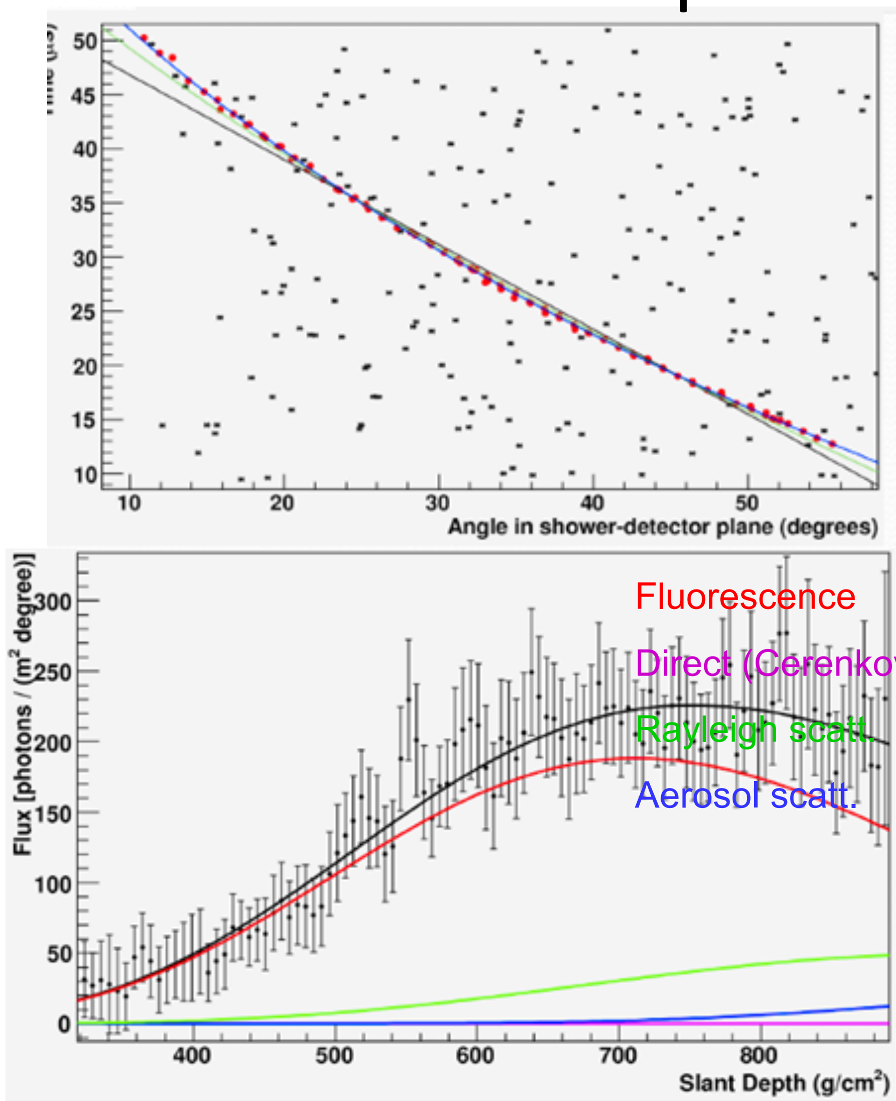

Black Rock Mesa

Xmax

Time fit

Profile fit

Composition from Xmax - HiRes and Auger

- Shower longitudinal development depends on primary particle type.
- FD observes shower development directly.
- Xmax is the most efficient parameter for determining primary particle type.

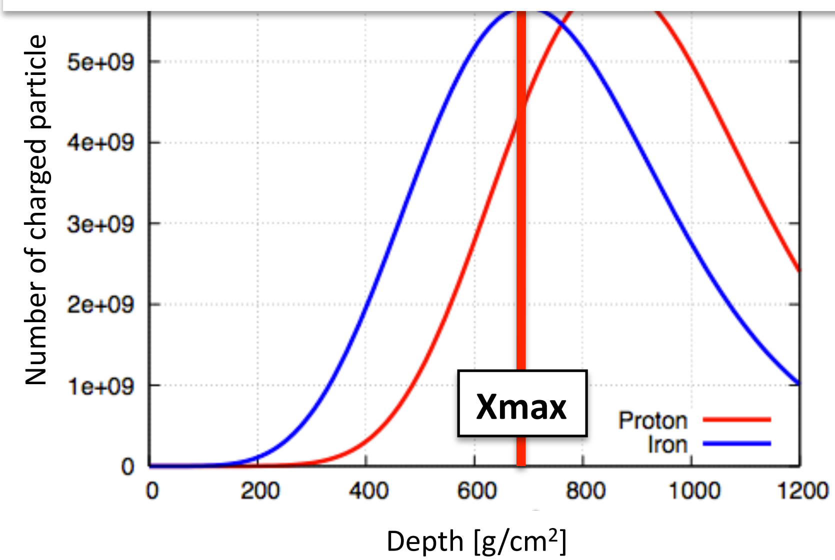

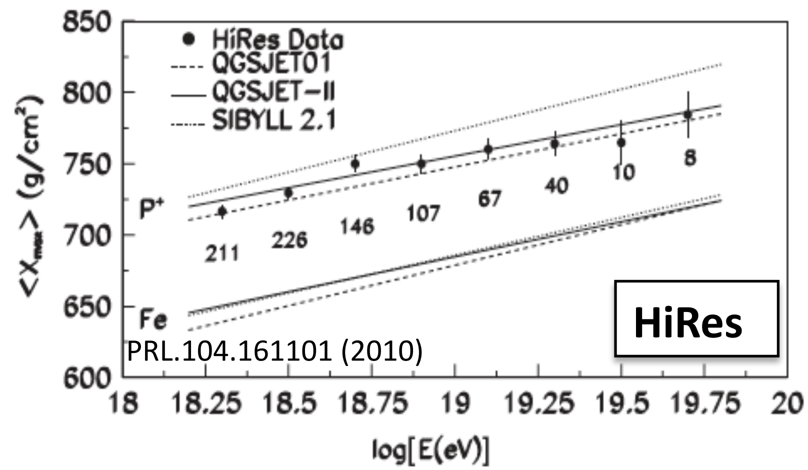

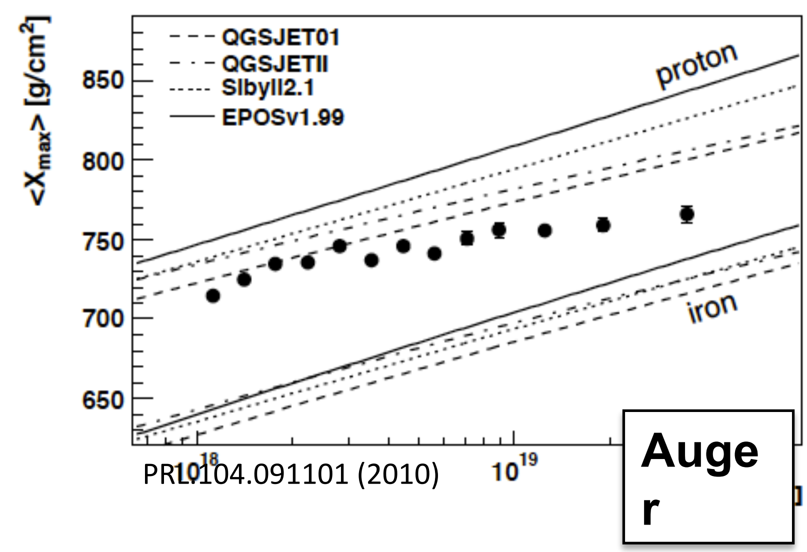

Difference above $10^{18.5}$ eV

PAO composition result

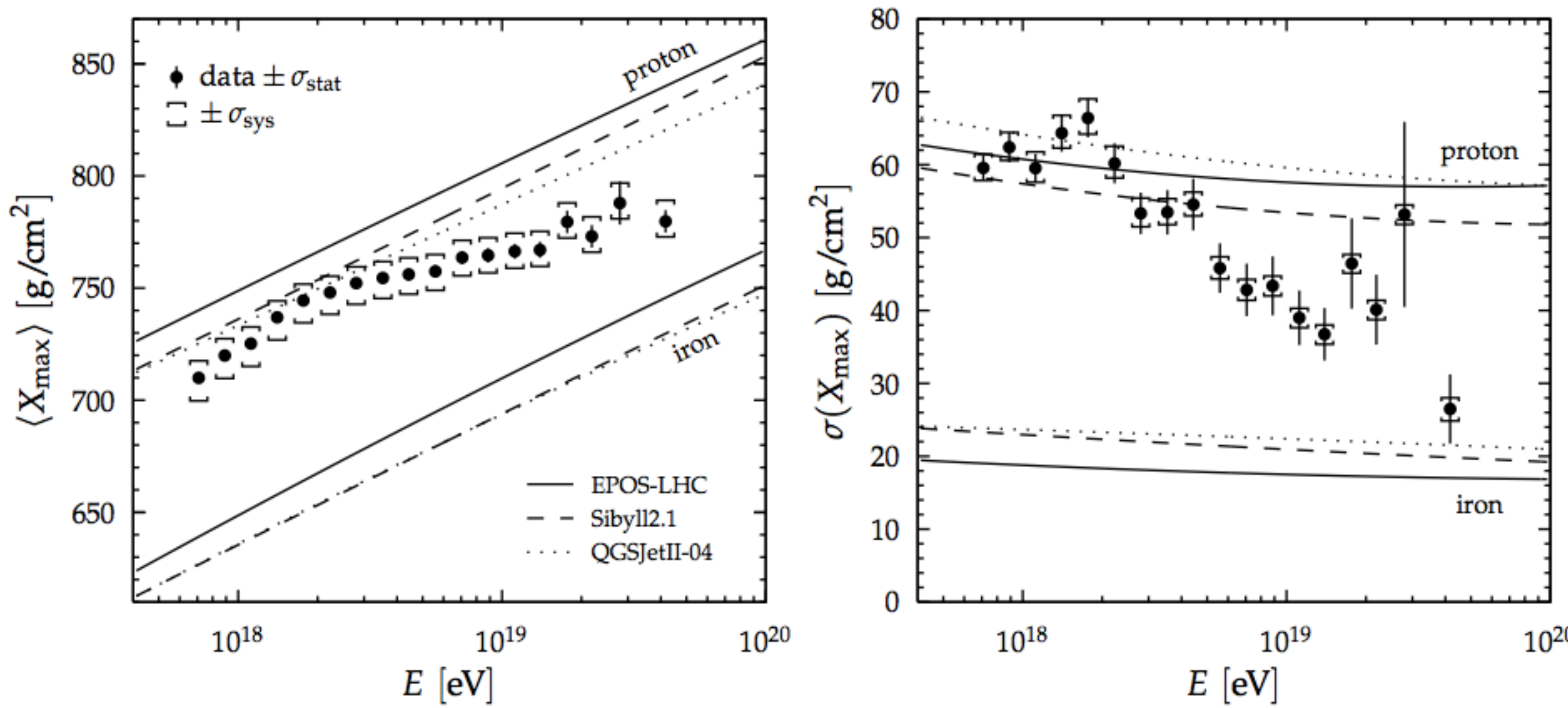

Figure 13: Energy evolution of the first two central moments of the $X_{\max}$ distribution compared to air-shower simulations for proton and iron primaries [80, 81, 95–98].

Detailed fits to MC predictions for different hadronic models

Auger Xmax Results

- Latest Auger Xmax paper.
- Performed fits to <Xmax> and RMS(Xmax) using 3 models.

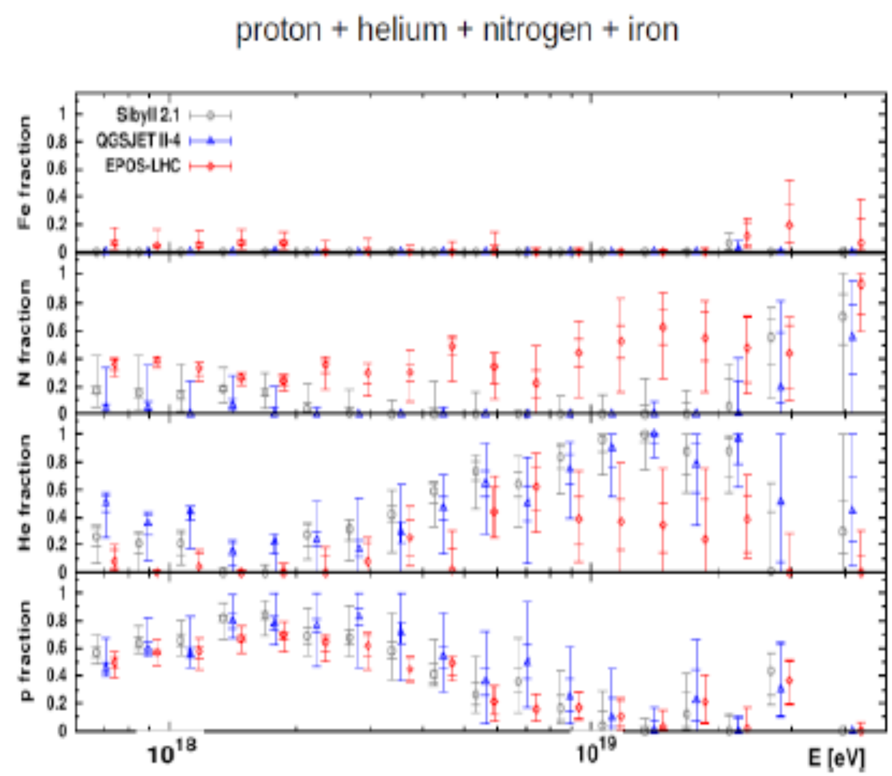

<u>3 comments:</u>

- No significant iron appears in any model.
- Test of models?

  Can't have Helium above $10^{19.1}$ eV:

Updated Auger data

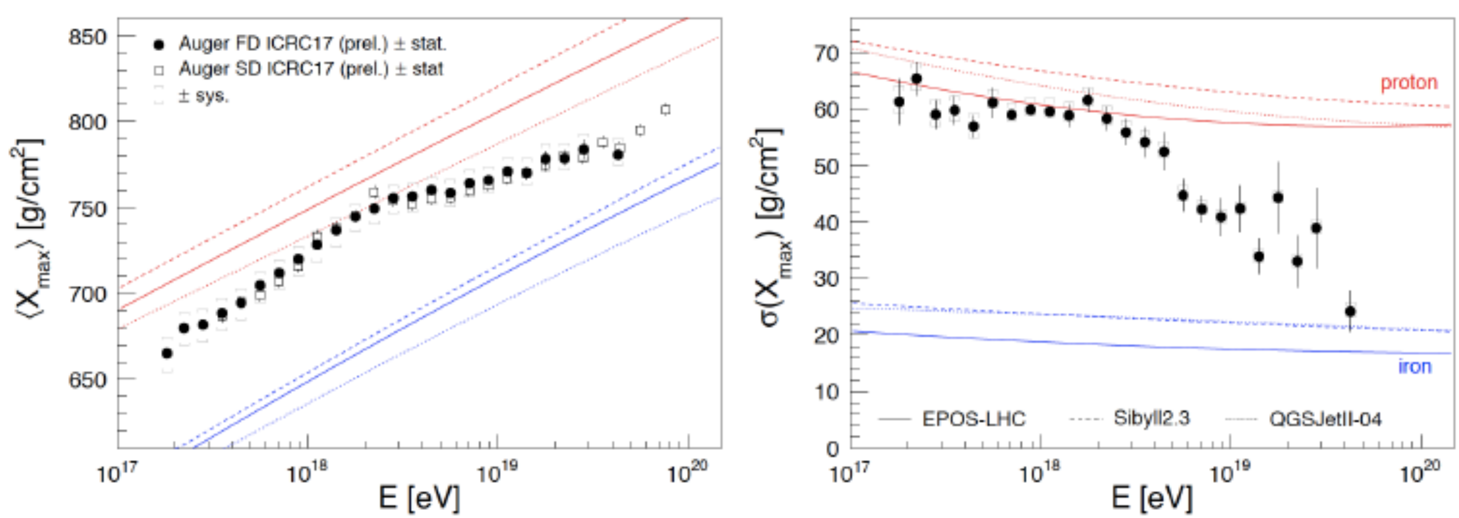

HiRes/MIA and HiRes elongation rate

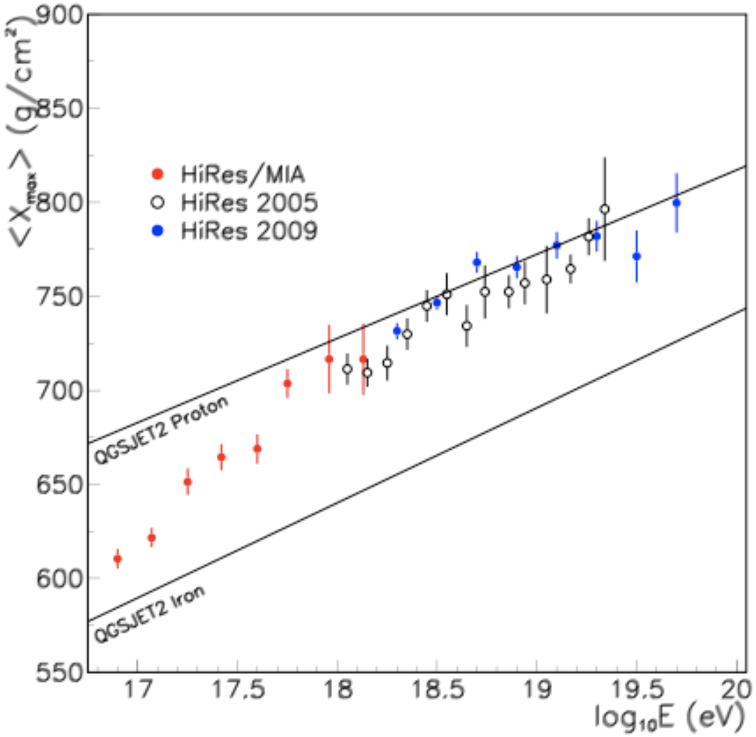

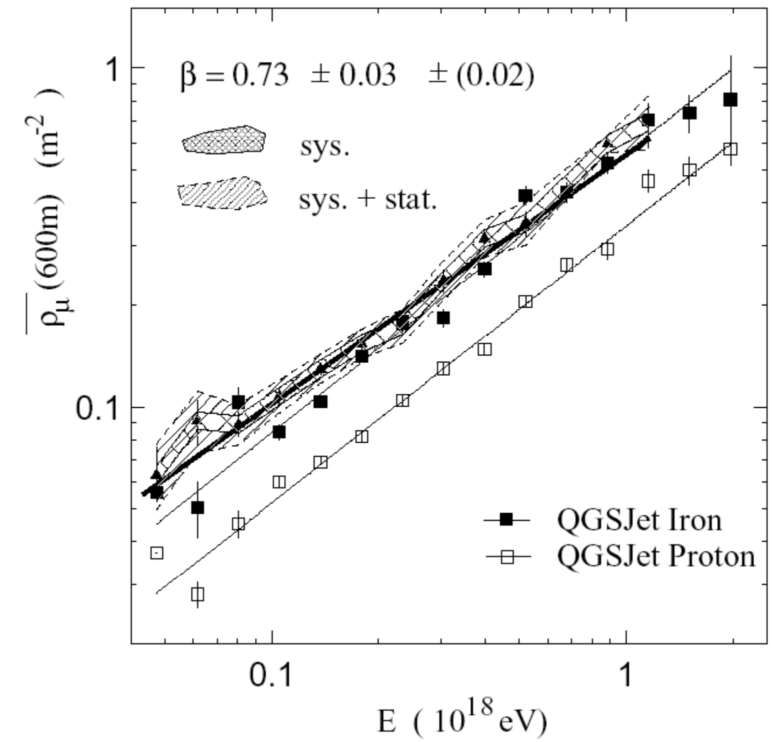

FIG. 2. Average Muon density at 600 m from the shower core. Same as FIG 1.

TA Elongation Rate and Sigma

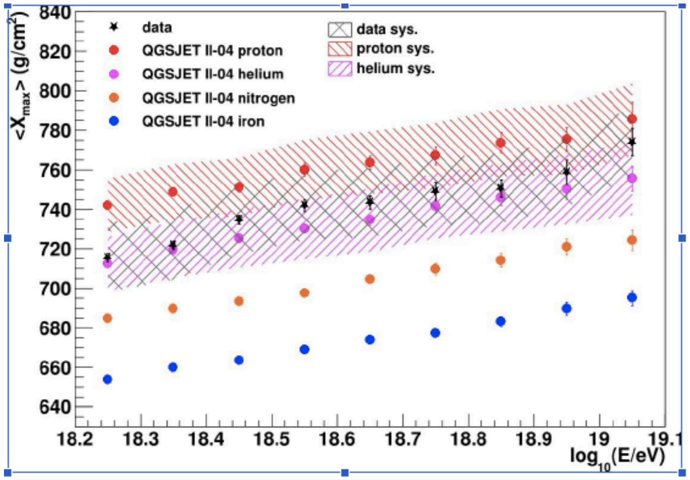

$\sigma(\langle X_{max}\rangle)$ of QGSJET II-04 p/He ≅ ± 3 g/cm^2 @ 10^{17} eV [lab] ($\sqrt{s}$ = 14 TeV)
$\sigma(\langle X_{max}\rangle)$ of QGSJET II-04 p/He ≅ ± 18 g/cm^2 @ $10^{19.5}$ eV [lab] ($\sqrt{s}$ = 250 TeV)
$\sigma(\langle X_{max}\rangle)$ of TA data = ±17.4 g/cm^2 ($10^{18.2} \le E < 10^{19.9}$ eV)

Conservative lower bounds on uncertainties from total cross-section, multiplicity, and elasticity dependence. (Abbasi & Thomson, arXiv:1605.05241 (2016))

x 5.62 in

10 year BR/LR hybrid $\langle X_{max}\rangle$

Hybrid events from TA BR/LR FD detectors in coincidence with SD array

3560 events, $18.2 \le \log_{10}(E/\text{eV}) < 19.1$

Elongation rate

- D_{10} = 66 ± 5 (g/cm²)/decade
- χ^2/dof = 10.66/7 (p = 0.154)

TA $\langle X_{max}\rangle$ appears consistent with $\langle X_{max}\rangle$ of predominantly light elements such as protons and helium using the QGSJET II-04 model.

$\langle X_{max}\rangle$ systematic uncertainty: ± 17 g/cm^2

Systematic uncertainty of QGSJET II-04 models are shown as well.

5

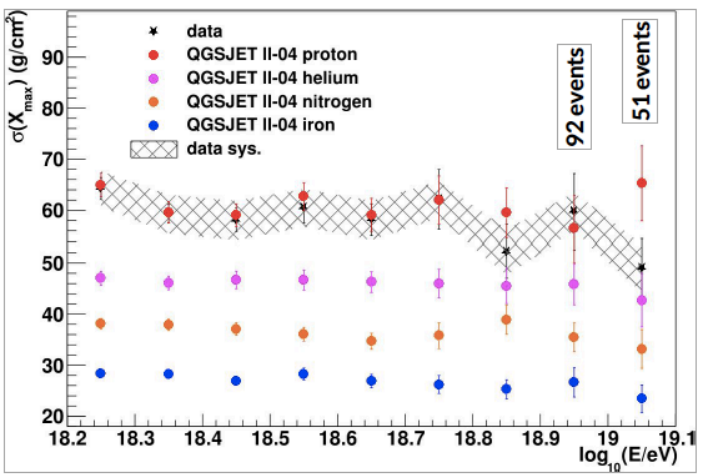

10 year BR/LR hybrid $\sigma(X_{max})$

Hybrid events from TA BR/LR FD detectors in coincidence with SD array

3560 events, $18.2 \le \log_{10}(E/\text{eV}) < 19.1$

Where statistics are large, $\sigma(X_{max})$ is consistent with QGSJET II-04 protons. Note that $\sigma(X_{max})$ is relatively model independent, unlike $\langle X_{max}\rangle$ which can vary by 20 g/cm² between models.

Above $10^{19.1}$ eV, statistics are depleted* due to the combination of acceptance (primarily loss of small zenith angle events) and falling spectrum. TA loses its ability to distinguish between even single element predictions of composition.

*96 events, $19.1 \le \log_{10}(E/\text{eV}) < 19.9$

Examaple of TA Xmax distribution shape analysis.

$18.4 \leq \log_{10}(E/\mathrm{eV}) < 18.5$

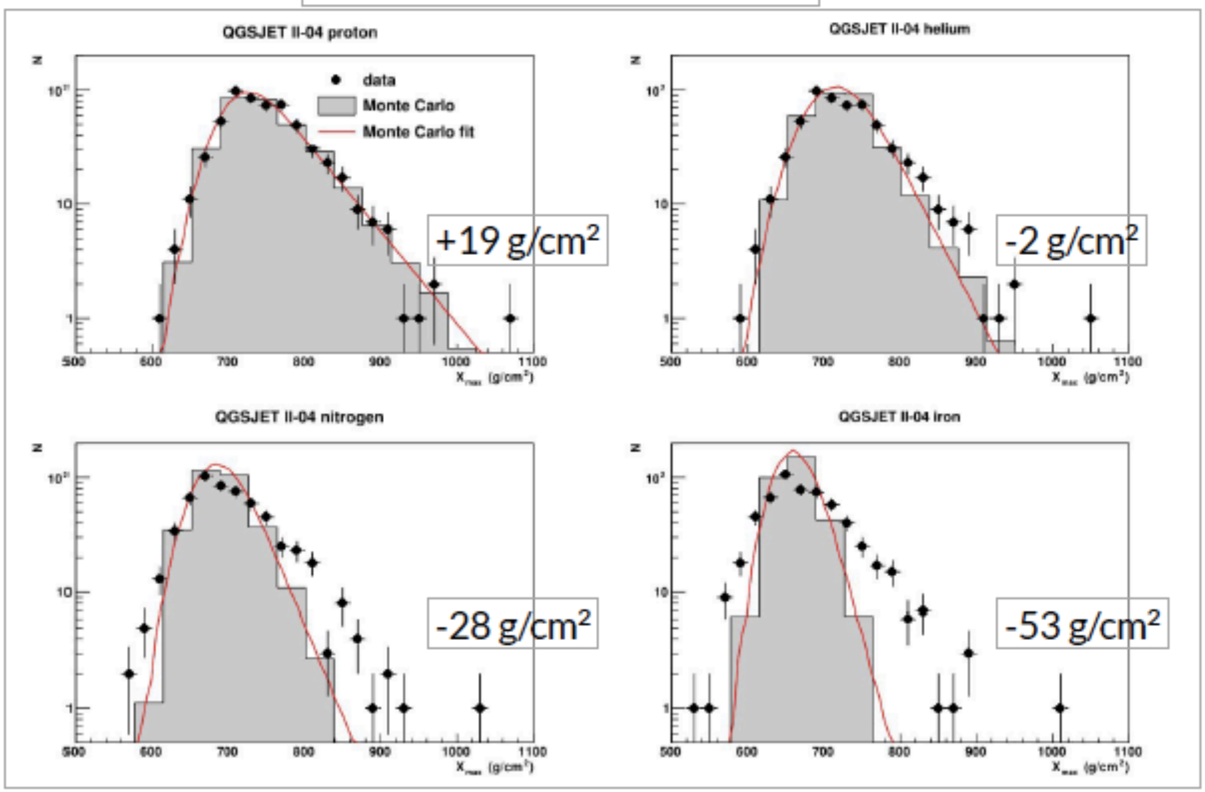

Depth of Ultra High Energy Cosmic Ray Induced Air Shower Maxima Measured by the Telescope Array Black Rock and Long Ridge Fluorescence Detectors and Surface Array In Hybrid Mode, Abbasi, et al., [Astrophys.J. 858 (2018) no.2, 76]

x 5.62 in

In [Astrophys.J. 858 (2018) no.2, 76] we tested TA hybrid X_{max} data against predictions of single element composition using the QGSJET II-04 model ([Phys.Rev. D83 (2011) 014018]).

To account for systematic uncertainties in X_{max} of our data and the model, we fit the data to reconstructed distributions of each element with a systematic shift in X_{max} and found the shift which maximized the likelihood of data and MC. This tests *the shapes* of the distributions.

For the shift which provides the maximum likelihood, calculate the probability of observing a ML at least as extreme as observed in the shifted data.

Best Single Element Fits to Xmax Shape with Energy (TA)

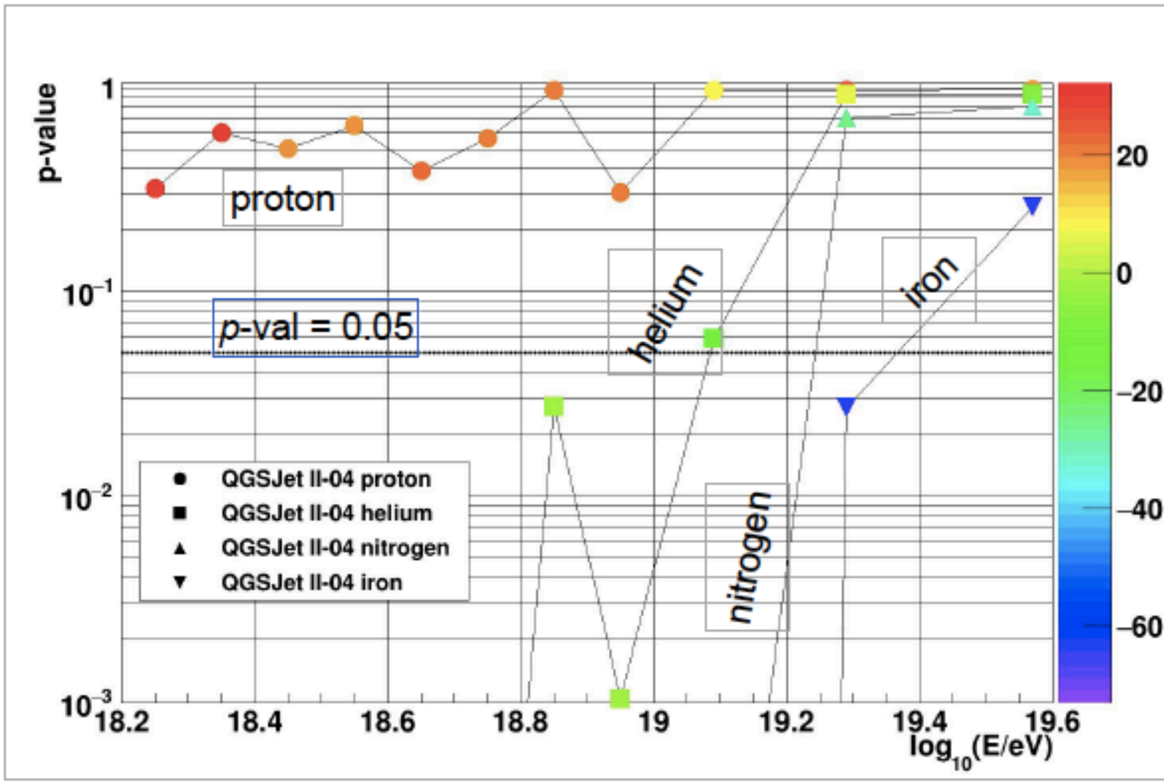

Depth of Ultra High Energy Cosmic Ray Induced Air Shower Maxima Measured by the Telescope Array Black Rock and Long Ridge Fluorescence Detectors and Surface Array in Hybrid Mode, Abbasi, et al., Astrophys.J. 858 (2018) no.2, 76

We demonstrated that at the 95% confidence level, TA data is compatible with a pure QGSJET II-04 proton composition for all energies $18.2 \le \log_{10}(E/\mathrm{eV}) < 19.9$, with X_{max} shifts ~+20 g/cm² applied to the data. TA $\langle X_{max} \rangle$ systematic uncertainty is ± 17 g/cm².

Below 10^{19} eV all other single elements tested were not compatible with TA data. For iron, shifts of 50 g/cm² were needed to make the data match the MC prediction.

Above 10^{19} eV TA data is compatible with all four pure QGSJET II-04 elements using this test because statistics are poor and the deep X_{max} tail is not seen.

Best 4-component (Auger type) fit to TA data

QGSJET II-04 proton, helium, nitrogen & iron mix

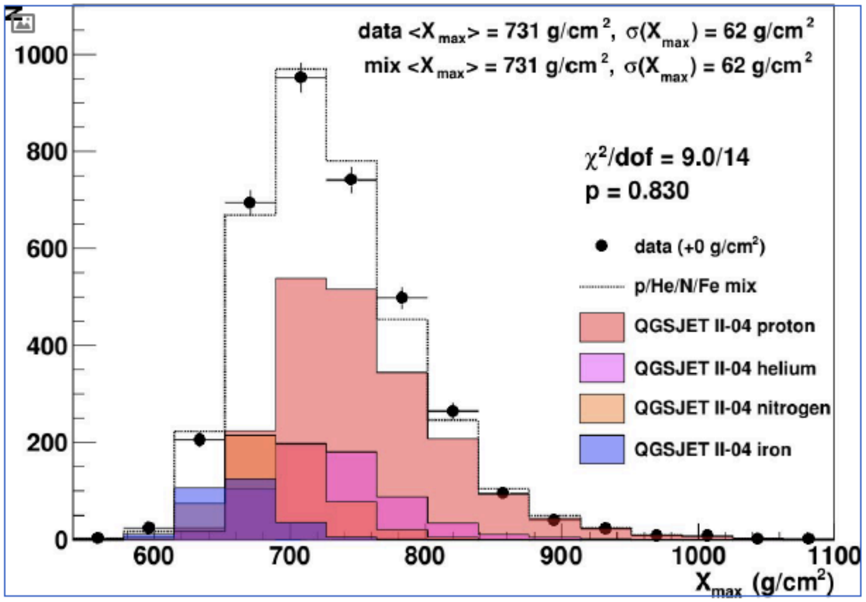

Fitting to a four component mix, proton, helium, nitrogen, and iron, results in a fit to TA hybrid data without a need to shift to find acceptable χ^2. Proton and helium combined (light elements) result in 75% of the mix between $18.2 \leq \log_{10}(E/eV) < 19.1$.

Fitting with elements with similar shapes and $<X_{max}>$, mainly proton and helium, is problematic due to correlations.

f_p = 57.3 ± 1.3%
f_{He} = 18.0 ± 0.7%
f_N = 16.8 ± 0.7%
f_{Fe} = 8.0 ± 0.5%

Light components (p + He): 75%

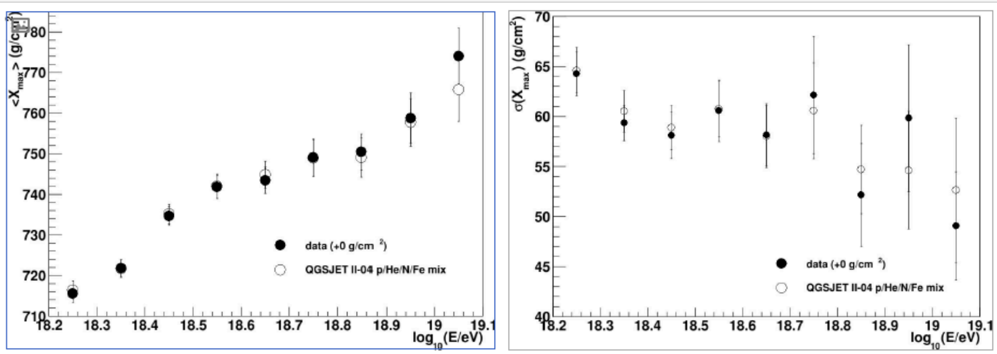

$<X_{max}>$ and $\sigma(X_{max})$ of QGSJET II-04 p/He/N/Fe mix with +0 g/cm^2 uniform shift applied to TA 10 year data

Why investigate a four component ad hoc model? We do not know what the composition is at UHE and we should not presuppose without further evidence that it is solely extra-galactic protons. New UHECR experiments such as TA may be able to answer this question via direct measurement, being mindful of our limitations due to resolution, acceptance, and statistics.

A similar, independent experiment has already made such a measurement using the same methods we have access to, and we may be able to verify or refute their claims.

Composition above 1 EeV

- Auger and TA data consistent within systematic errors from 1 to 10 EeV.
- Above 10 EeV, TA still has insufficient statistics for a detailed Xmax distribution analysis – need to confirm narrowing of distribution (Auger)
- From 1 to 10 EeV, TA is consistent with a light composition, not excluding a 4 component mix dominated by p/He.
- Results may change with more refined hadronic models, but difficult to explain Xmax tails without significant protons (below 10 EeV)

Evolution of composition

- Important: Auger and TA both agree on a proton dominated composition from 1 to~5 EeV → Any emergent differences at higher energies are unlikely to be due to systematics.
- Below 1 EeV, composition measurements rely on Cherenkov dominated events: systematic differences may still exist.

Example Xmax distributions (2)

- 16.9 < $\log_{10}(E_{cal})$ < 17.0
- All Plots: (Black) **Data**
- Top left: **Iron**
- Top right: **CNO**
- Bottom left: **Helium**
- Bottom right: **Proton**

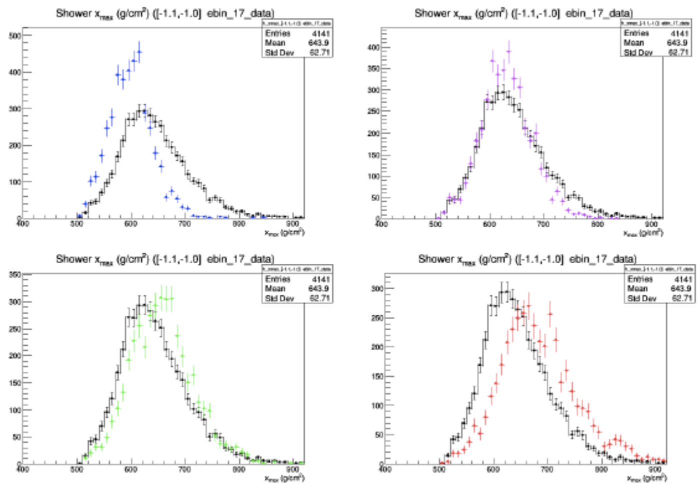

Example Xmax distributions (1)

- 15.7 < $\log_{10}(E_{cal})$ < 15.8
- All Plots: (Black) **Data**
- Top left: **Iron**
- Top right: **CNO**
- Bottom left: **Helium**
- Bottom right: **Proton**

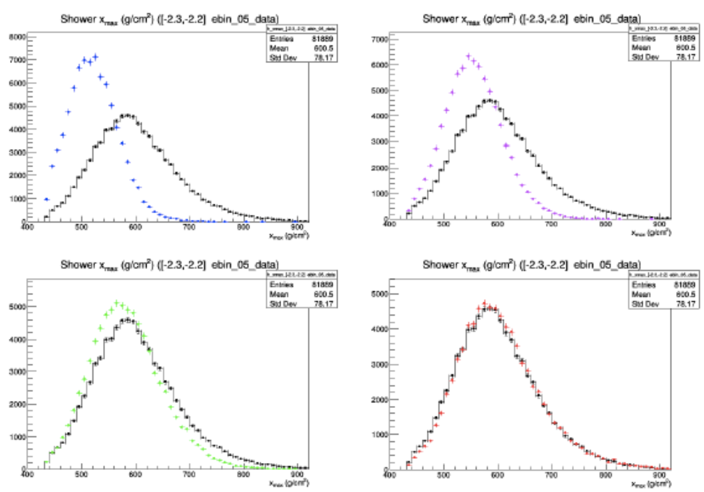

TALE Cherenkov data
Compared to expectatios
For p/He/CNO/Fe using
EPOS-LHC model

Mean Reconstructed X_{max} vs. Shower Energy

- (Top Figure): Reconstructed Data $\langle X_{max} \rangle$ vs. Shower total Energy starting at log(E [eV]) = 15.3
  - Also shown, results for 4 MC primaries.
- (Bottom Figure): A broken line fit to TALE data $\langle X_{max} \rangle$
  - Break point: 17.23 +/- 0.05
  - Slope before: 35.13 +/- 0.35
  - Slope after: 62.40 +/- 4.95
- (Bottom Figure): Also shown (red squares) are $\langle X_{max} \rangle$ reported by TA using hybrid events from Black Rock / Long Ridge FD's and the main SD array.

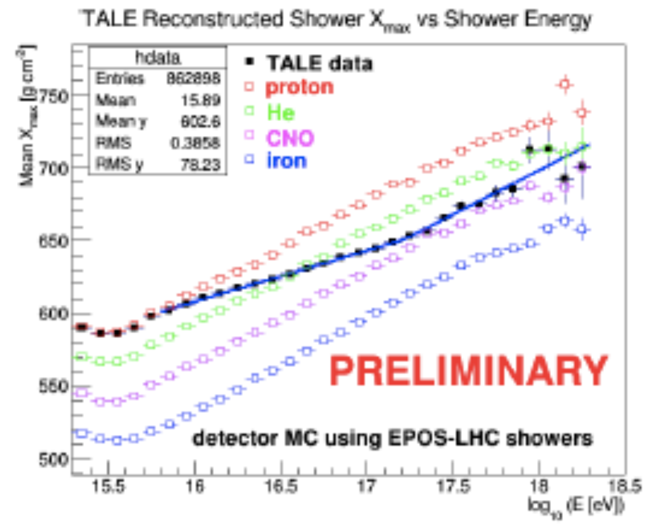

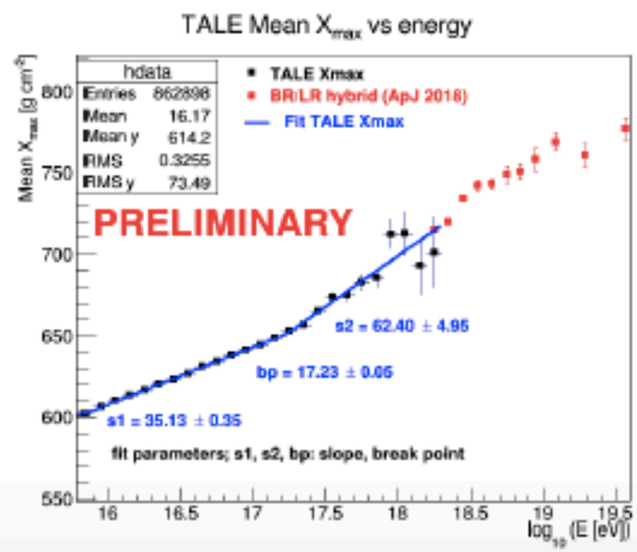

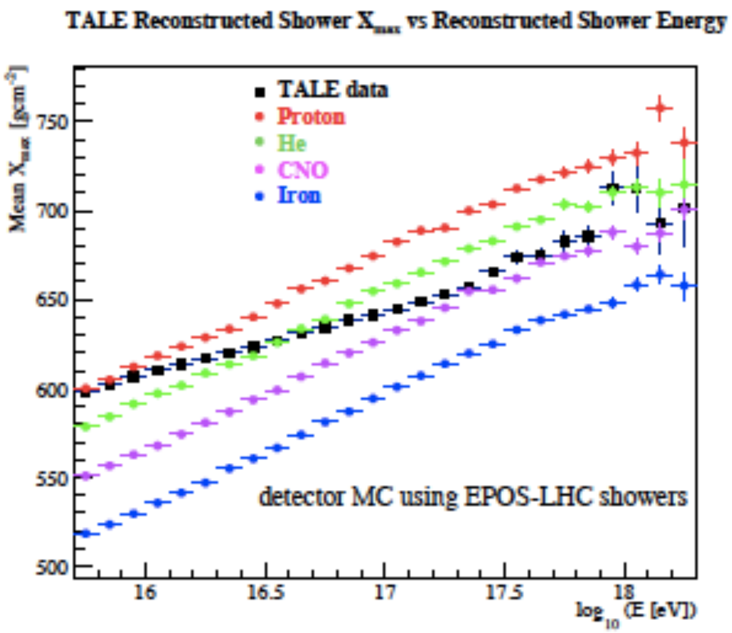

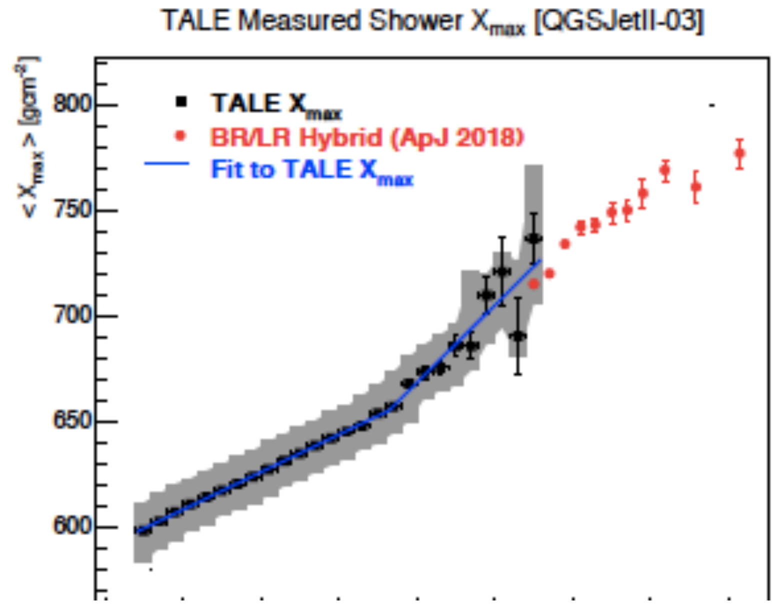

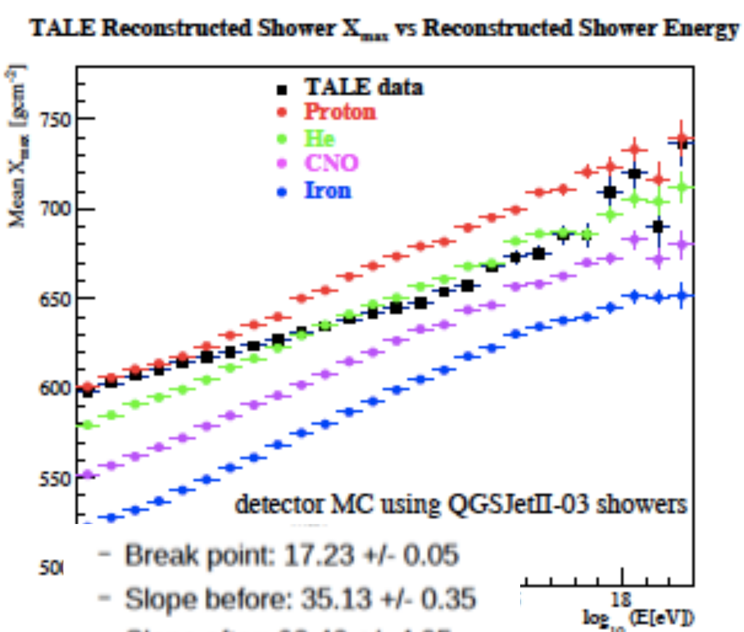

- Break point: 17.23 +/- 0.05
- Slope before: 35.13 +/- 0.35
- Slope after: 62.40 +/- 4.95

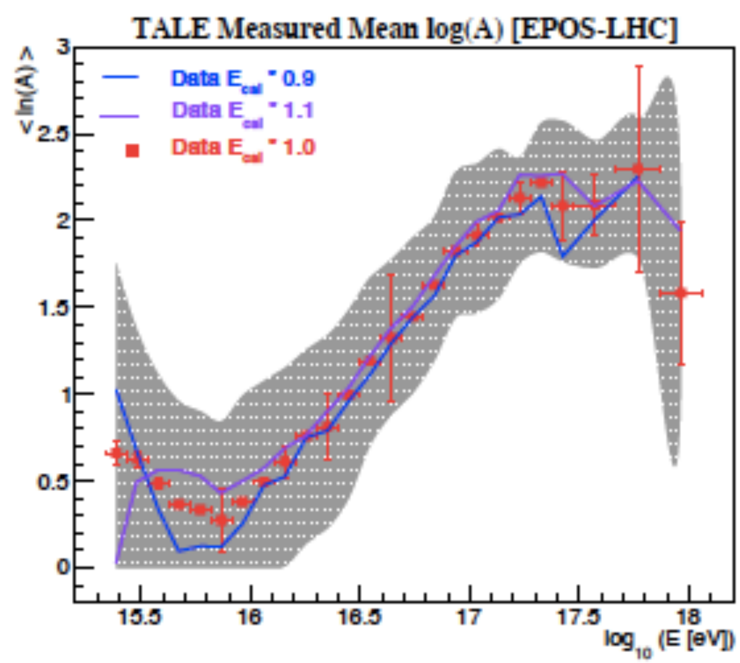

TALE data imply that the cosmic ray composition near the first knee is light, mainly protonic. At energies near 10^{17} eV the composition becomes mixed with heavier elements becoming important. The trend at energies near 10^{18} eV
Is to a lighter composition again.

TALE data smoothly matches the TA hybrid composition results around 10^{18} EV.

Hadronic Physics

- UHECR Air Shower development is sensitive to the p-Air inelastic cross-section.
- Using Glauber Model can relate to p-p total cross-section well beyond accelerator energies.
- Muon content of EAS is sensitive to primary particle composition.
- However, there is an excess of muons relative to any existing model. This seems true over a wide range of energies.

Slope of tail of Xmax distribution is sensitive to the proton-air cross section.

Most recent TA result using hybrid BR/LR data shows good agreement with previous measurements.

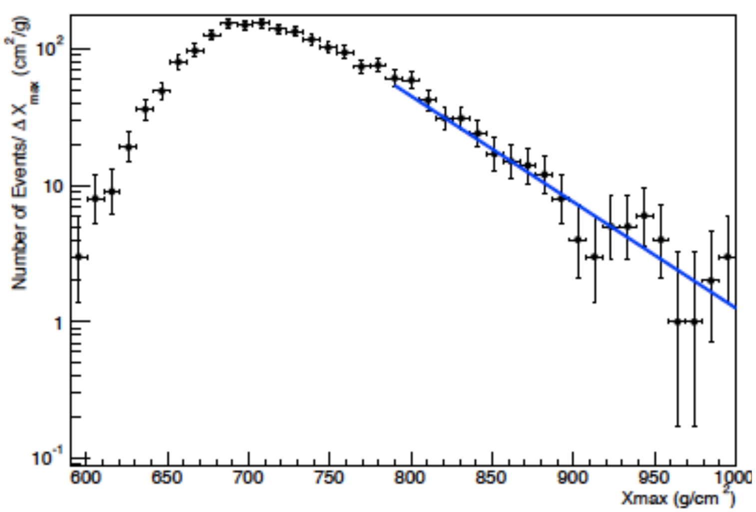

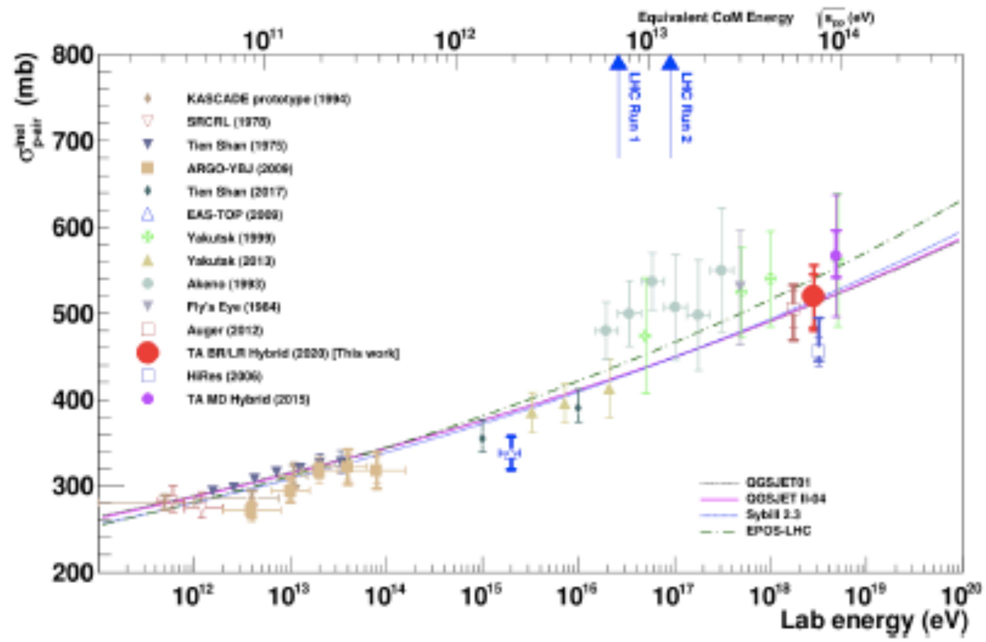

There have been persistent problems with hadronic simulation models underproducing muons in EAS. TA data confirms this problem –

Select events to enhance muon purity in SD signal using geometrical cuts

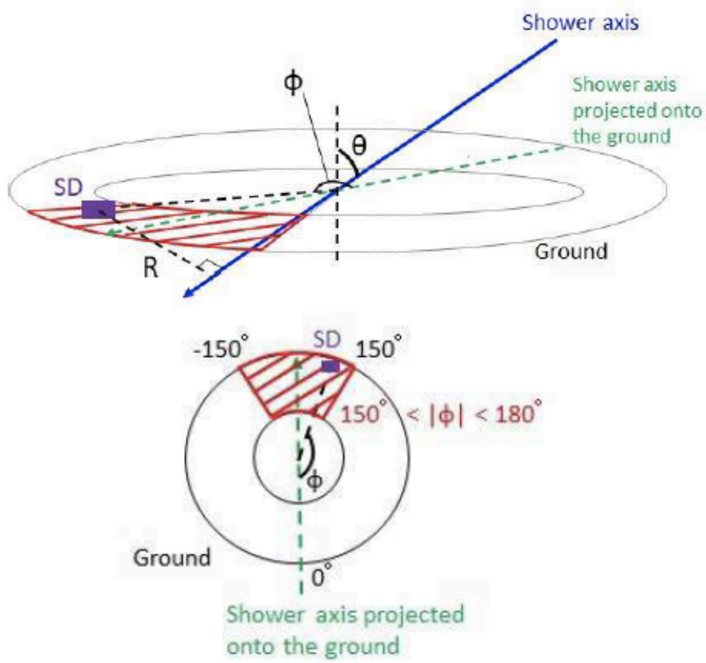

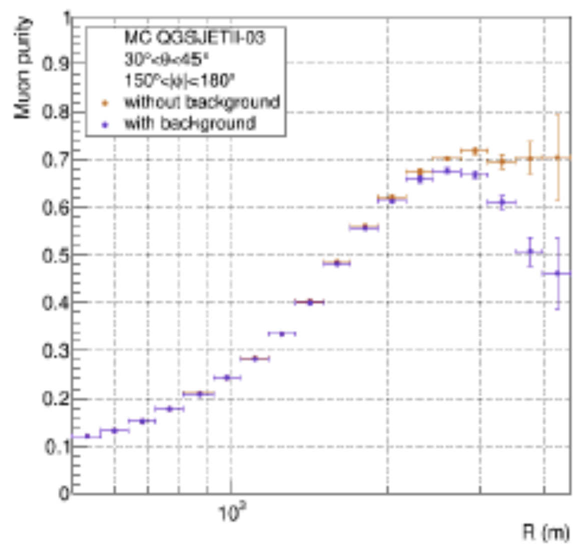

FIG. 4. (color online). (top) Lateral distributions of the air shower average signal of the MC with QGSJET II-03 for $30° < \theta < 45°, 150° < |\phi| < 180°$, $500 \text{ m} < R < 4500$ m. The red, green, blue, yellow, magenta and black represent gamma, electron, muon, other shower components, atmospheric muon background and the total of them, respectively. The vertical error bar shows the standard deviation. (bottom) Lateral distributions of the muon purity. The violet and orange show calculations with and without the atmospheric muon background, respectively.

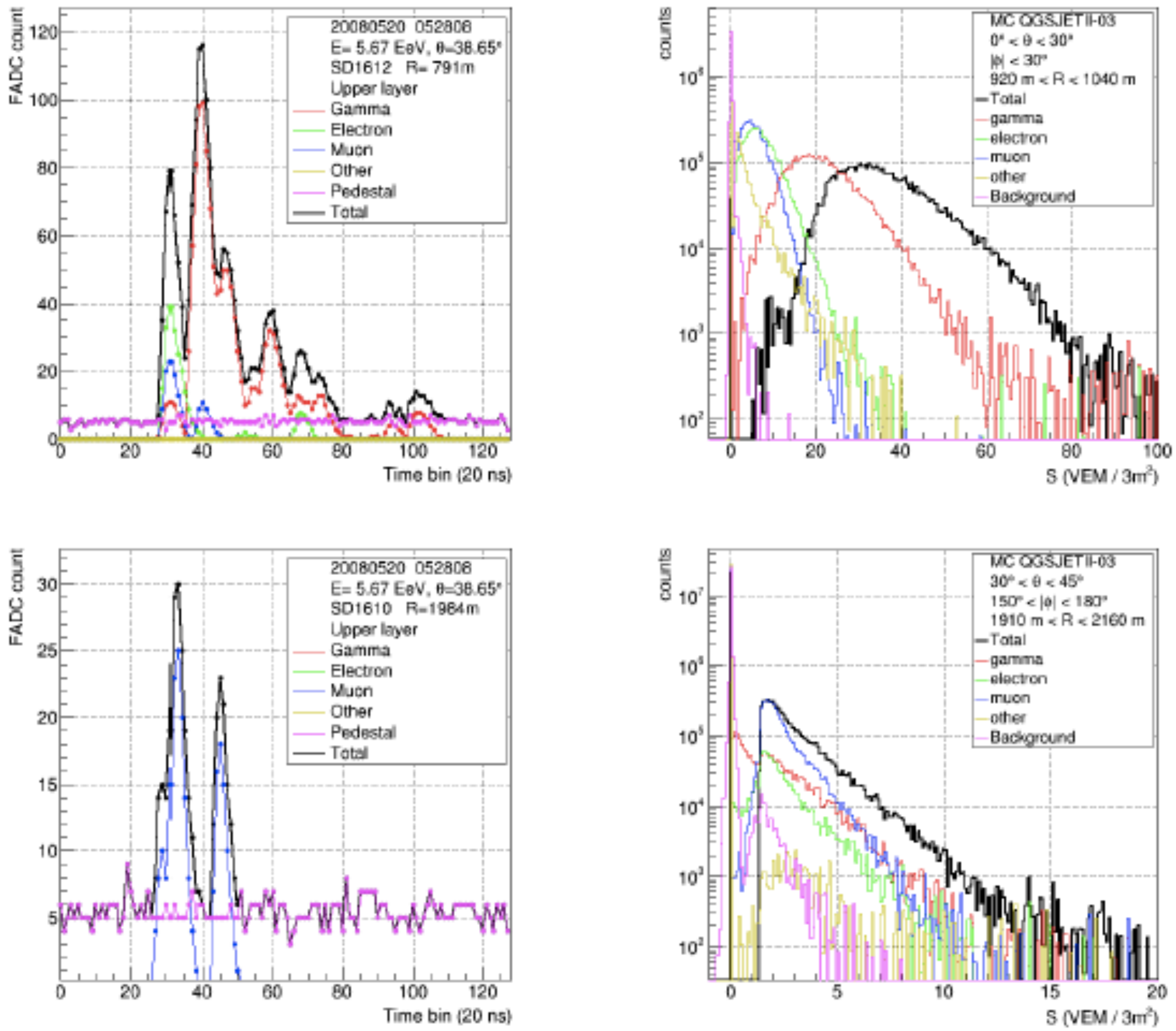

Typical SD signal development (L) and SD signal distribution (R)
Top: standard cuts, Bottom: muon enrichment cuts.

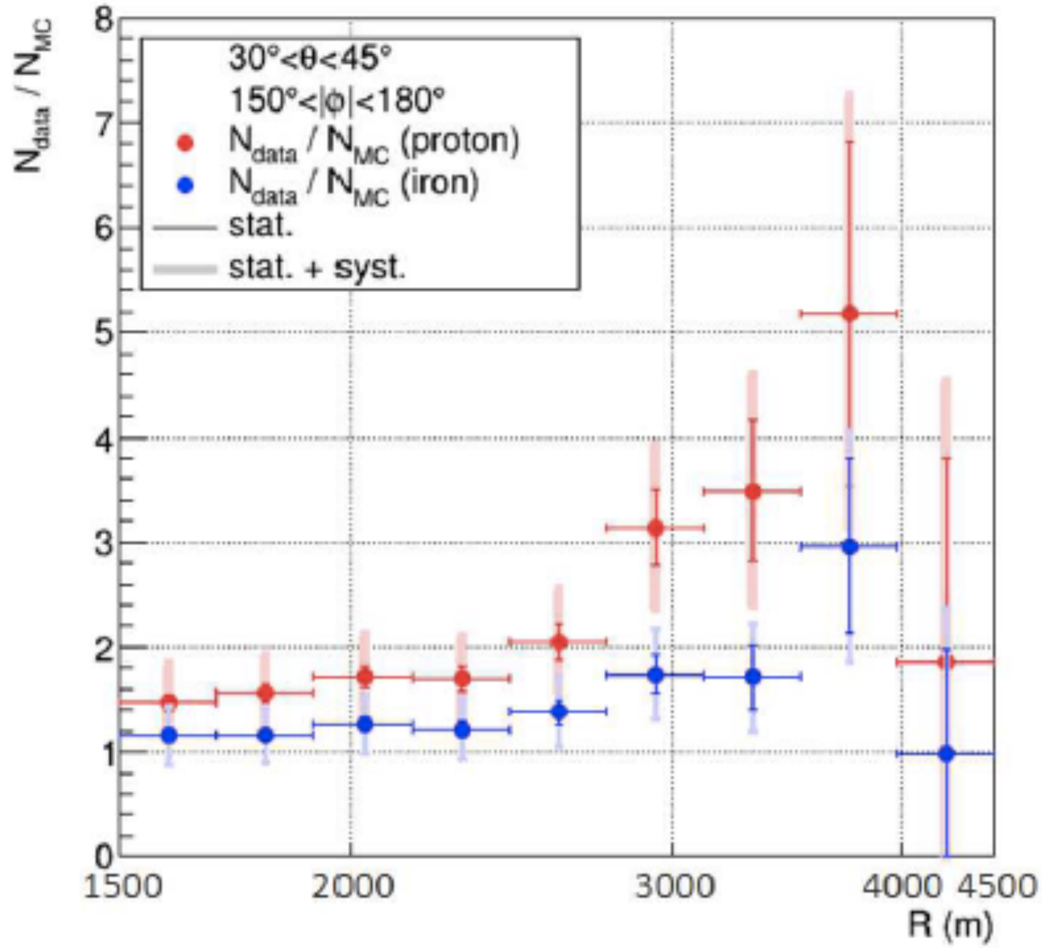

Muon pure data signals consistently higher than MC at large distances from the core
Reason for muon deficiency in models is not clear.

Local LSS as source of UHECR

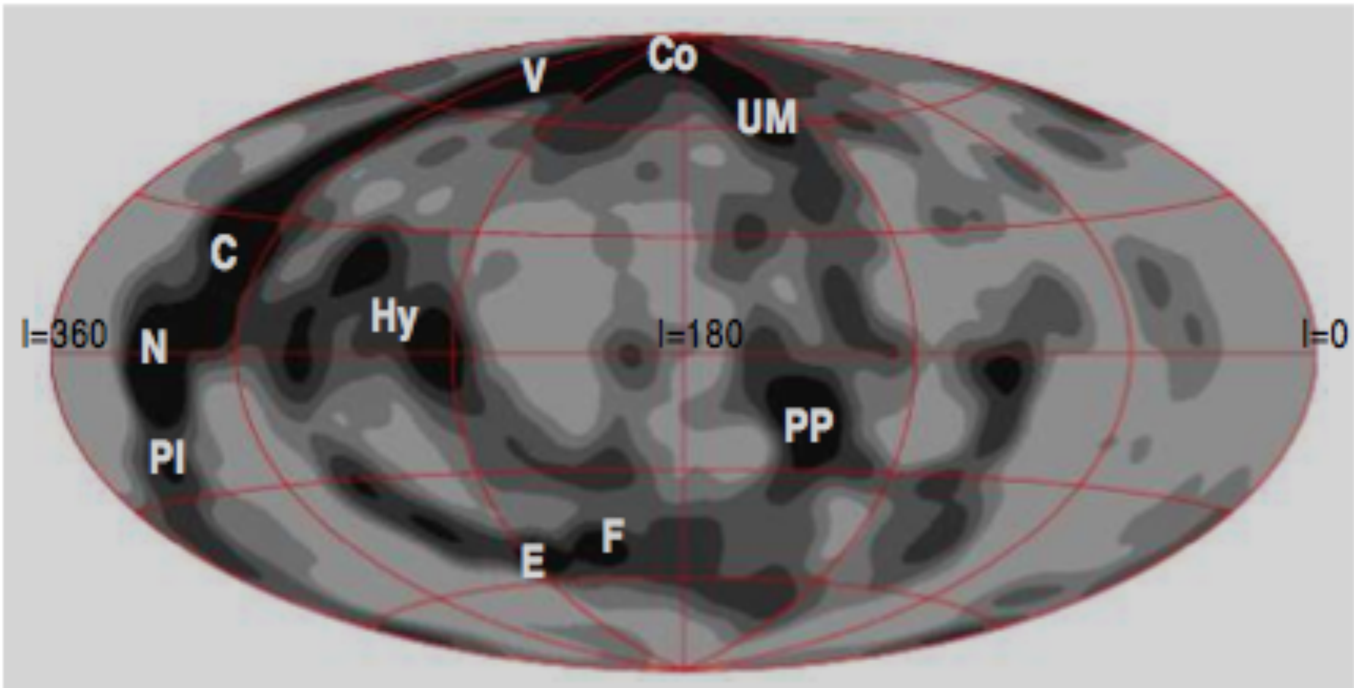

FIG. 5.— Sky map of expected flux at $E > 57$ EeV (Galactic coordinates). The smearing angle is 6°. Letters indicate the nearby structures as follows: **C**: Centaurus supercluster (60 Mpc); **Co**: Coma cluster (90 Mpc); **E**: Eridanus cluster (30 Mpc); **F**: Fornax cluster (20 Mpc); **Hy**: Hydra supercluster (50 Mpc); **N**: Norma supercluster (65 Mpc); **PI**: Pavo-Indus supercluster (70 Mpc); **PP**: Perseus-Pisces supercluster (70 Mpc); **UM**: Ursa Major (20 Mpc); **V**: Virgo cluster (20 Mpc).

Auger Dipole – UHECR Anisotropy

- Significance of dipole increased
- Strength increases with energy
- Transition of dipole phase around 1 EeV: hint for Galactic-to-extragalactic transition

FLUX MAP FOR E > 8 EeV

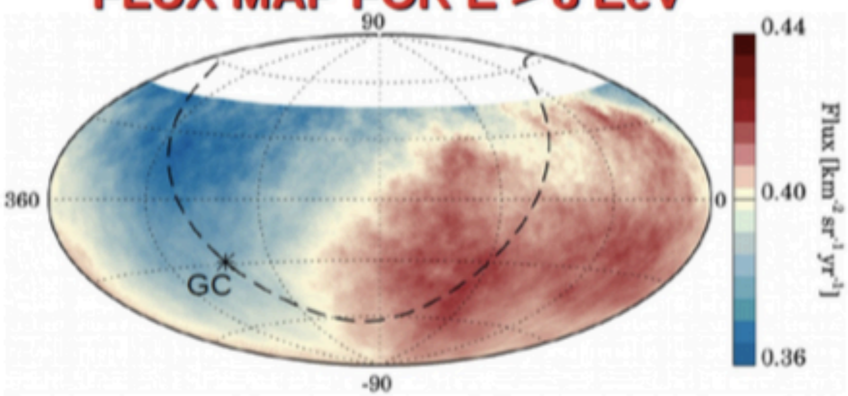

equatorial coordinates, smoothed on 45° radius windows

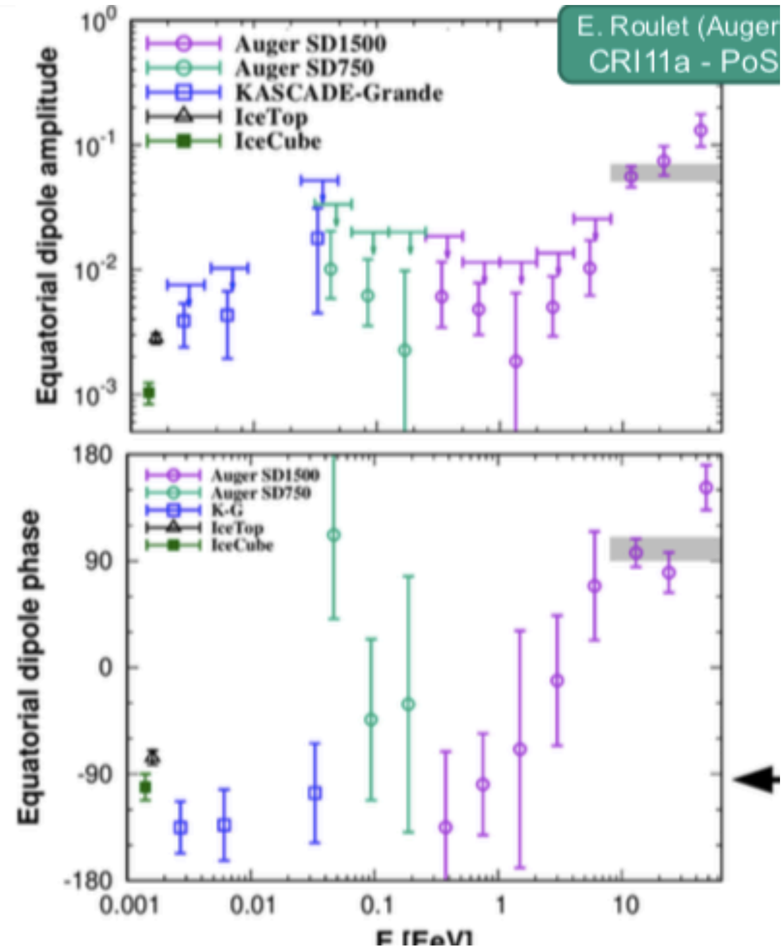

TA sees excess of events above 5.7×10^{19}

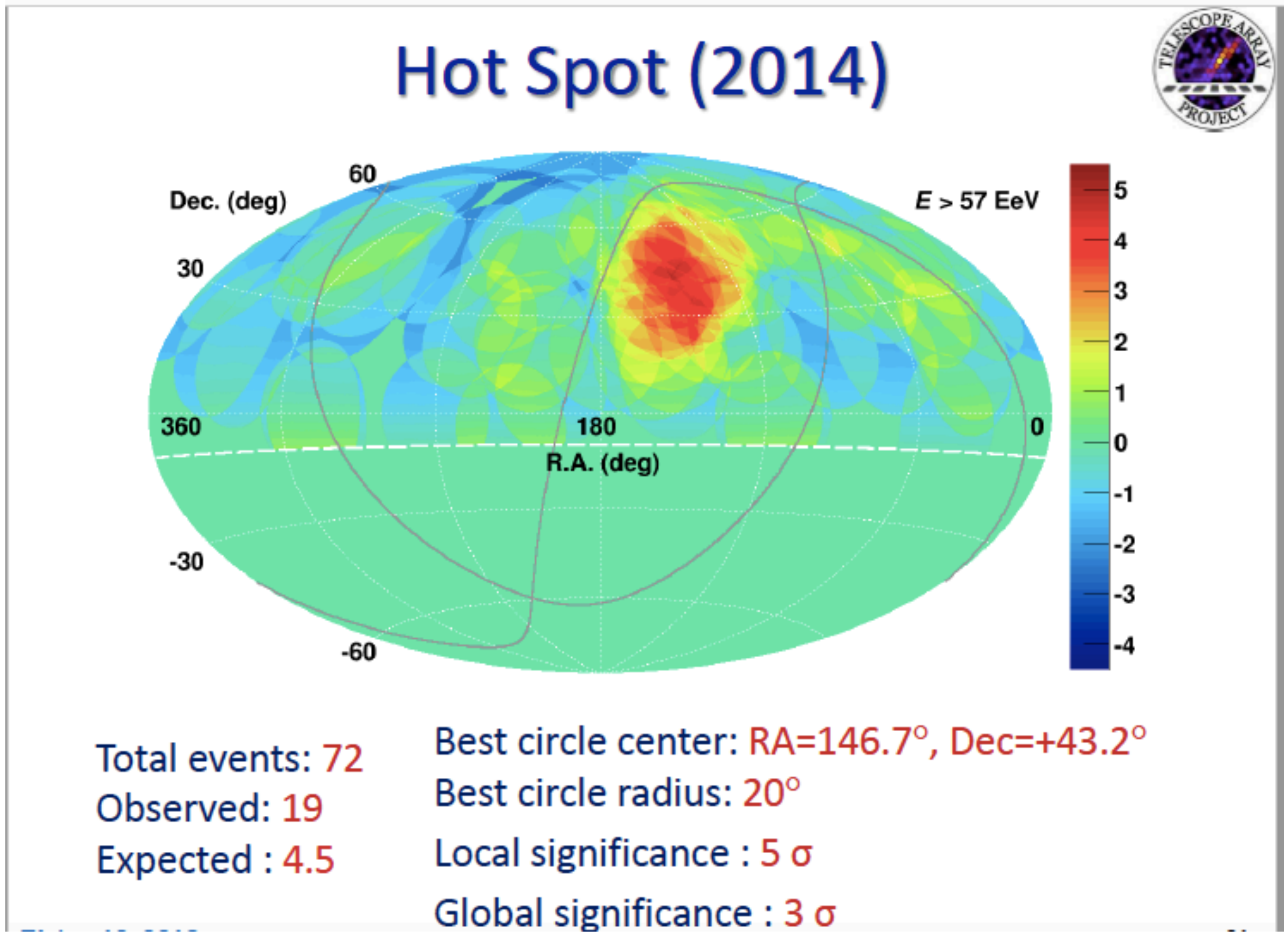

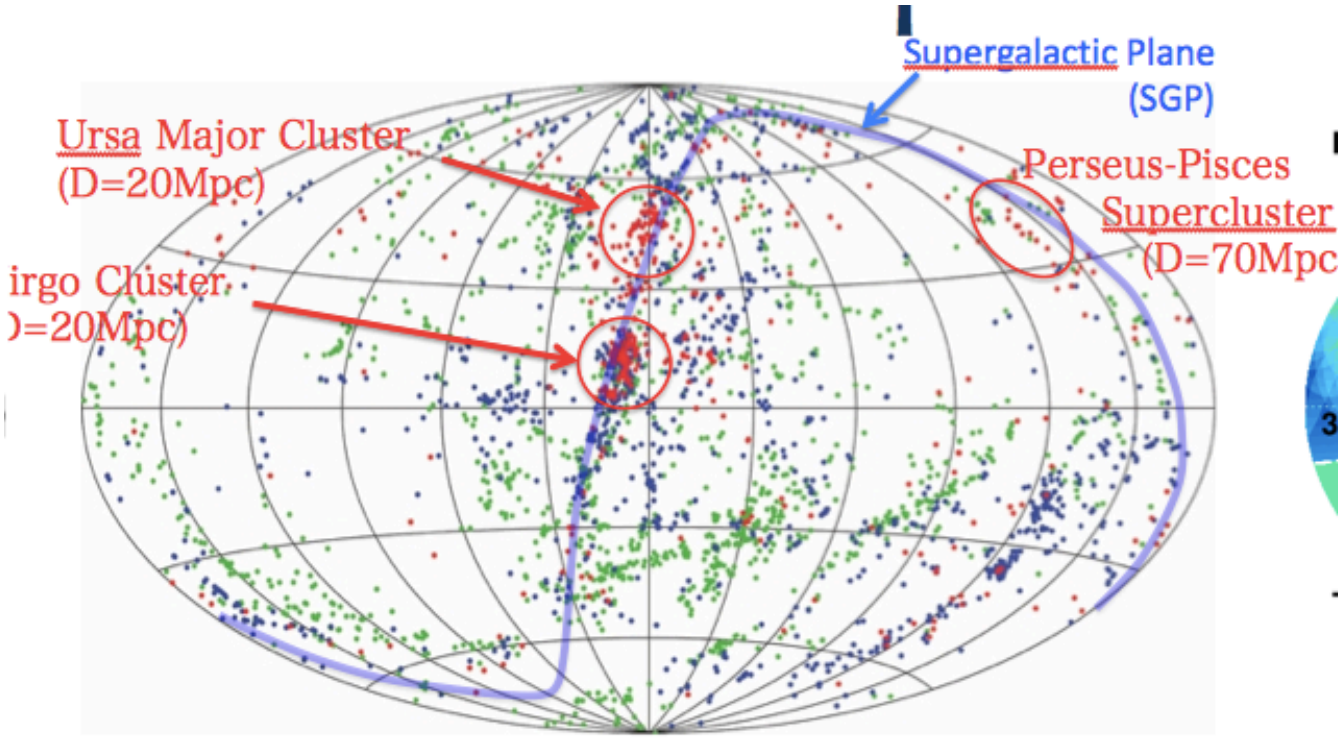

2MASS Galaxies D<50Mpc

Most recent update

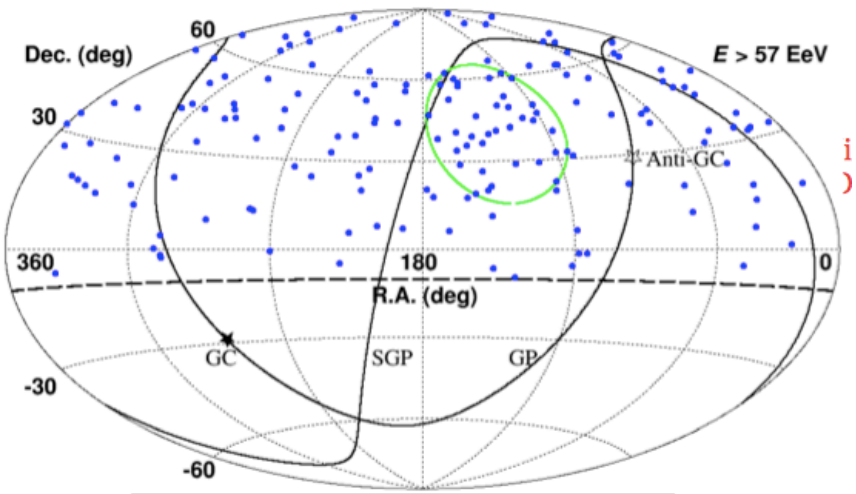

>57EeV Cosmic Rays

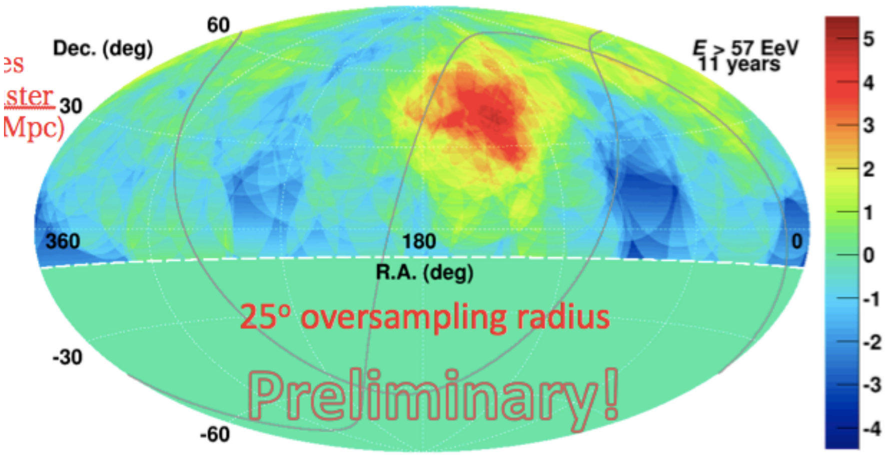

>57EeV Significance

Telescope Array - Hotspot

K. Kawata (TA Coll.)
PS3-173 - PoS 310

- number of events grows slightly slower than in the past, but still grows faster than background rate

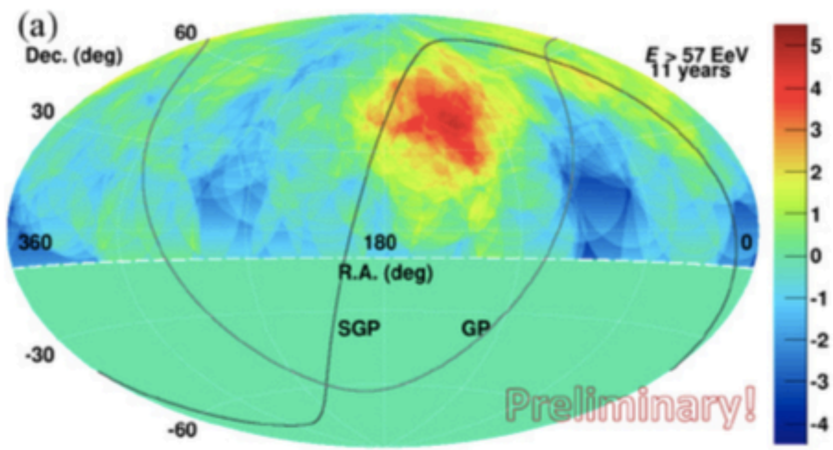

Hotspot from 11 years of TA SD data, from May 11, 2008 to May 11, 2019

E > 57 EeV, in total 168 events
38 events fall in Hotspot (α=144.3°, δ=40.3°, 25° radius, 22° from SGP), expected=14.2 events
local significance = 5.1 σ, chance probability → 2.9σ
25° over-sampling radius shows the highest local significance (scanned 15° to 35° with 5° step)

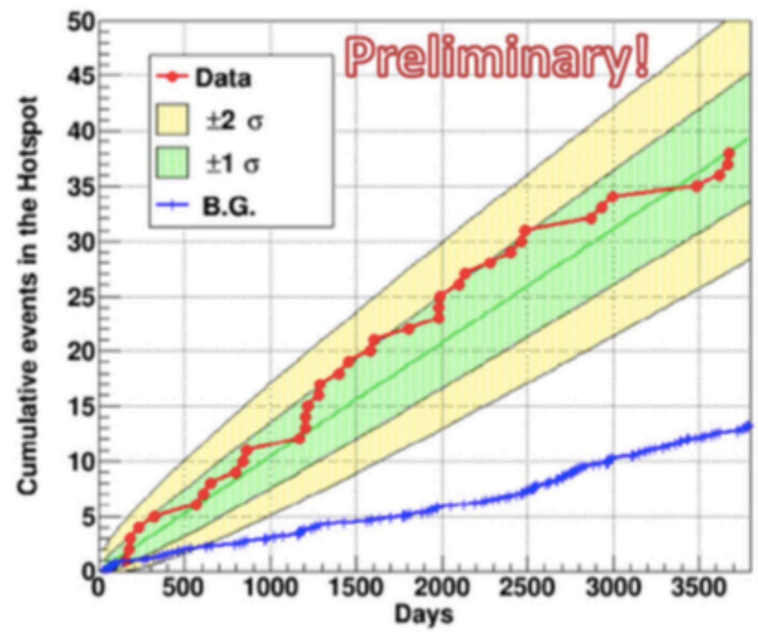

Global Anisotropy (Auger + TA)

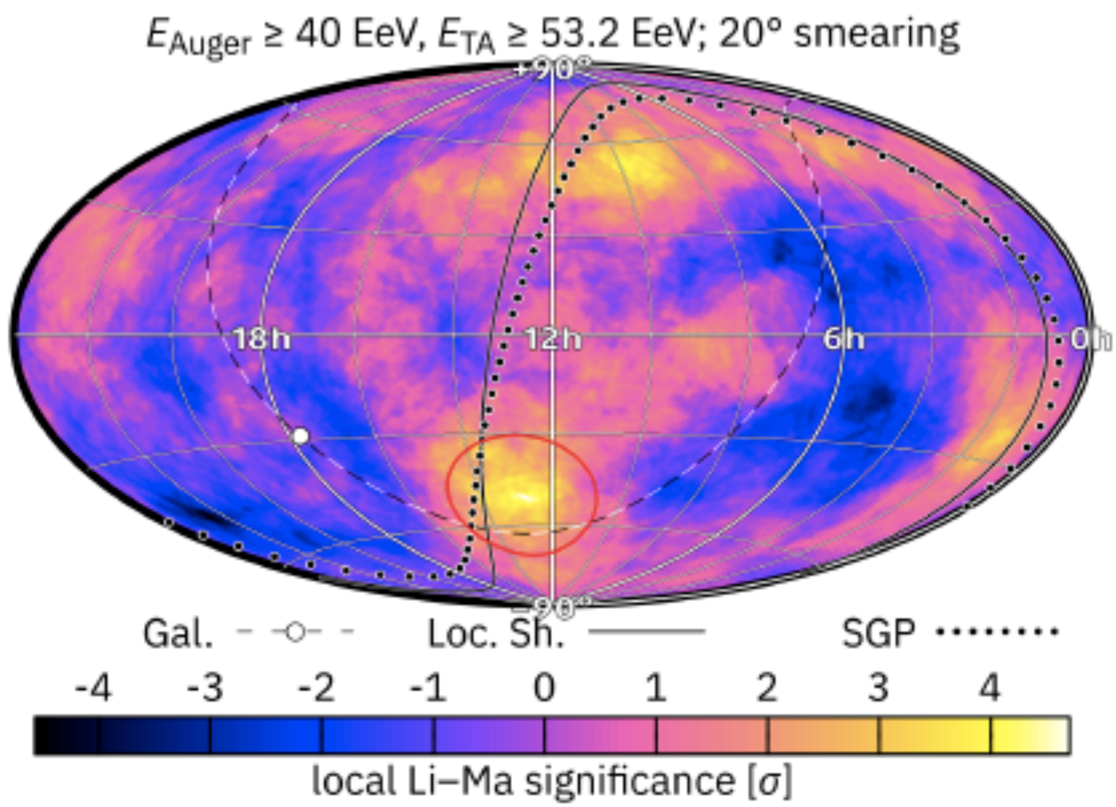

Energy spectrum anisotropy: Distributions of significance across sky

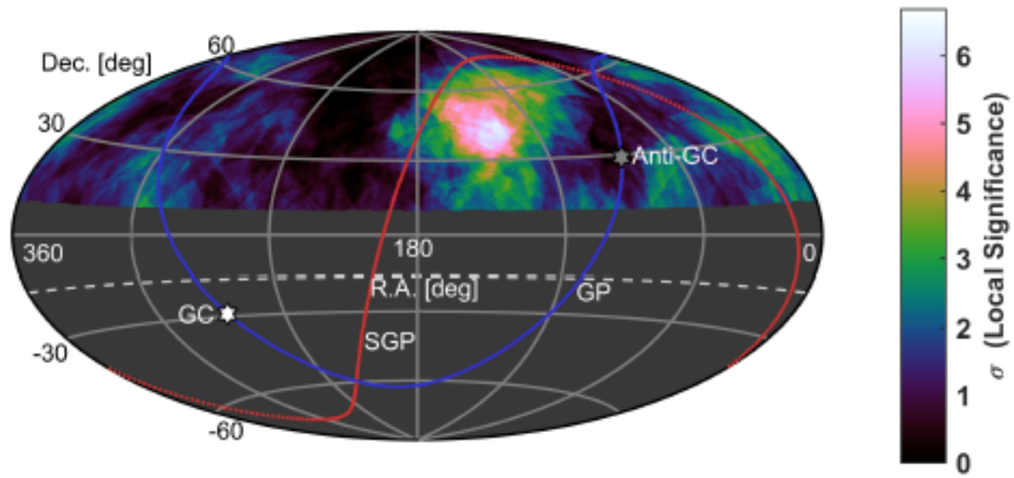

Figure 4: Hammer-Aitoff projection in equatorial coordinates. The local pre-trial energy spectrum anisotropy significance, for each spherical cap bin of radius 30° <bin> and $\log_{10}(E/eV) \geq 19.2$. The maximum significance is $6.7\sigma_{local}$ at 139° R.A., 45° Decl. This is 7° from the previously published "hotspot" location [2]. The dashed curve at Decl. = -16° defines the FoV. Solid curves indicate the galactic plane (GP) and supergalactic plane (SGP). White and grey hexagrams indicate the Galactic center (GC) and anti-galactic center (Anti-GC).

Spectrum at point of most significant deviation

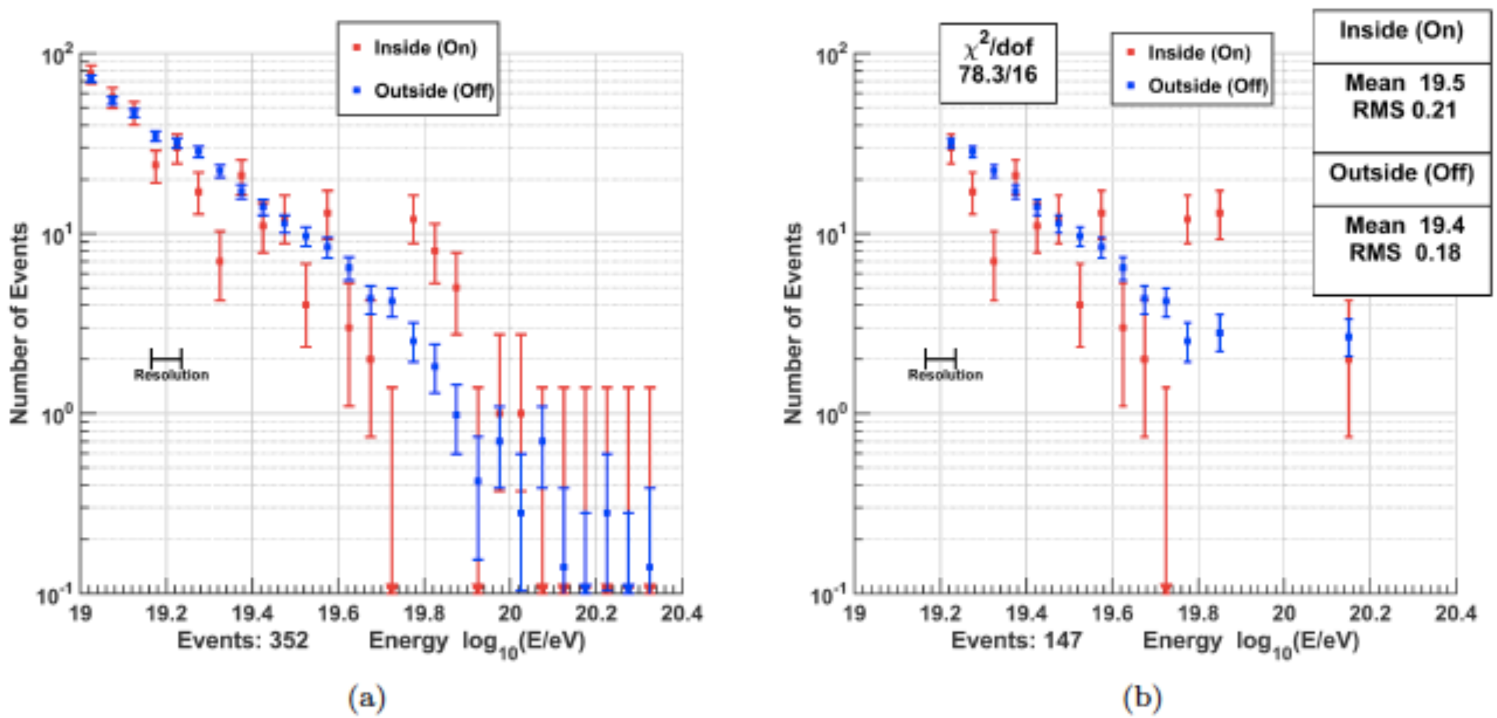

Hot/cold spot begs the question of magnetic field effect

- Search for anisotropies in energy –angle correlations.
- Since possible sources near hot/cold spot located on or near supergalactic plane, use SG coordinates.
- Wedge correlation analysis suggested by Auger paper using rectangular boxes.

Wedge origin placed on equal angle 2 deg grid. Scan over wedge length, width pointing direction and threshold energy. Calculate ranked correlation of event energy and angle from origin.

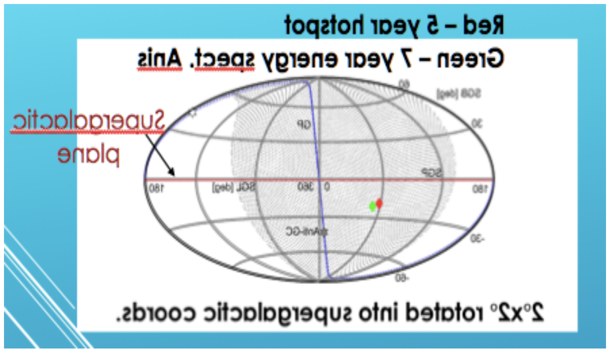

- All values are ranked 1 to n. Kendall's correlation is used.

$$\tau = \frac{(\text{number of concordant pairs}) - (\text{number of discordant pairs})}{\frac{1}{2}n(n-1)}.$$

- *Any monotonic function* F(x,y) results in τ= 1. Removes model assumption

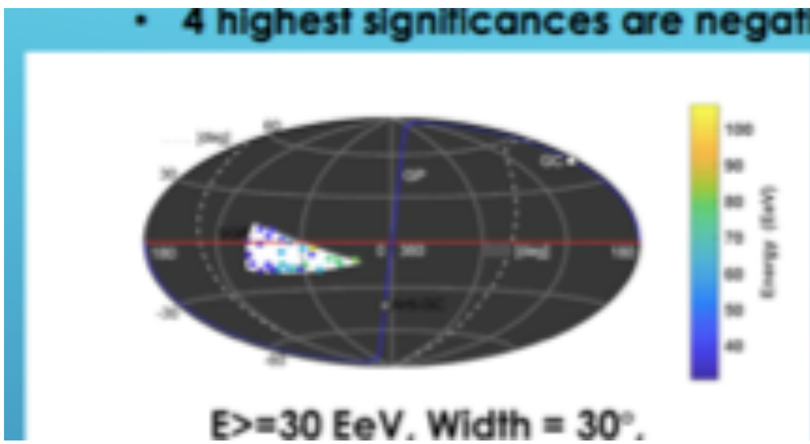

E>=30 EeV. Width = 30°.

- Energy Threshold
  - 10, 15, 20…100 EeV
- Wedge width (spherical cap sections)
  - 10°, 20°, 30°…90° (steps of 5° on each side of the pointing direction)
- Maximum Distance
  - 15°, 20°, 25°…90°
- Pointing Direction (0° “up” counterclockwise)
  - 0°, 5°, 10°…355°

UNIFORM FIELD ESTIMATE

- Fit 1/E to straight line

$$\delta \approx 0.5^{\circ} Z \frac{S}{kpc}\frac{B}{\mu G}\frac{10^{20} eV}{E}$$

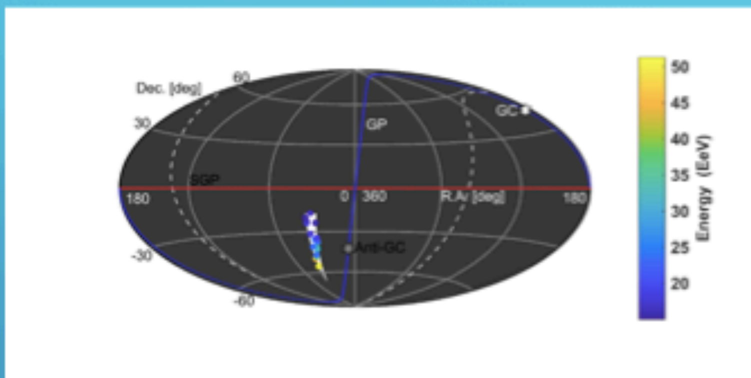

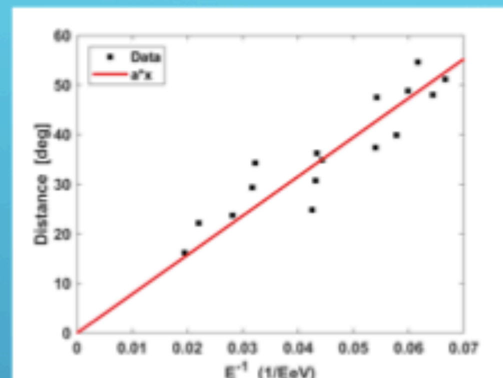

E>=15 EeV, Width = 10°, Distance<=55°, Direction = 345°

- $\frac{788.7}{E} = 50 * Z \frac{S}{kpc}\frac{B}{\mu G}\frac{1}{E}$
- If Z = 1 then $\frac{S}{kpc}\frac{B}{\mu G} = 15.774$
- If S = 3.7 Mpc (M82) then B = 4nG

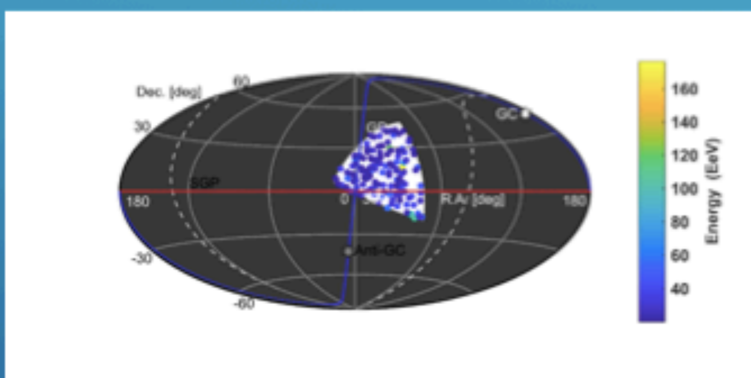

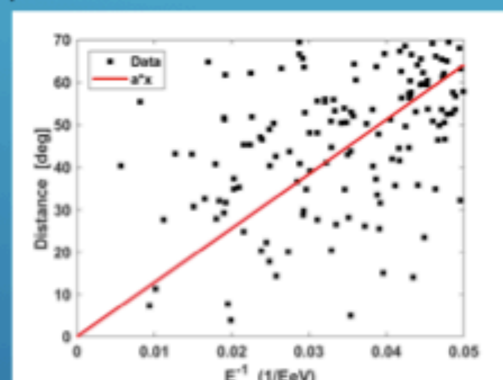

E>=30 EeV, Width = 30°, Distance<=70°, Direction = 320°

- $\frac{1128}{E} = 50 * Z \frac{S}{kpc}\frac{B}{\mu G}\frac{1}{E}$
- If Z = 1 then $\frac{S}{kpc}\frac{B}{\mu G} = 22.56$
- If S = 3.7 Mpc (M82) then B = 6nG

Distribution of maximum correlation strength

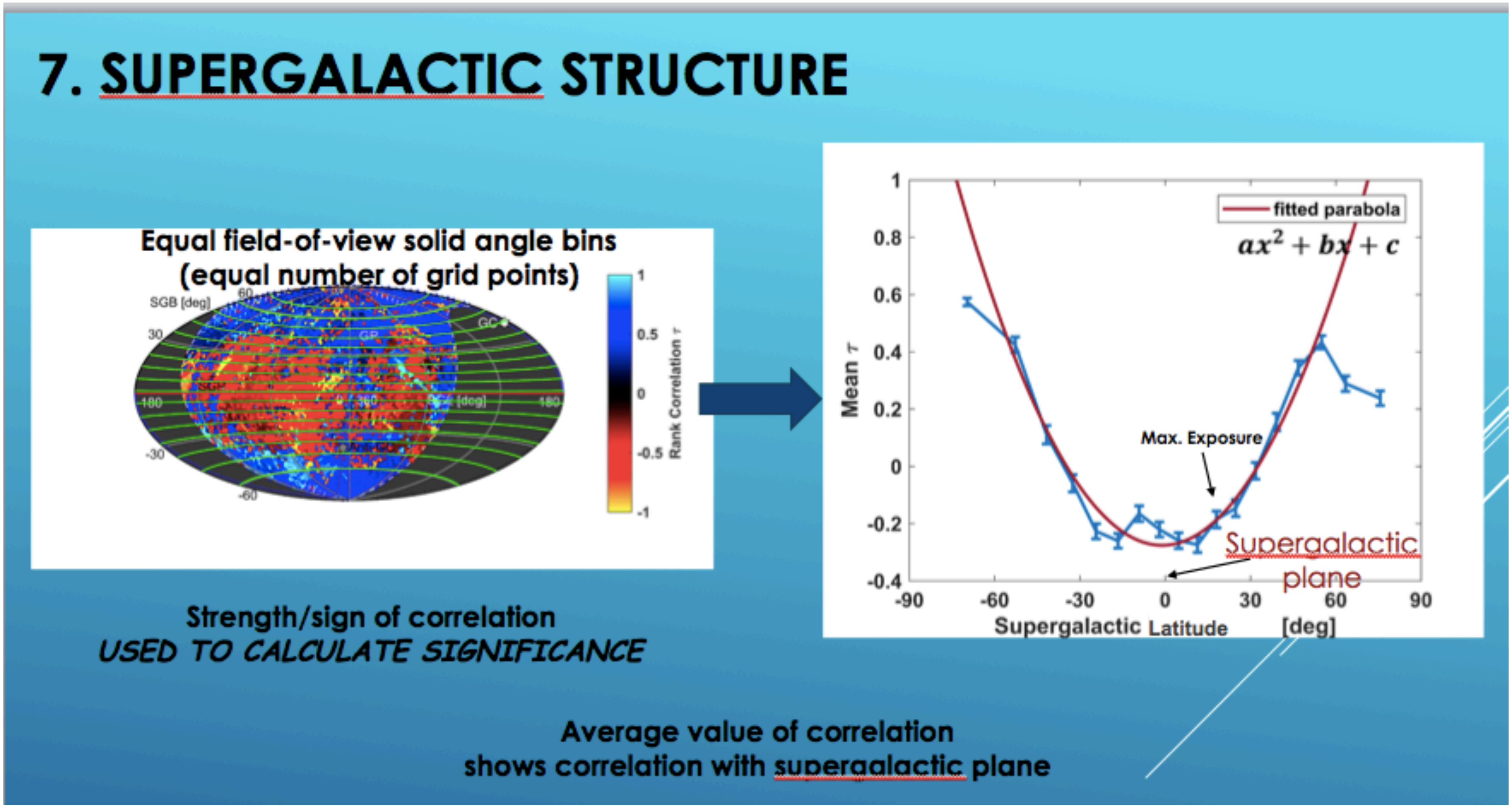

Simulated background sets generated by scrambling energies.

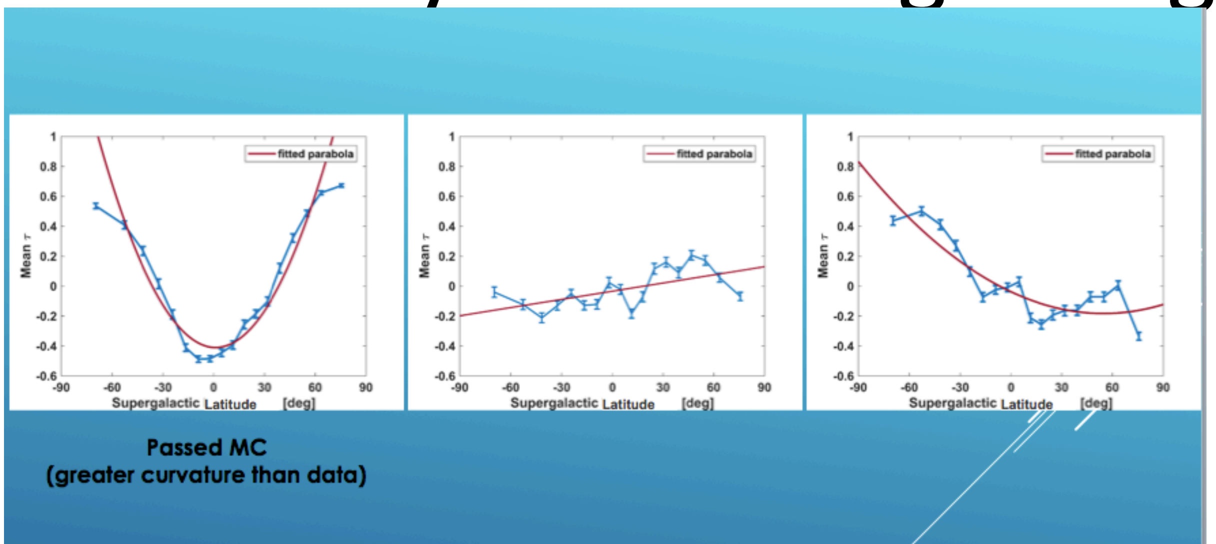

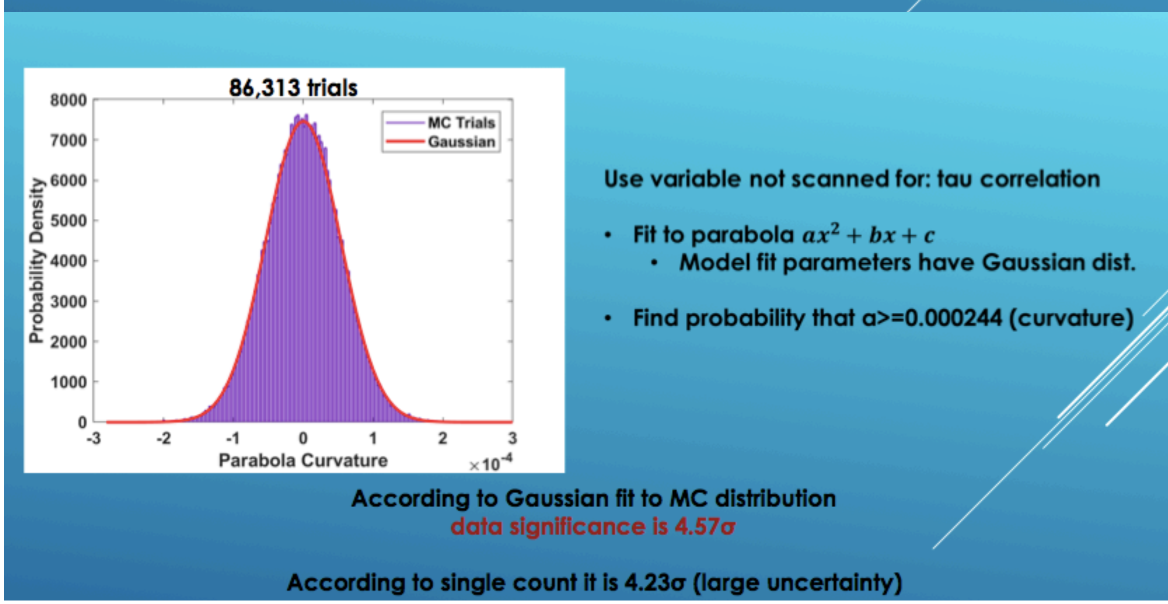

10 year result

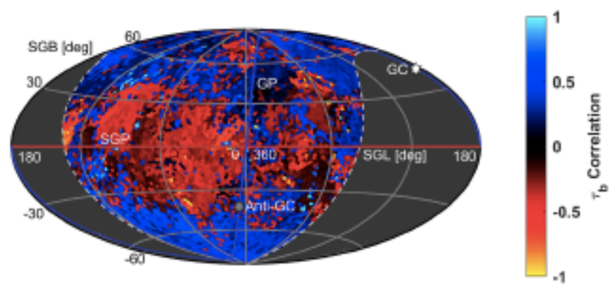

(a)

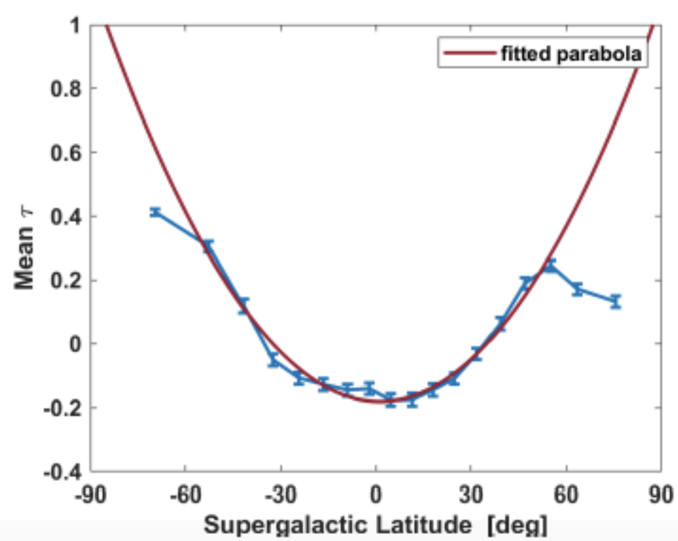

(b)

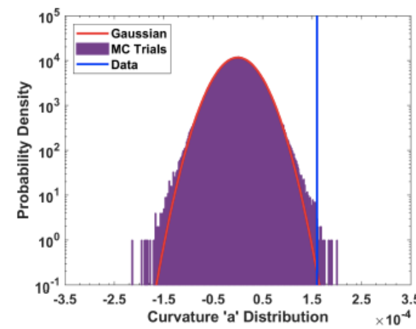

Figure 10. The distribution of the curvature parameter a of the mean τ parabola chosen as the supergalactic structure of multiplets test statistic for 900,000 isotropic MC sets. The purple bars are the MC PDF. The red line is a Gaussian distribution fit to the MC distribution. The curvature for the data is a=1.60$\times$10^{-4} shown as a blue vertical line. There are 22 MC with a larger curvature than data, which gives a significance of 4.09σ.

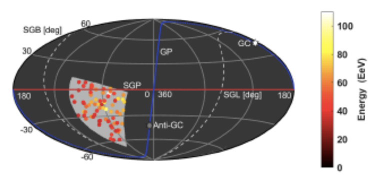

(a)

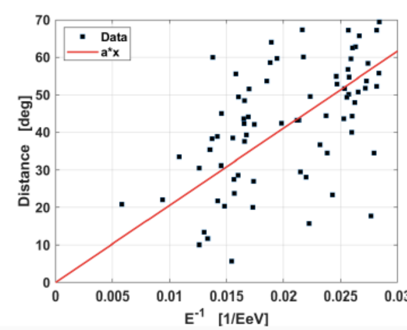

(b)

Apparent curl of B field in hot/cold spot region

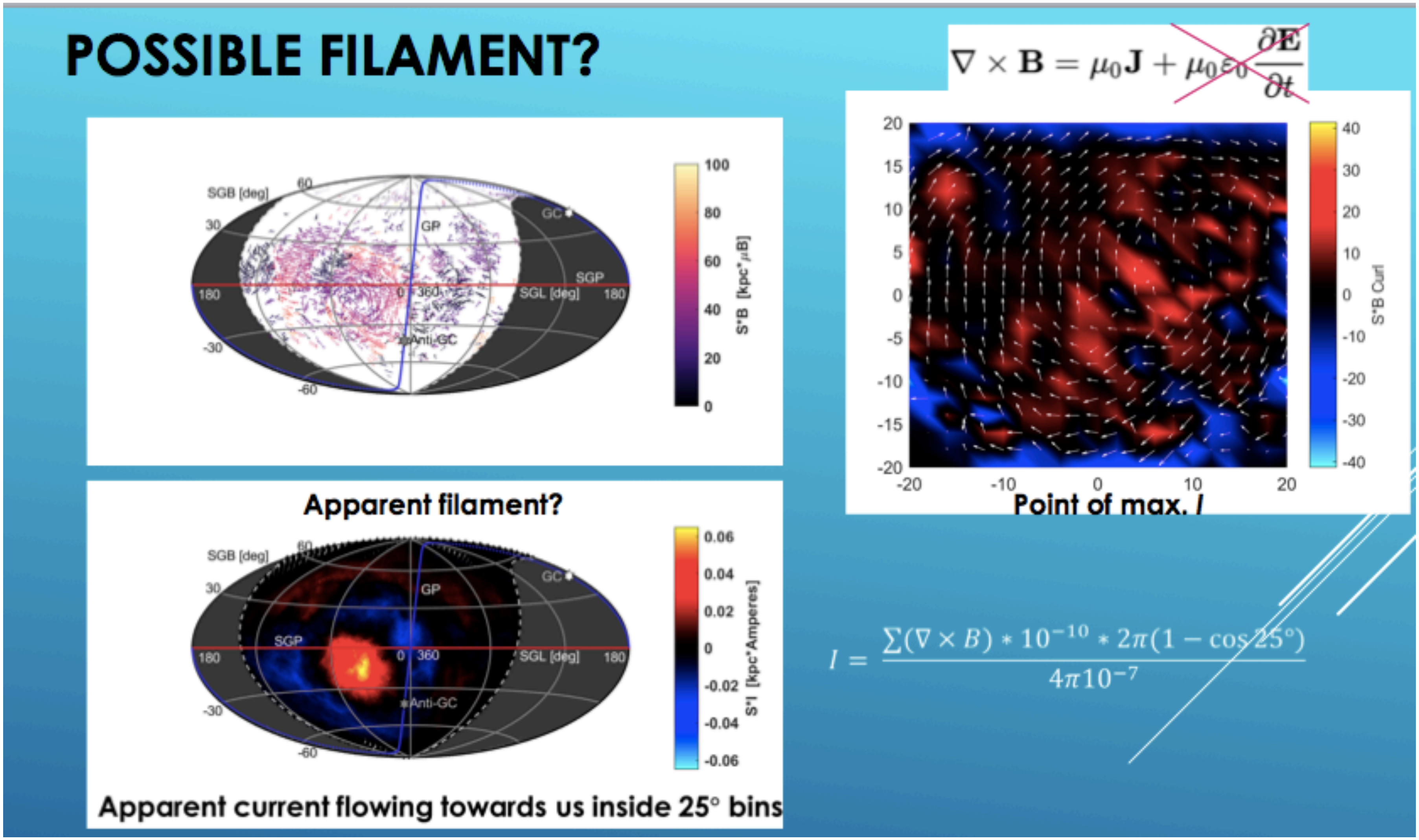

Composition and Anisotropy requires more statistics above 10^{19} eV:TAx4

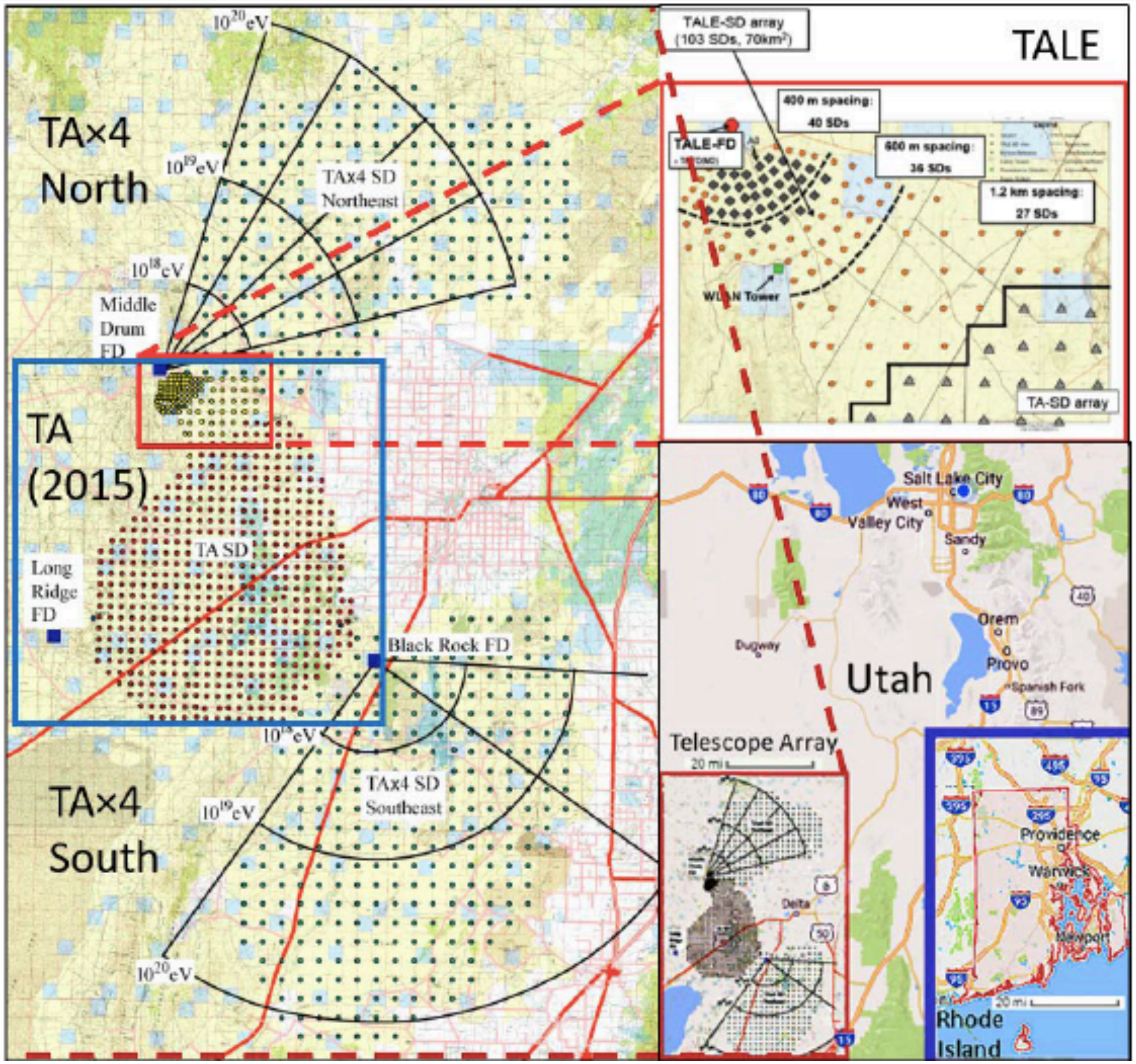

TAx4 under construction:

Helicopter Deployment

Middle Drum Telescope Station
All FDs Operational

Black Rock Mesa
All FD's Operational

TAx4 SD array is fully operational

Number of the SDs Listed in DAQ

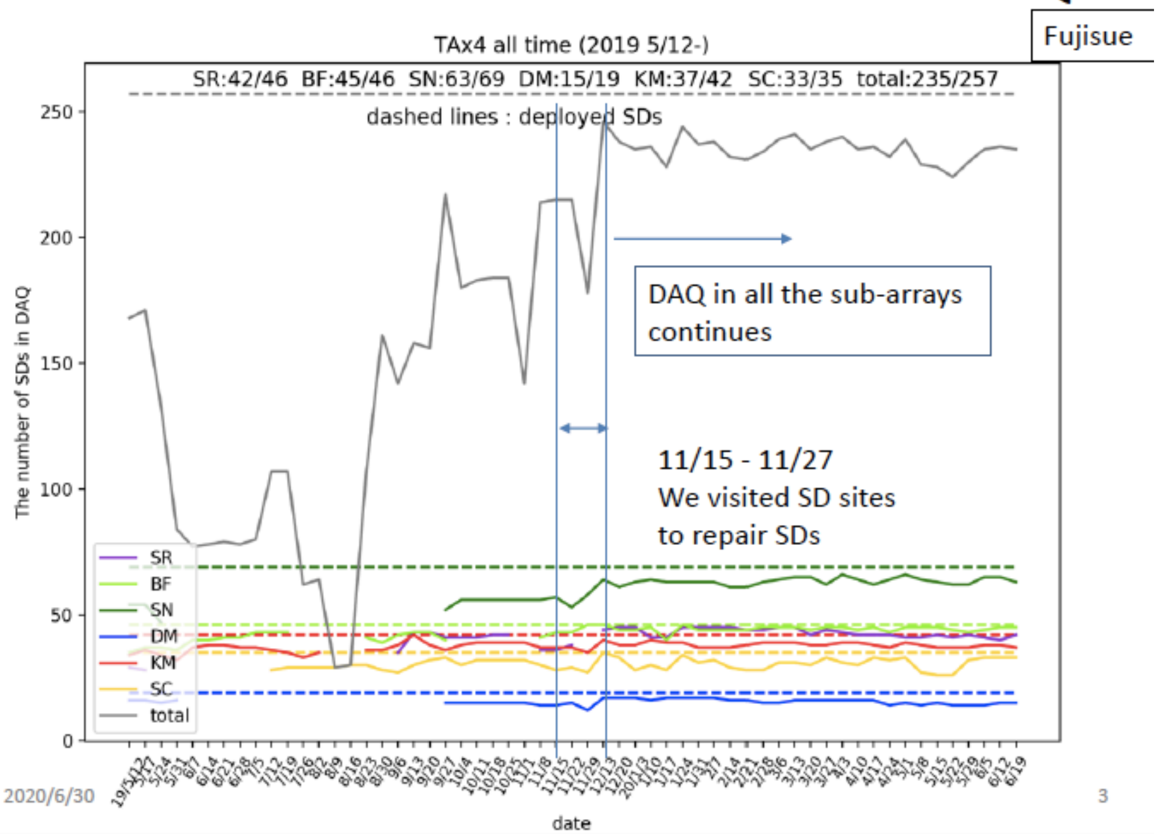

- Everything we have learned has come from improvements in technique: aperture and resolution.
- We now have additional tools: multi-messenger particle astrophysics.
- Neutrino, gravitational and gamma-ray astronomy will provide important complementary data in the search for UHECR origin.

- Diffuse neutrino flux must be related to the GZK cutoff and the flux of UHECR protons.
- Diffuse gamma-ray flux must be similarly related.
- Gamma Ray direct observation of SN at TeV and greater energies can pinpoint galactic cosmic ray accelerators. Correlate with galactic cosmic ray flux.

- Observation of neutrino point sources will generate a class of potential UHECR sources.
- Improved knowledge of galactic magnetic field will enable much better resolution of sources.
- We are now collaborating with the PHAESTOS group in Crete to use starlight polarimetry and known star distances from the Gaia survey to de-convolute the effect of the galactic magnetic field.

What have we learned?

- The featureless and uninteresting Cosmic Ray spectrum was an instrumental effect. Early detectors had poor energy resolution and calibration. The spectrum is rich with features.
- The composition of UHECR below ~ 10^{19} eV is reasonably well known and exhibits interesting features corresponding to spectral structures.
- The galactic/extragalactic transition is now in hand and details of galactic acceleration can now be studies.

- Persistent hints of intermediate angular scale anisotropies at the highest energies seem to show concentrations of sources near the supergalactic plane.
- Magnetic deflections are beginning to be studied and correlations with supergalactic sheets or filaments may be important.

Telescope Array Collaboration

RU Abbasi[1], M Abe[13], T Abu-Zayyad[1], M Allen[1], R Anderson[1], R Azuma[2], E Barcikowski[1], JW Belz[1], DR Bergman[1], SA Blake[1], R Cady[1], MJ Chae[3], BG Cheon[4], J Chiba[5], M Chikawa[6], WR Cho[7], T Fujii[8], M Fukushima[8,9], T Goto[10], W Hanlon[1], Y Hayashi[10], N Hayashida[11], K Hibino[11], K Honda[12],D Ikeda[8], N Inoue[13], T Ishii[12], R Ishimori[2], H Ito[14], D Ivanov[1], CCH Jui[1], K Kadota[16], F Kakimoto[2], O Kalashev[17], K Kasahara[18], H Kawai[19], S Kawakami[10], S Kawana[13], K Kawata[8], E Kido[8], HB Kim[4], JH Kim[1], JH Kim[25], S Kitamura[2], Y Kitamura[2], V Kuzmin[17], YJ Kwon[7], J Lan[1], SI Lim[3], JP Lundquist[1], K Machida[12], K Martens[9], T Matsuda[20], T Matsuyama[10], JN Matthews[1], M Minamino[10], K Mukai[12], I Myers[1], K Nagasawa[13], S Nagataki[14],T Nakamura[21], T Nonaka[8], A Nozato[6], S Ogio[10], J Ogura[2], M Ohnishi[8], H Ohoka[8], K Oki[8], T Okuda[22], M Ono[14], A Oshima[10], S Ozawa[18], IH Park[23], MS Pshirkov[24], DC Rodriguez[1], G Rubtsov[17], D Ryu[25], H Sagawa[8], N Sakurai[10], AL Sampson[1], LM Scott[15], PD Shah[1], F Shibata[12], T Shibata[8], H Shimodaira[8], BK Shin[4], JD Smith[1], P Sokolsky[1], RW Springer[1], BT Stokes[1], SR Stratton[1,15], TA Stroman[1], T Suzawa[13], M Takamura[5], M Takeda[8], R Takeishi[8], A Taketa[26], M Takita[8], Y Tameda[11], H Tanaka[10], K Tanaka[27], M Tanaka[20], SB Thomas[1], GB Thomson[1], P Tinyakov[17,24], I Tkachev[17], H Tokuno[2], T Tomida[28], S Troitsky[17], Y Tsunesada[2], K Tsutsumi[2], Y Uchihori[29], S Udo[11], F Urban[24], G Vasiloff[1], T Wong[1], R Yamane[10], H Yamaoka[20], K Yamazaki[10], J Yang[3], K Yashiro[5], Y Yoneda[10], S Yoshida[19], H Yoshii[30], R Zollinger[1], Z Zundel[1]

[1]High Energy Astrophysics Institute and Department of Physics and Astronomy, University of Utah, Salt Lake City, Utah, USA, [2]Graduate School of Science and Engineering, Tokyo Institute of Technology, Meguro, Tokyo, Japan, [3]Department of Physics and Institute for the Early Universe, Ewha Womans University, Seodaaemun-gu, Seoul, Korea, [4]Department of Physics and The Research Institute of Natural Science, Hanyang University, Seongdong-gu, Seoul, Korea, [5]Department of Physics, Tokyo University of Science, Noda, Chiba, Japan, [6]Department of Physics, Kinki University, Higashi Osaka, Osaka, Japan, [7]Department of Physics, Yonsei University, Seodaemun-gu, Seoul, Korea, [8]Institute for Cosmic Ray Research, University of Tokyo, Kashiwa, Chiba, Japan, [9]Kavli Institute for the Physics and Mathematics of the Universe (WPI), Todai Institutes for Advanced Study, the University of Tokyo, Kashiwa, Chiba, Japan, [10]Graduate School of Science, Osaka City University, Osaka, Osaka, Japan, [11]Faculty of Engineering, Kanagawa University, Yokohama, Kanagawa, Japan, [12]Interdisciplinary Graduate School of Medicine and Engineering, University of Yamanashi, Kofu, Yamanashi, Japan, [13]The Graduate School of Science and Engineering, Saitama University, Saitama, Saitama, Japan, [14]Astrophysical Big Bang Laboratory, RIKEN, Wako, Saitama, Japan, [15]Department of Physics and Astronomy, Rutgers University - The State University of New Jersey, Piscataway, New Jersey, USA, [16]Department of Physics, Tokyo City University, Setagaya-ku, Tokyo, Japan, [17]Institute for Nuclear Research of the Russian Academy of Sciences, Moscow, Russia, [18]Advanced Research Institute for Science and Engineering, Waseda University, Shinjuku-ku, Tokyo, Japan, [19]Department of Physics, Chiba University, Chiba, Chiba, Japan, [20]Institute of Particle and Nuclear Studies, KEK, Tsukuba, Ibaraki, Japan, [21]Faculty of Science, Kochi University, Kochi, Kochi, Japan, [22]Department of Physical Sciences, Ritsumeikan University, Kusatsu, Shiga, Japan, [23]Department of Physics, Sungkyunkwan University, Jang-an-gu, Suwon, Korea, [24]Service de Physique Theorique, Universite Libre de Bruxelles, Brussels, Belgium, [25]Department of Physics, School of Natural Sciences, Ulsan National Institute of Science and Technology, UNIST-gil, Ulsan, Korea, [26]Earthquake Research Institute, University of Tokyo, Bunkyo-ku, Tokyo, Japan, [27]Graduate School of Information Sciences, Hiroshima City University, Hiroshima, Hiroshima, Japan, [28]Advanced Science Institute, RIKEN, Wako, Saitama, Japan, [29]National Institute of Radiological Science, Chiba, Chiba, Japan, [30]Department of Physics, Ehime University, Matsuyama, Ehime, Japan

USA, Japan, Korea, Russia, Belgium

Associated Experiments

- Gamma rays from Lightning (with N. Mexico Tech) – first observation of downward MeV gamma rays from lightning strikes.
- 40 MeV electron linac beam studies: - radio emission
- Tests of detectors for proposed space-based air-fluorescence experiments (JEM-EUSO)
- JPL-CalTech radio astronomy station: Recent observation of FRB from galactic source

In Memoriam

Clicerio Avilez Valdez

Clicerio Avilez Valdez, the director of the Institute de Fisica at the Universidad de Guanajuato, Mexico, died suddenly of a massive cerebral hemorrhage on 10 May 1991. He was 45. Avilez believed that Latin American participation in the high-technology and frontier research of elementary-particle physics was important to foster the growth of science, engineering and graduate education in Mexico and other Latin American countries. He devoted his career to the pursuit of that goal. In 1980 Avilez decided to become an experimenter in high-energy physics and spent a year at Nevis Laboratories at Columbia University. With the support of Jorge Flores, the director of the Institute de Fisica at UNAM, he then joined with colleagues from Columbia and the University of Massachusetts in experiments at both Brookhaven and Fermilab. He was cospokesman of an experiment at Brookhaven that studied the hadronic production of strange particles. His efforts were instrumental in starting Fermilab experiment E690, which explores the hadronic production of strange, charm and bottom particles. In 1986 Avilez went to the Universidad de Guanajuato and became the director of the Institute de Fisica. Avilez organized several important conferences to encourage interactions between Latin American scientists and the world scientific community. He and Leon Lederman ran the Pan- American Symposium on High-Energy Physics and Technology in Cocoyoc, Mexico, in 1982. This meeting sparked the birth of many research groups throughout Latin America. Avilez worked tirelessly to further the development of high-technology endeavors in Mexico and elsewhere. His energy, enthusiasm and leadership will be missed by his colleagues
and students.

Clicerio invited me to give a series of lectures on cosmic ray physics at a summer school in Mexico in 1986. I was unable to come at the last minute, but the lecture notes became the basis for my book "Introduction to Ultrahigh Energy Cosmic Rays" – the second edition of which (co-authored with Gordon Thomson) just came out. I will always remember his energy, enthusiasm and determination to improve the standing of physics in Mexico and Latin America. His kindness in inviting me then wound up making a big impact on my career.


Thank You!

Energy calibration

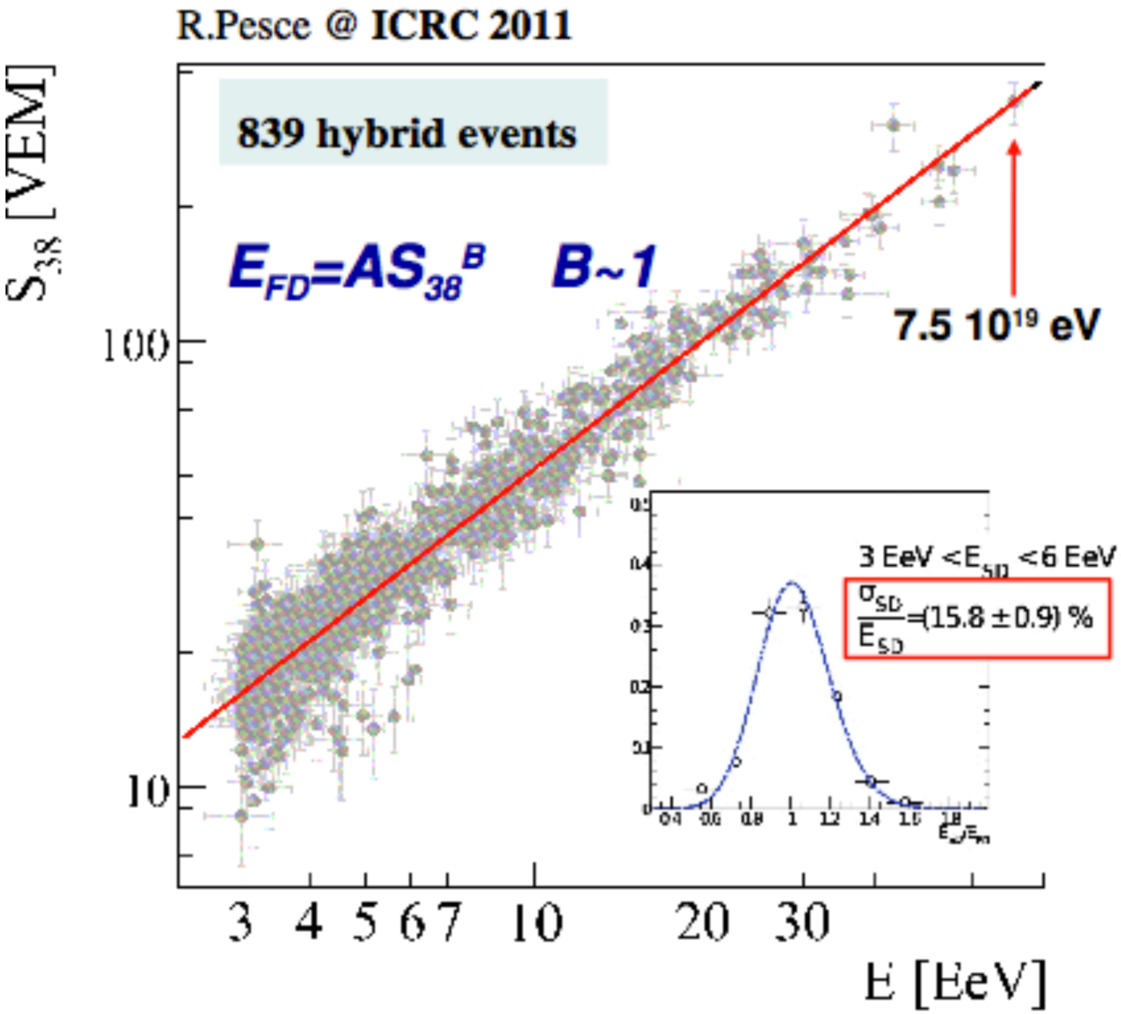

Jan 2004 – Sept 2010
E > 3 EeV - zenith < 60°

Using hybrid events, the SD energy estimator is calibrated without relying on Monte Carlo

Method Systematic Uncertainties
7% a 10^{19} eV
15% a 10^{20} eV

FD Energy Systematics
■ fluorescence yield 14%
■ FD absolute calibration 9.5%
■ invisible energy 4%
■ reconstruction 10%
■ atmospheric effects 8%
TOTAL: 22%

***S_{38}* -> S1000 that a shower would have produced had it arrived with a zenith angle of 38°**

TA Fluorescence Detectors

Refurbished from HiRes

Observation started Dec. 2007

Middle Drum

14 cameras/station
256 PMTs/camera

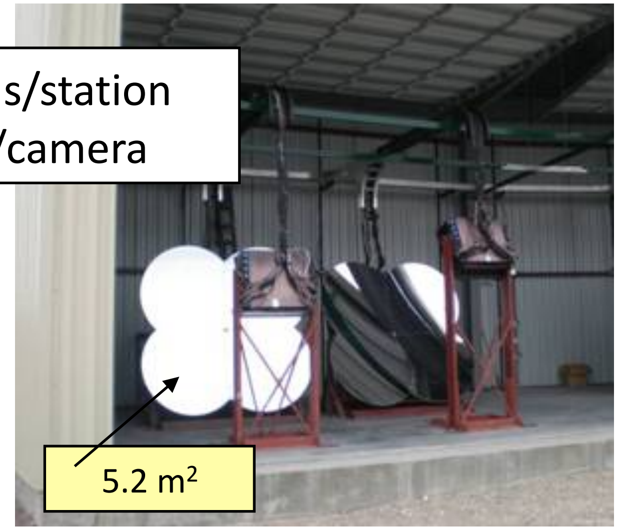

5.2 m^2

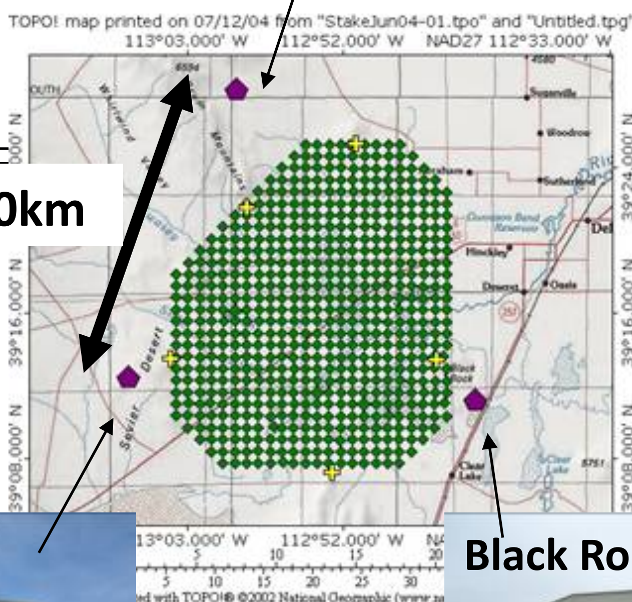

~30km

Observation started Nov. 2007

Long Ridge

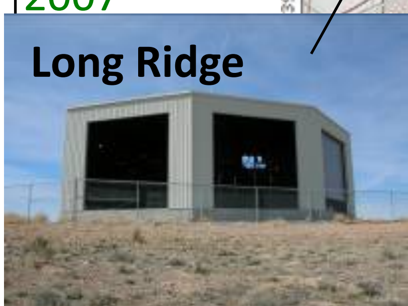

Observation started Jun. 2007

Black Rock Mesa

New FDs

256 PMTs/camera
HAMAMATSU R9508
FOV~15x18deg
12 cameras/station

~1 m^2

6.8 m^2

97

< SD Deployment >

- 2006 Oct. – 2007 Mar.
- BLM restriction for Apr. – Sep.
- Tuning from 2007 Oct.

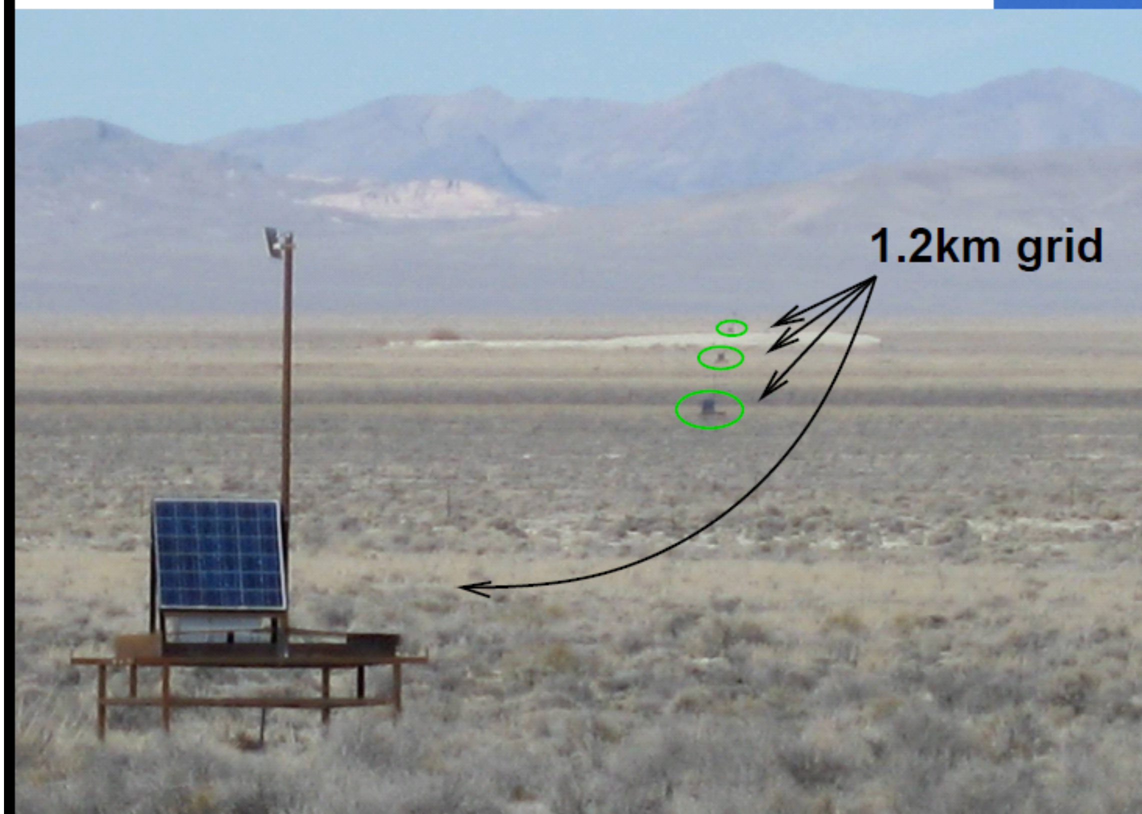

Energy Scale

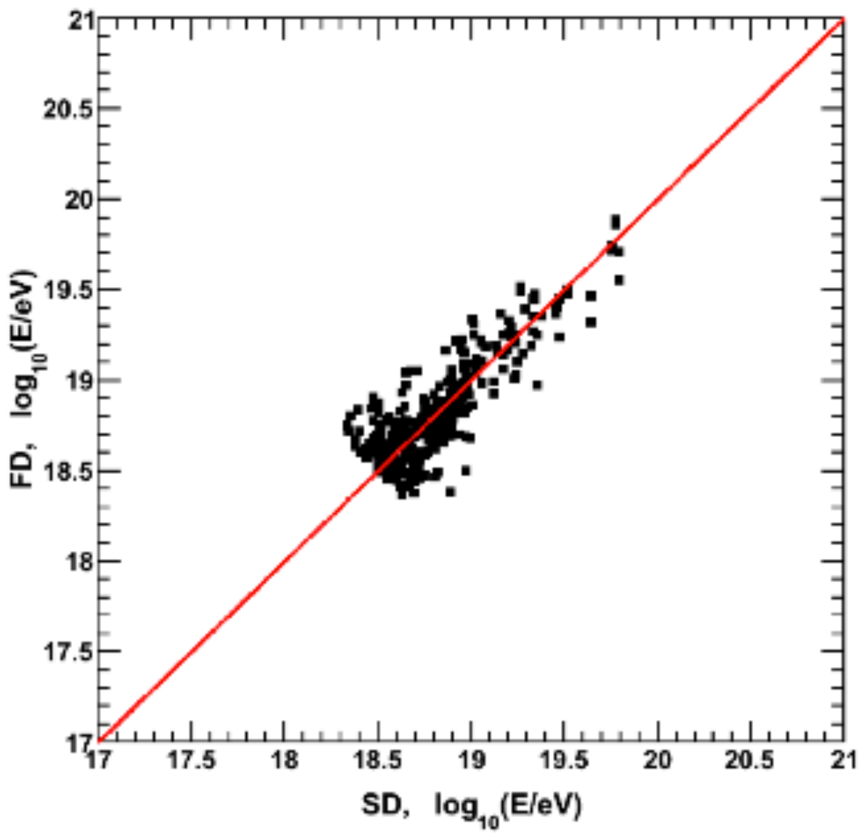

- SD and FD energy estimations disagree
- FD estimate possesses less model-dependence
- Set SD energy scale to FD energy scale using well-reconstructed events from all 3 FD detectors
- **27% renormalization.**

Acceptance

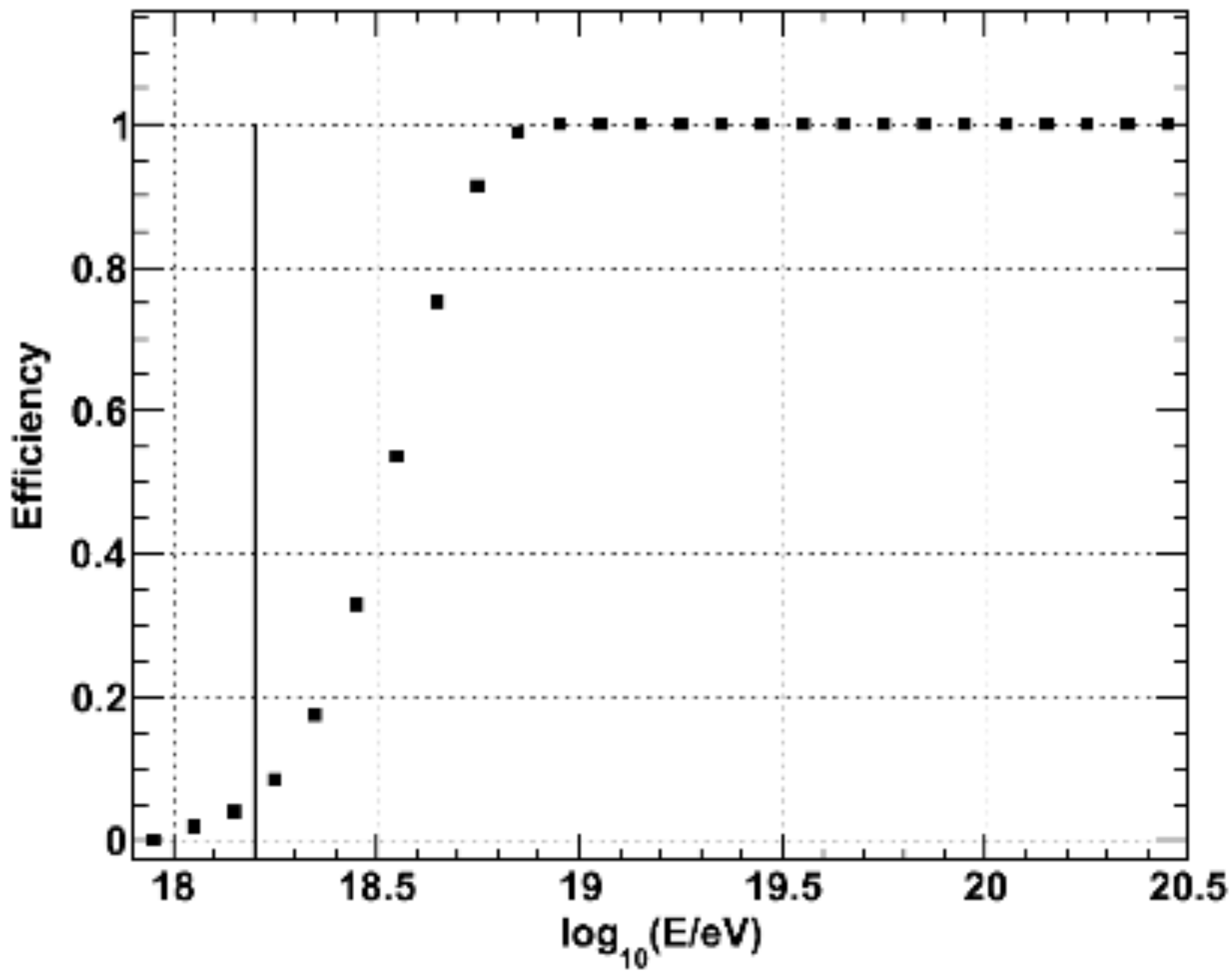

HiRes/TA stereo data elongation rate

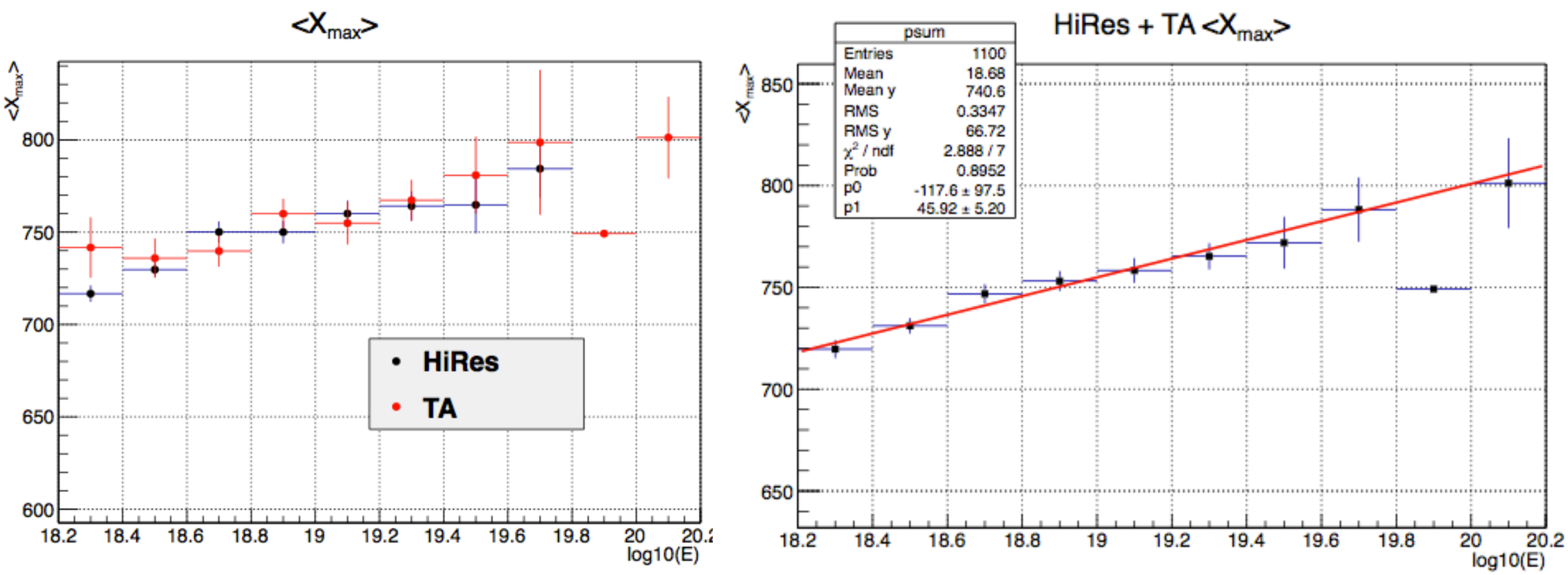

Composition does not seem to be changing rapidly over this energy range

HiRes/TA agreement is remarkable

- Different mirrors/electronics/pmt’s/calibration procedures
- Different geography/atmospheric aerosol loading
- Different reconstruction methodology, independent of HiRes/Utah group

Comparison of uncorrected HiRes/TA/PAO/Yakutsk data

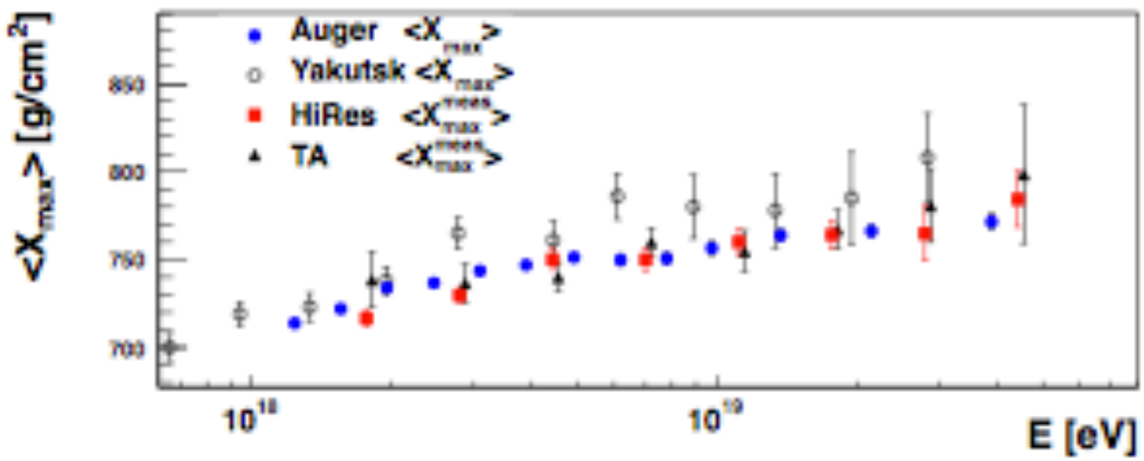

Fig. 2. $\langle X_{\rm max}\rangle$ measured by Auger and Yakutsk, together with the $\langle X_{\rm max}^{\rm meas}\rangle$ as measured by HiRes and TA. Data points are shifted to a common energy scale (text for details).

Interpretation of data

- HiRes/TA Xmax data is in excellent agreement
- Uncorrected HiRes/TA data elongation rate data is in excellent agreement with PAO
- HiRes/TA apertures very similar

- PAO cut philosophy is to minimize detector bias and compare to theory.
- HiRes/TA philosophy is to take care of bias by careful simulation of models using detector MC and reconstruction.
- Should be equivalent!

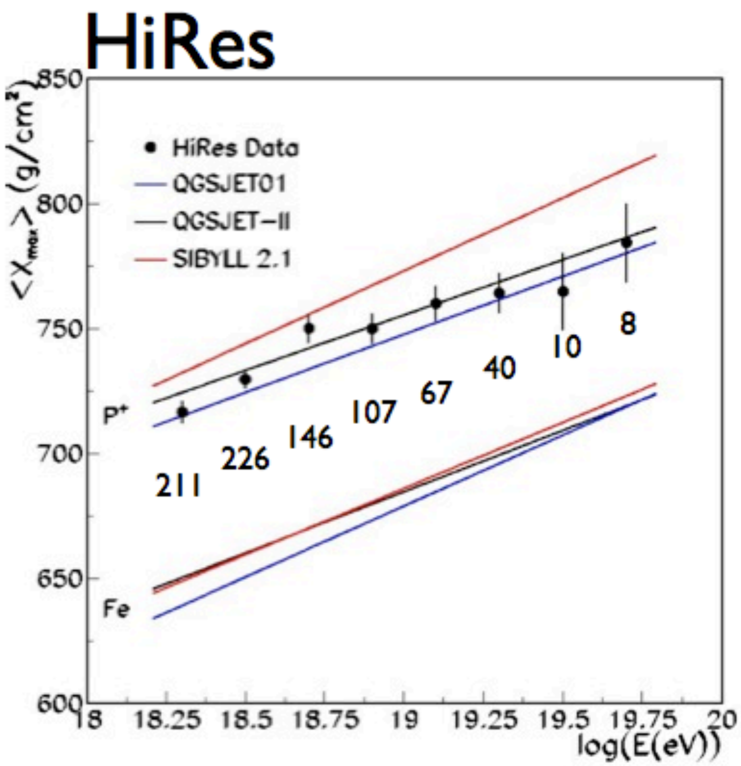

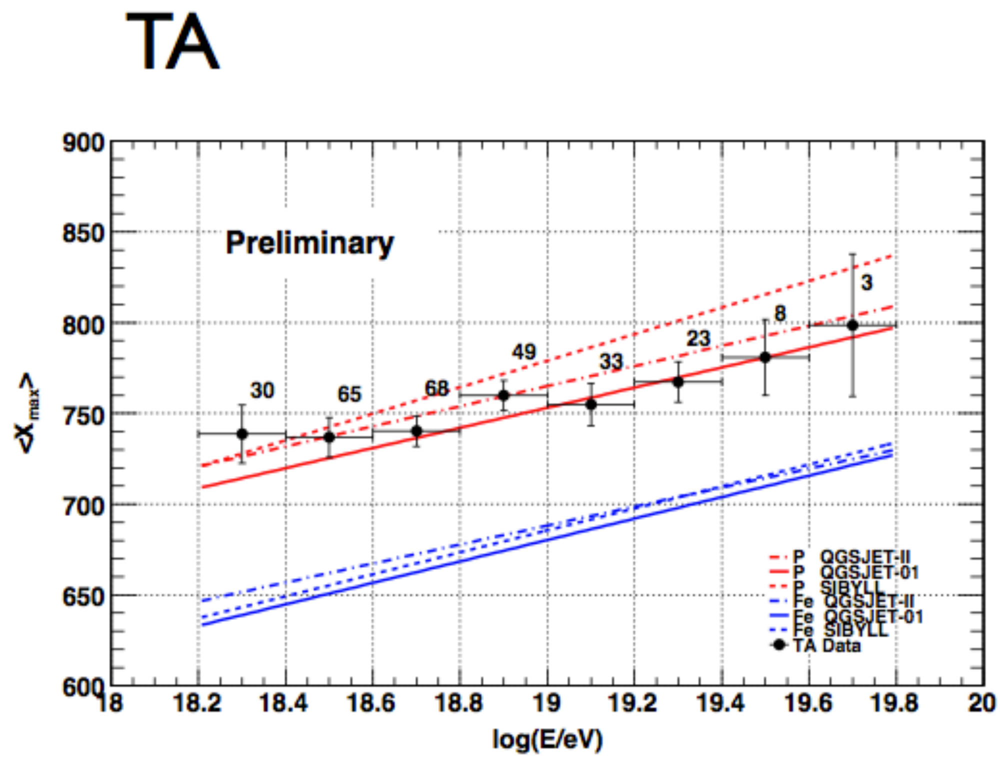

Note: p and Fe rails corrected for detector acceptance after cuts

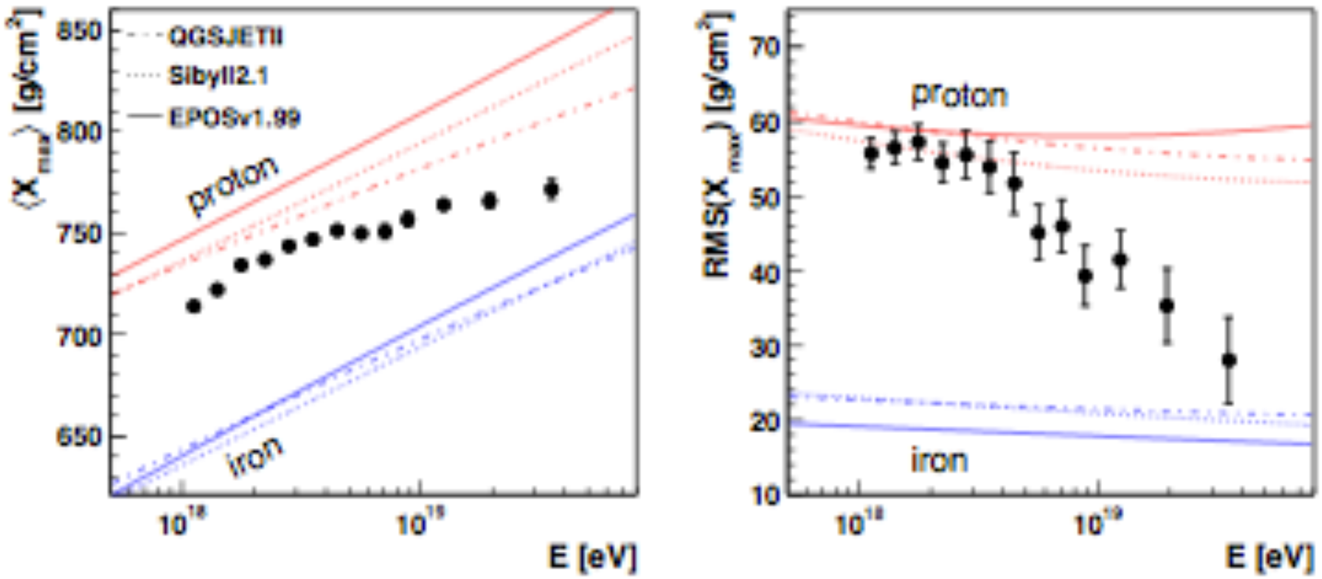

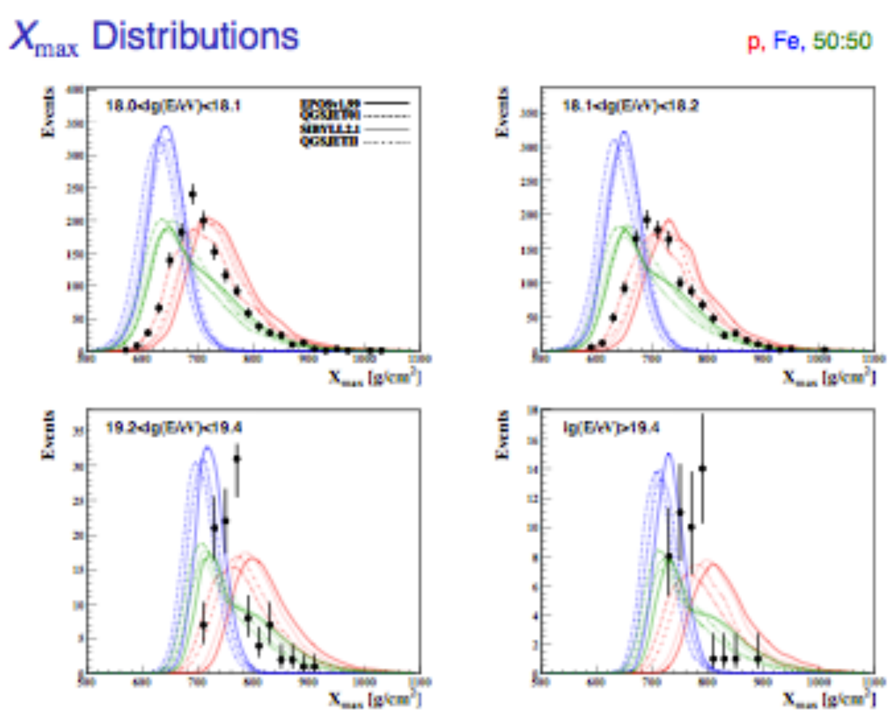

PAO elongation rate and fluctuation rms

Note: no bias expected for data so

Prediction rails uncorrected

HiRes/TA data should be shifted by

~20 gm/cm2 deeper if QGSJET p.

Measurement of the p-air cross-sectior

see R. Ulrich at this Conf

Tail of the distribution of X_{max} sensitive to cross-section

Fly's Eye → Ellsworth et al. Phys. Rev. D26 (1982) 336
Baltrusaitis et al. Phys. Rev. Lett. 52 (1984) 1380

$18 < \log_{10}(E/eV) < 18.5$

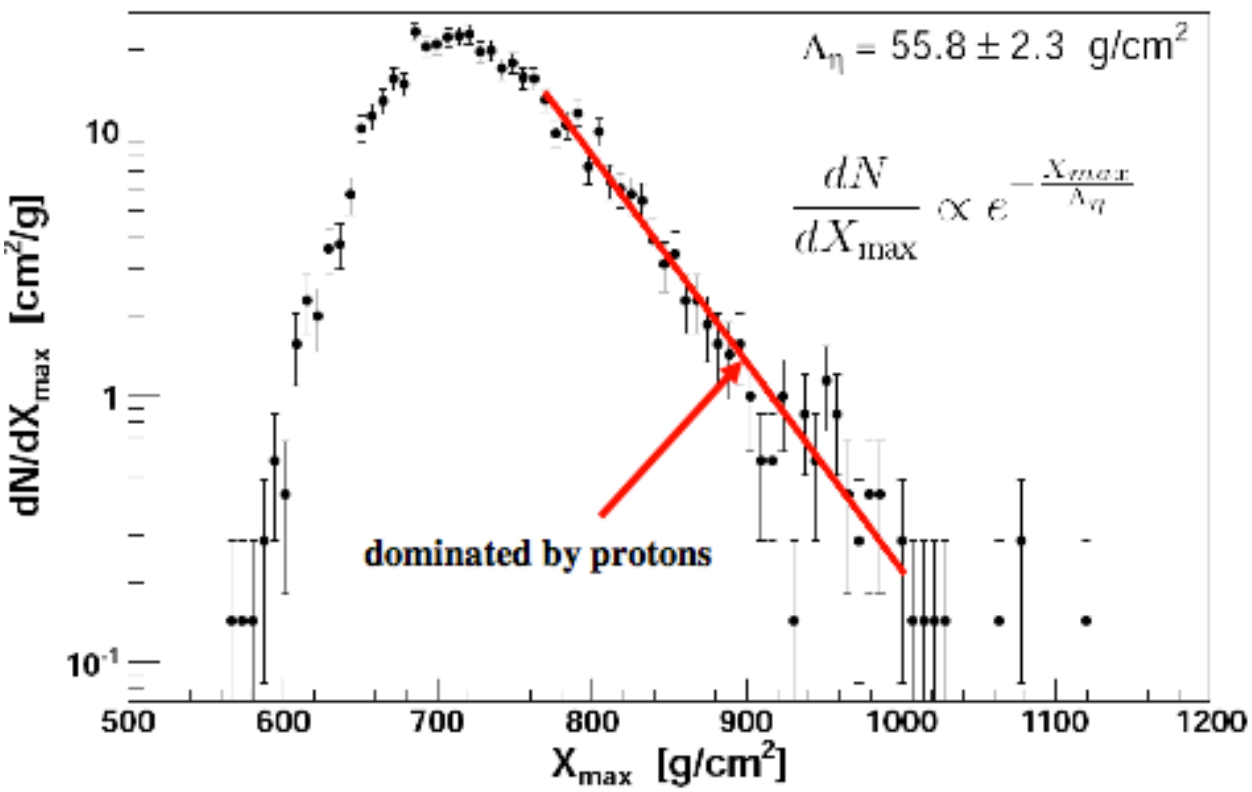

The Pierre Auger Collaboration, Phys. Rev. Lett. 109, 062002 (2012)

η is the fraction of "deepest" event from the unbiased X_{max} distribution

Why η = 20% ?
25% helium contamination produces a bias at the level of the statistical uncertainties

Use simulations to correlate Λ_η^{MC} with cross-sections

Λ_η^{MC} adjusted to reproduce the measured Λ_η

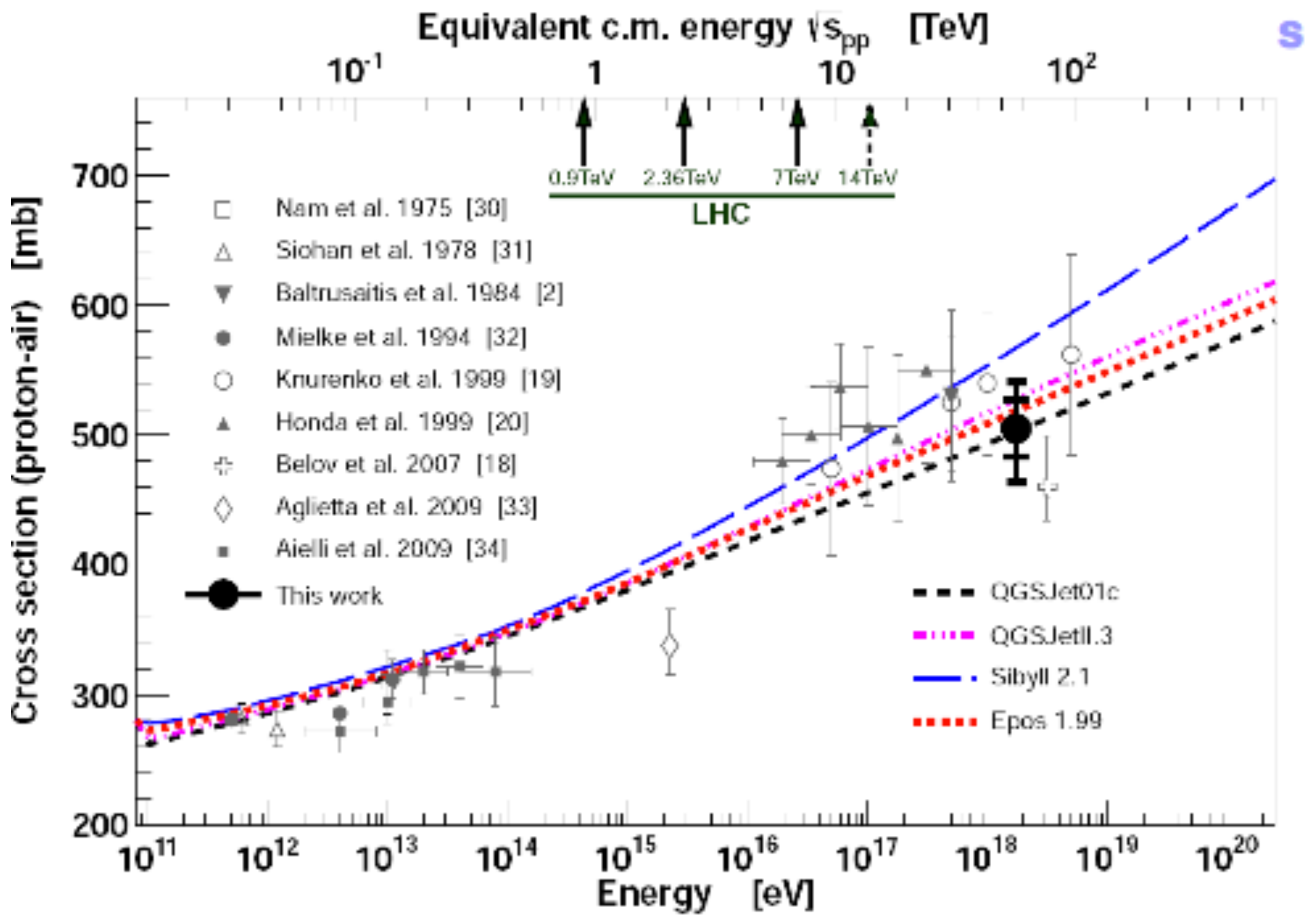

Equivalent c.m. energy √s_pp [TeV]
0.9TeV
2.36TeV
7TeV
14TeV
LHC
Nam et al. 1975 [30]
Siohan et al. 1978 [31]
Baltrusaitis et al. 1984 [2]
Mielke et al. 1994 [32]
Knurenko et al. 1999 [19]
Honda et al. 1999 [20]
Belov et al. 2007 [18]
Aglietta et al. 2009 [33]
Aielli et al. 2009 [34]
This work
QGSJet01c
QGSJetII.3
Sibyll 2.1
Epos 1.99
Cross section (proton-air) [mb]
Energy [eV]

Data X_{max} Distribution

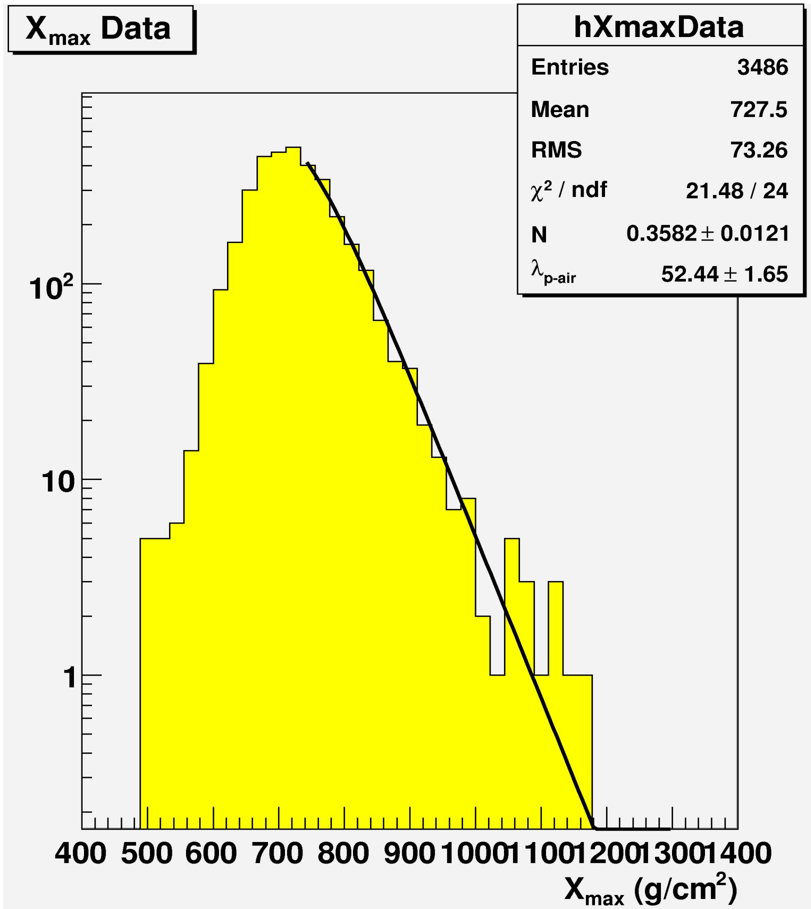

- Mean energy ~ $10^{18.5}$ eV;
- Only events with global fit are used;
- Without additional systematic errors due to heavier and lighter components

- **HiRes:**

HiRes 2007 Measurement.

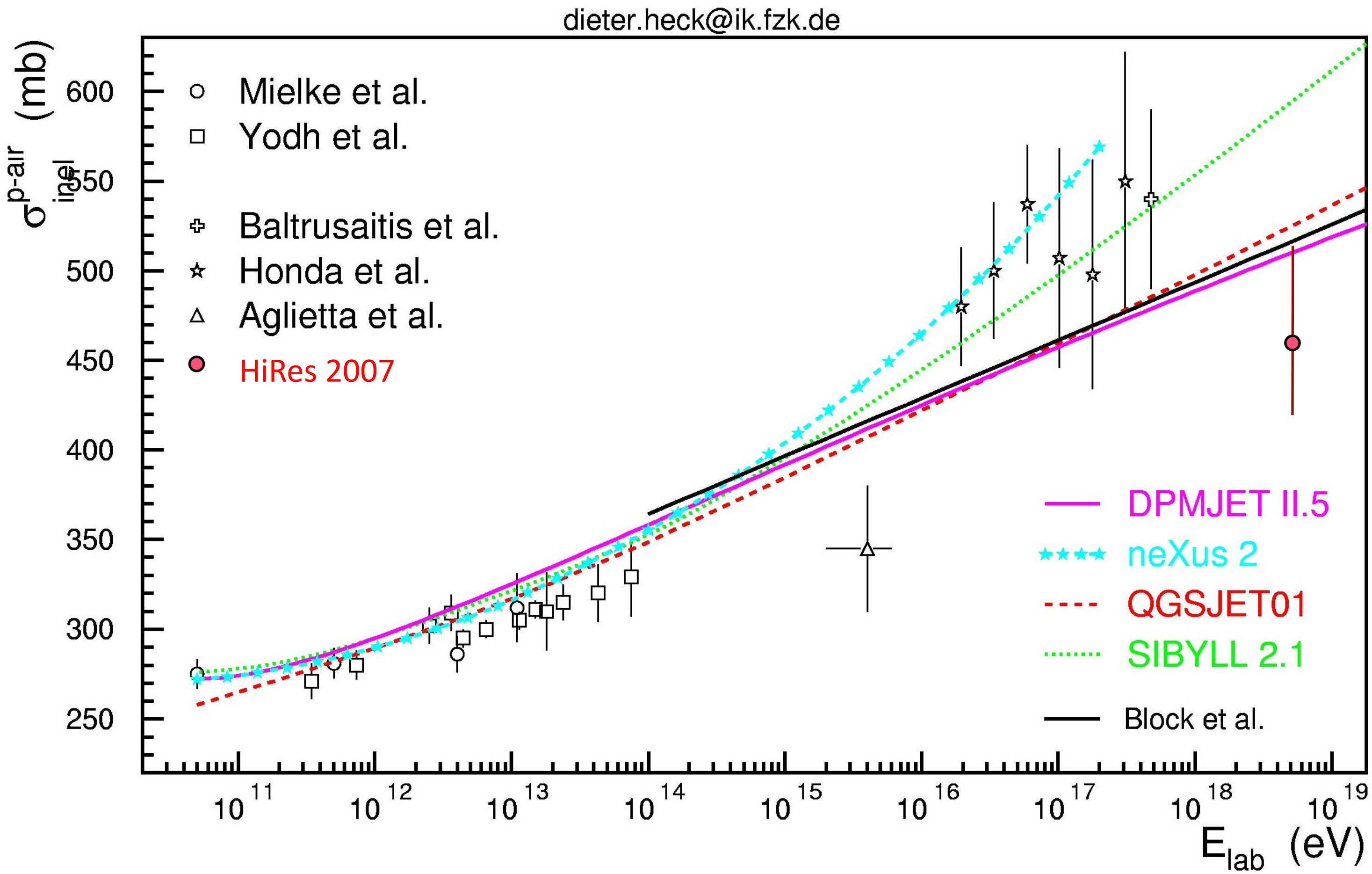

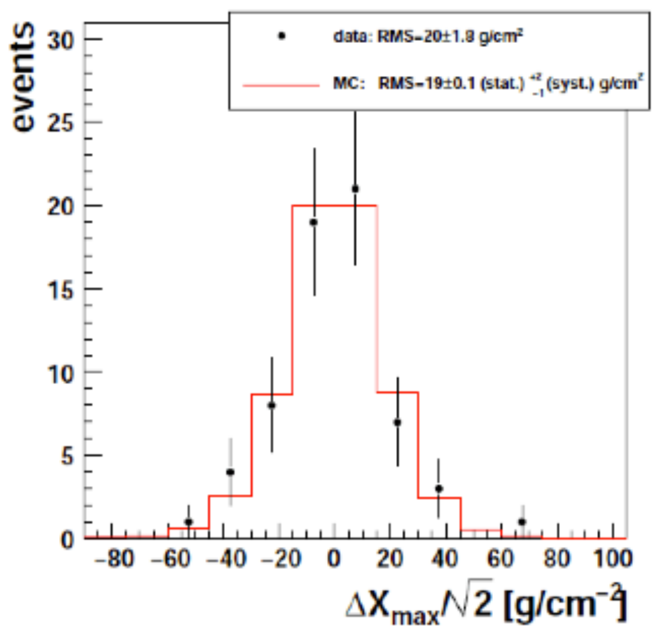

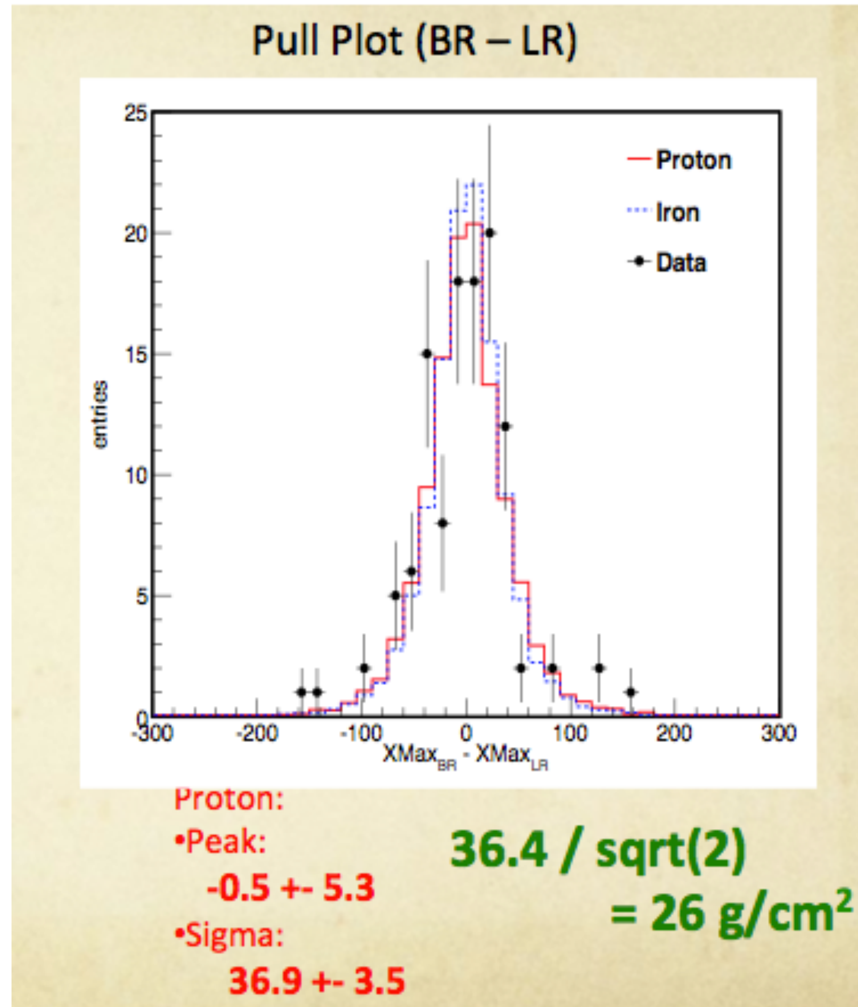

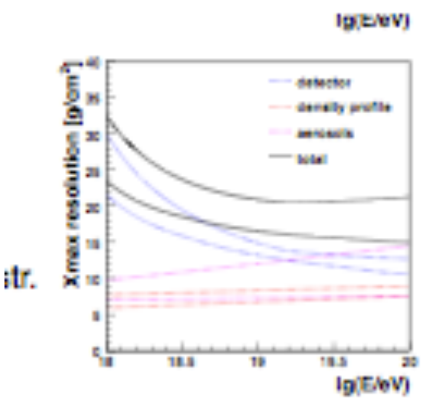

Calculated and measured Xmax resolutions for PAO and TA stereo hybrid events appear to be very similar

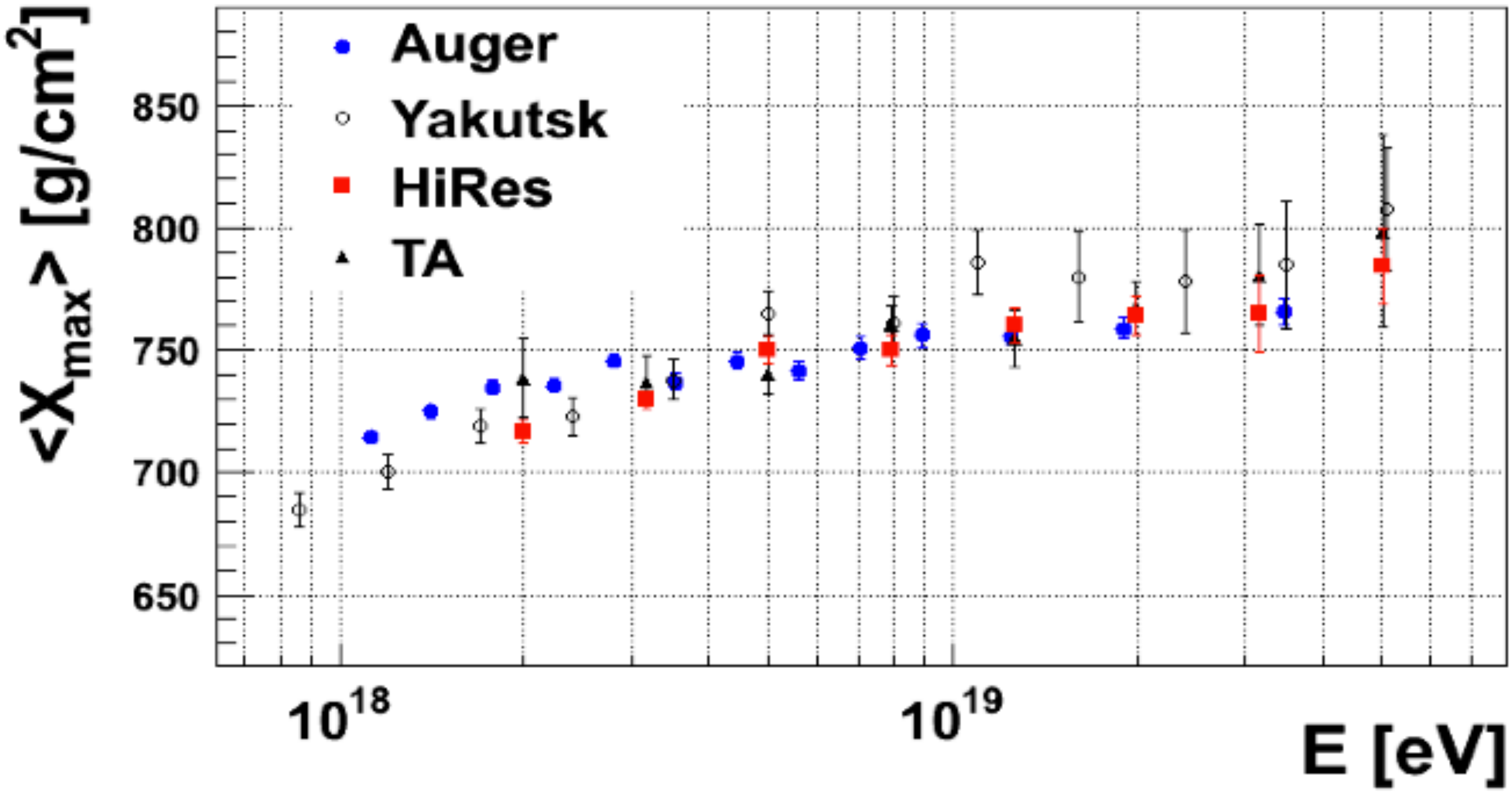

Actual data (before acceptance corrections) is in excellent agreement.
Is this telling us something about the proton simulations?

Mixed models – interplay of galactic and extragalactic spectra

COMPARISON of DIP and ANKLE MODELS

In the **dip model** transition occurs at $E_{\rm tr} \sim (5-7) \times 10^{17}$ eV, i.e. close to the end of Galactic Cosmic Rays (Iron knee at $E \sim 1 \times 1017$ eV).

In the **ankle model** transition occurs at $E_a = (0.3 - 1) \times 10^{19}$ eV, much higher than Iron knee, in contradiction with Standard Galactic Model.

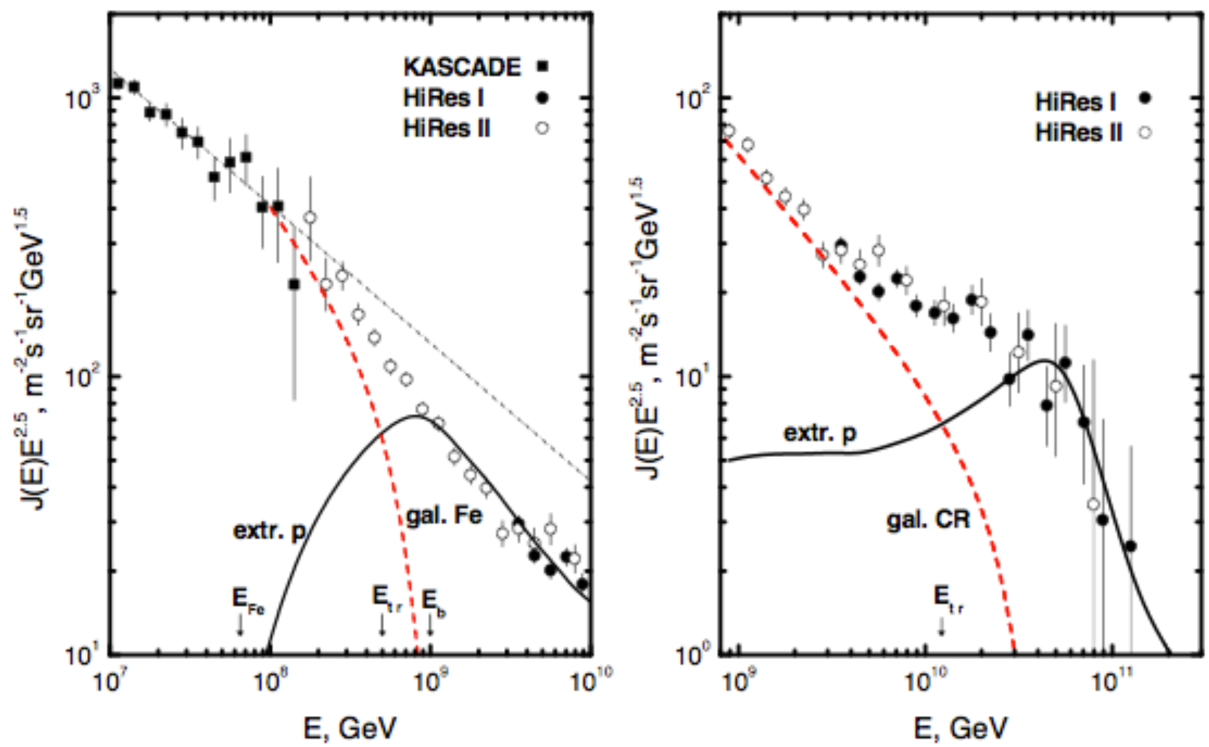

FD Auger enhancement: HEAT

H-J Mathes @ **ICRC 2011**

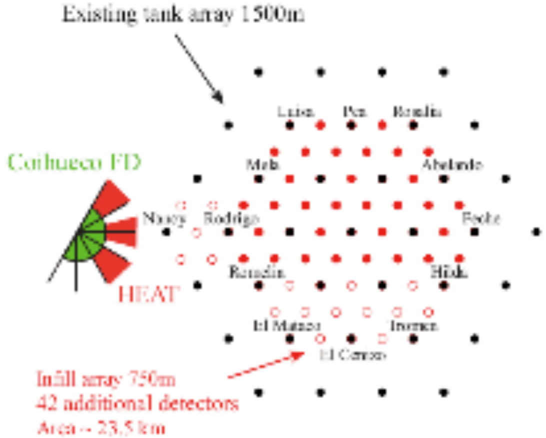

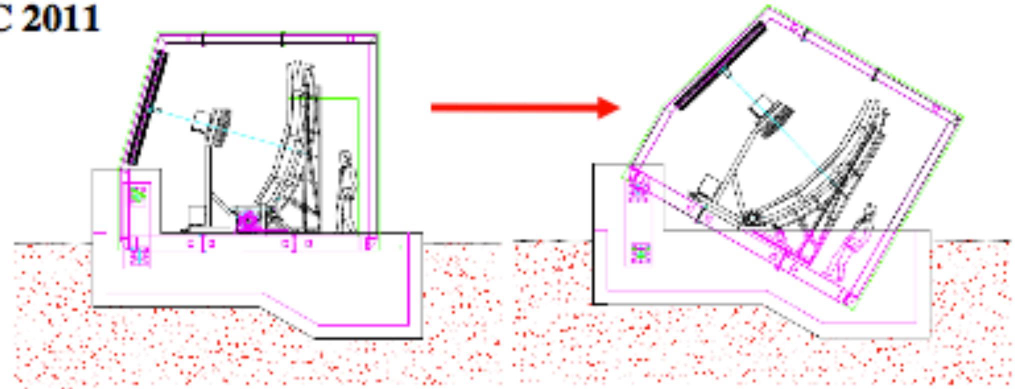

3 telescopes nearby Coihueco
30° up to 60° elevation

Taking data since Sept. 2009

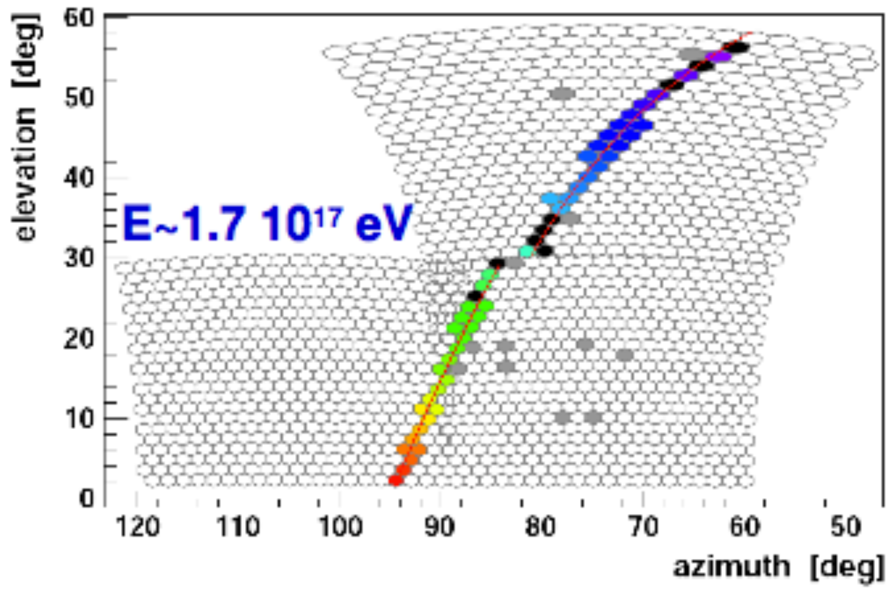

Higher elevation
lower energies (~ 10^{17} eV) unbiased
observation of longitudinal profile

SD Auger enhancement: AMIGA

I.Maris, F. Sanchez @ ICRC 2011

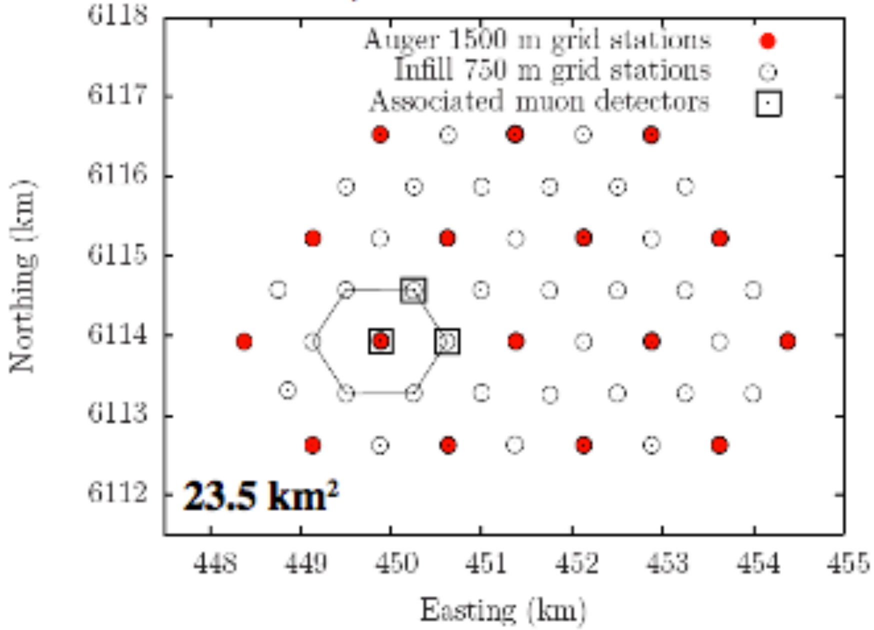

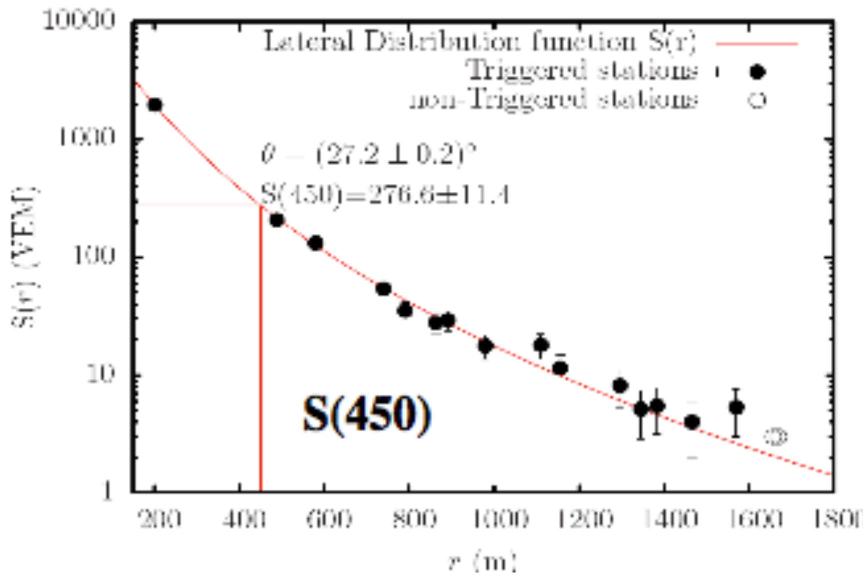

INFILL array (Cherenkov stations) and Muon detectors (scintillators)

- 53 (now 61) stations with spacing 750 m
- 4 (now 7) buried scintillator modules installed

Exposure: (26.4 ± 1.3) km² sr yr

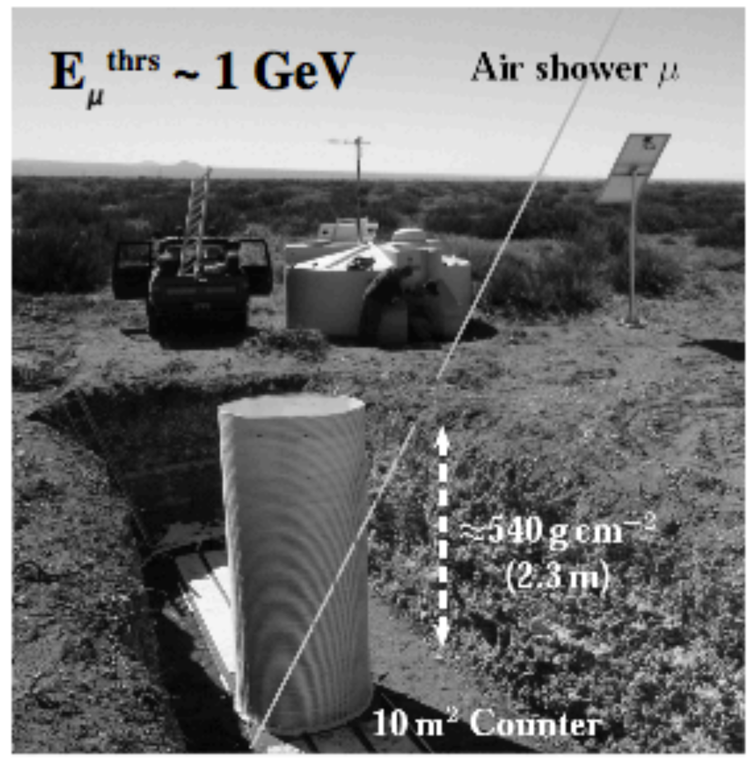

700 (20, 4) events/ month E > $10^{17.5\,(18,\,18.5)}$ eV

ELS (Electron Linac) Calibration

- 40 MeV beam at few hundred meters simulates EAS.
- Knowing beam intensity, energy and detector response gives end to end calibration and cross-check on air fluorescence efficiency
- Beam is also being used to study radio emission (Karlsruhe PAO group), radio reflection (TARA group), JEM/Euso prototype detector calibration

40 MeV electron Linac installed
100 m from BR FD site

Used for final end to end calibration of FD energy scale for TA

Useful for calibration of TARA

TA-JEM-EUSO detector calibration

KIT group study of GHz radio emission

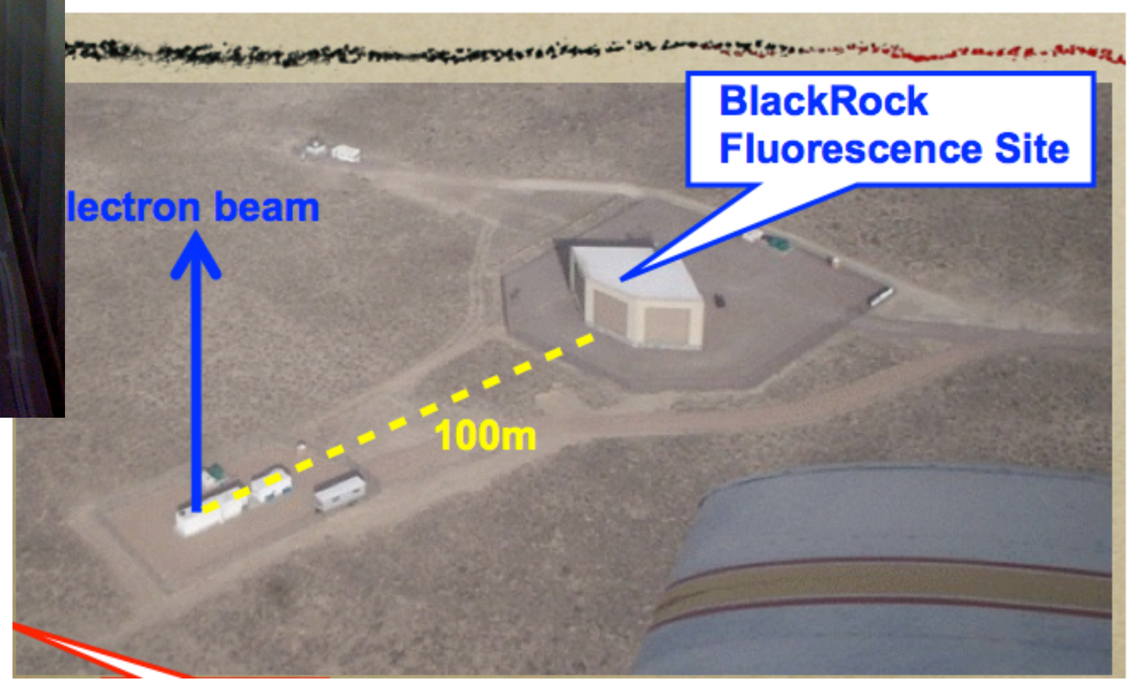

1992-1996: HiRes Prototype

- 14 (HiRes-1) + 4 (HiRes-2) mirror prototype detector operated between 1992 and 1996
- HiRes-1 field of view up to ~70°.
- HiRes-1 operated in hybrid mode with the MIA muon array (16 patches×64 underground scintillation counters each):

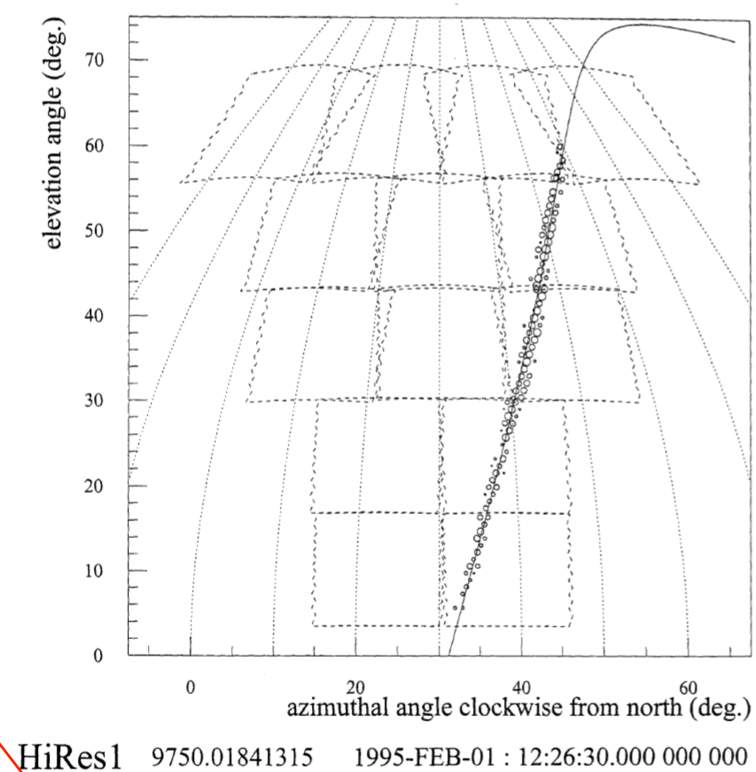

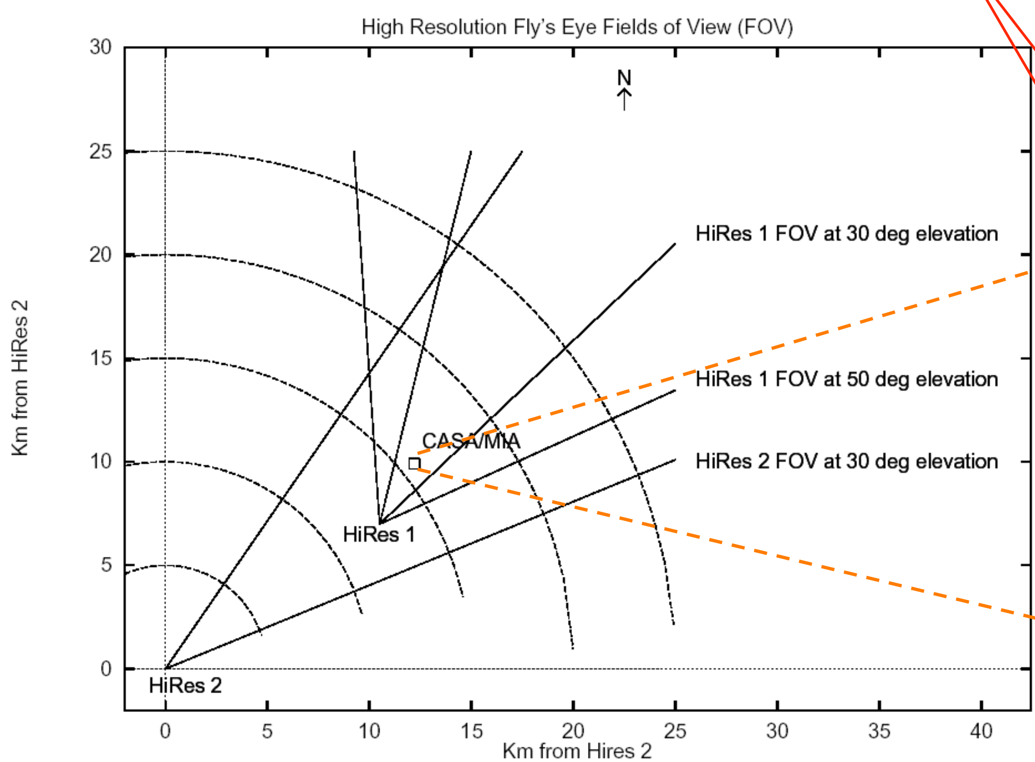

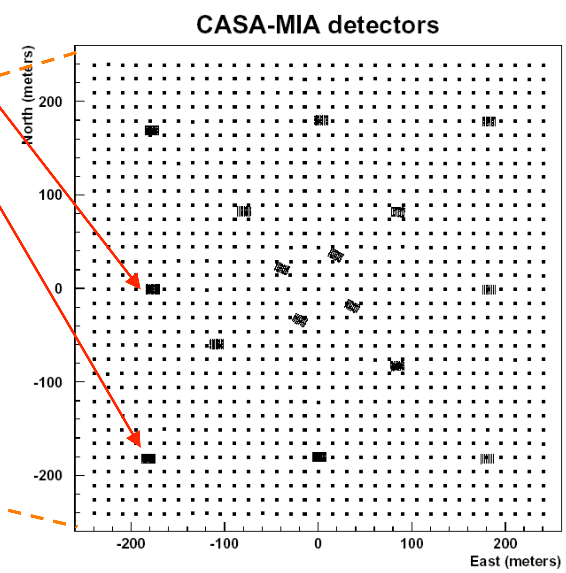

Dethinning Technique

- Change each Corsika "output particle" of weight *w* to *w* particles; distribute in space and time.
- Time distribution agrees with unthinned Corsika showers.

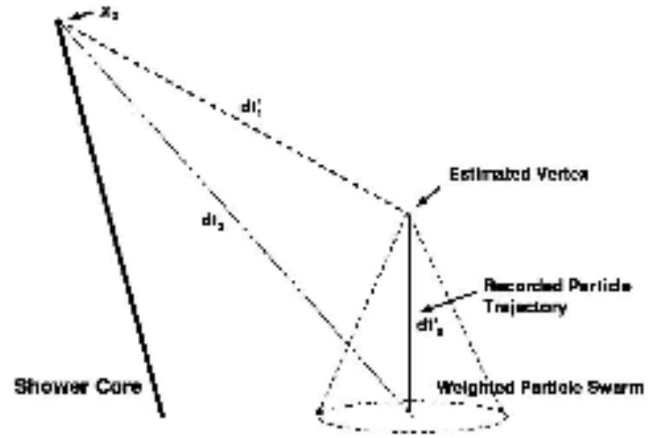

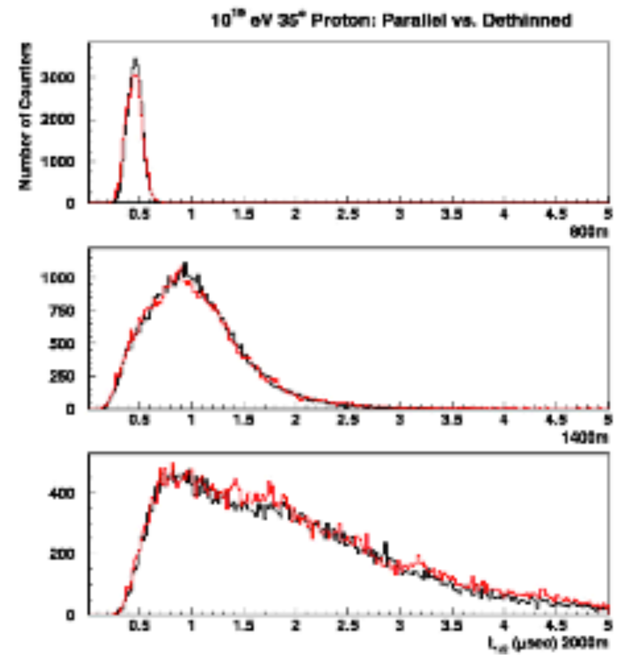

Reconstructed MC Primary Fractions (Equal fractions thrown)

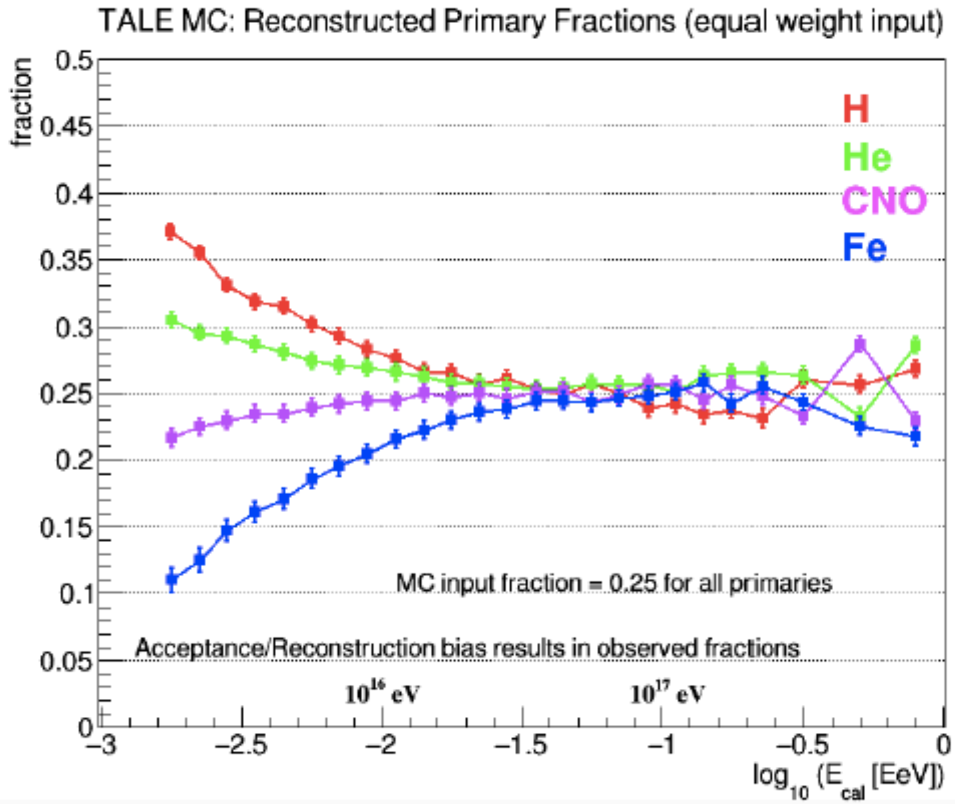

Reconstruction Resolution (Xmax)

- One histogram per decade in energy starting at $E = 10^{15.3}$ eV
- Shower X_{max} [g / cm^2]
- Histogram: ΔX_{max} [g / cm^2]

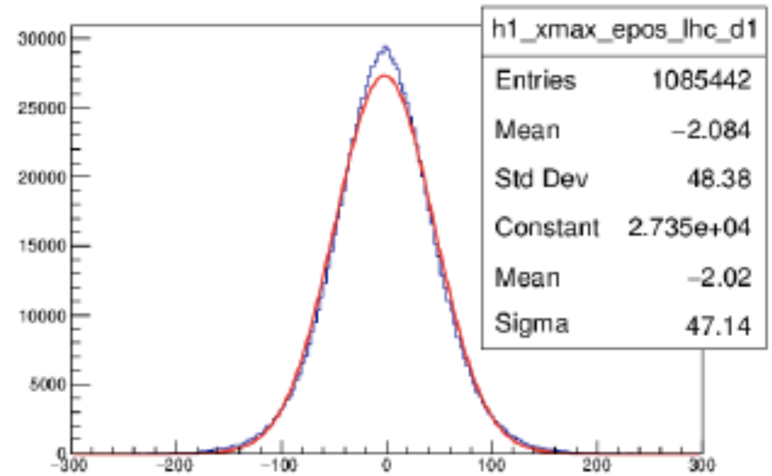

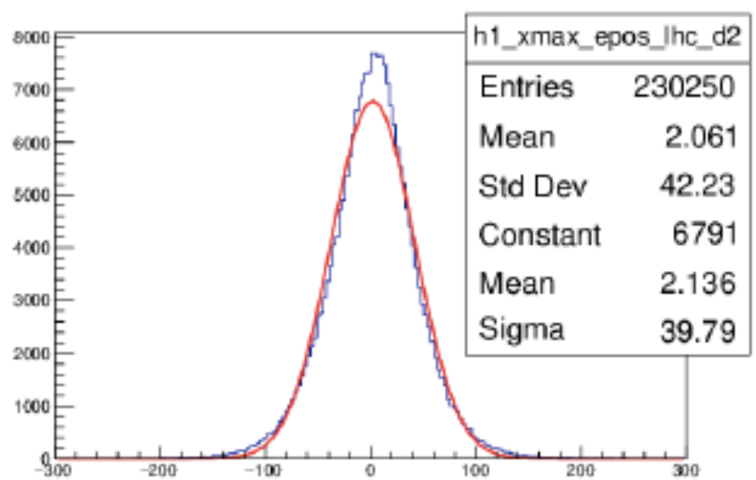

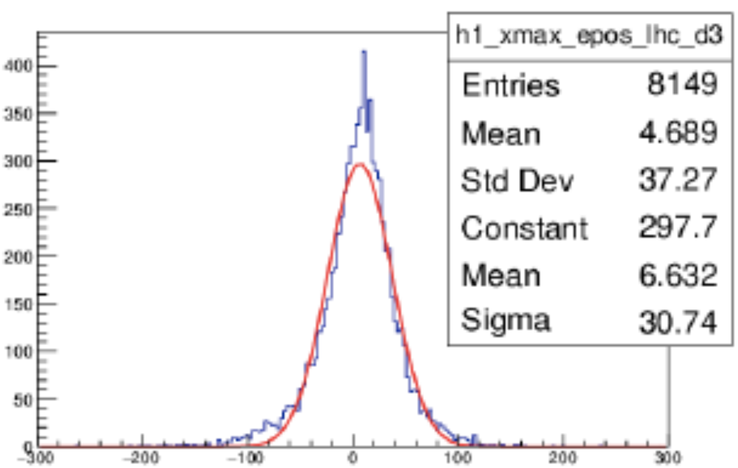

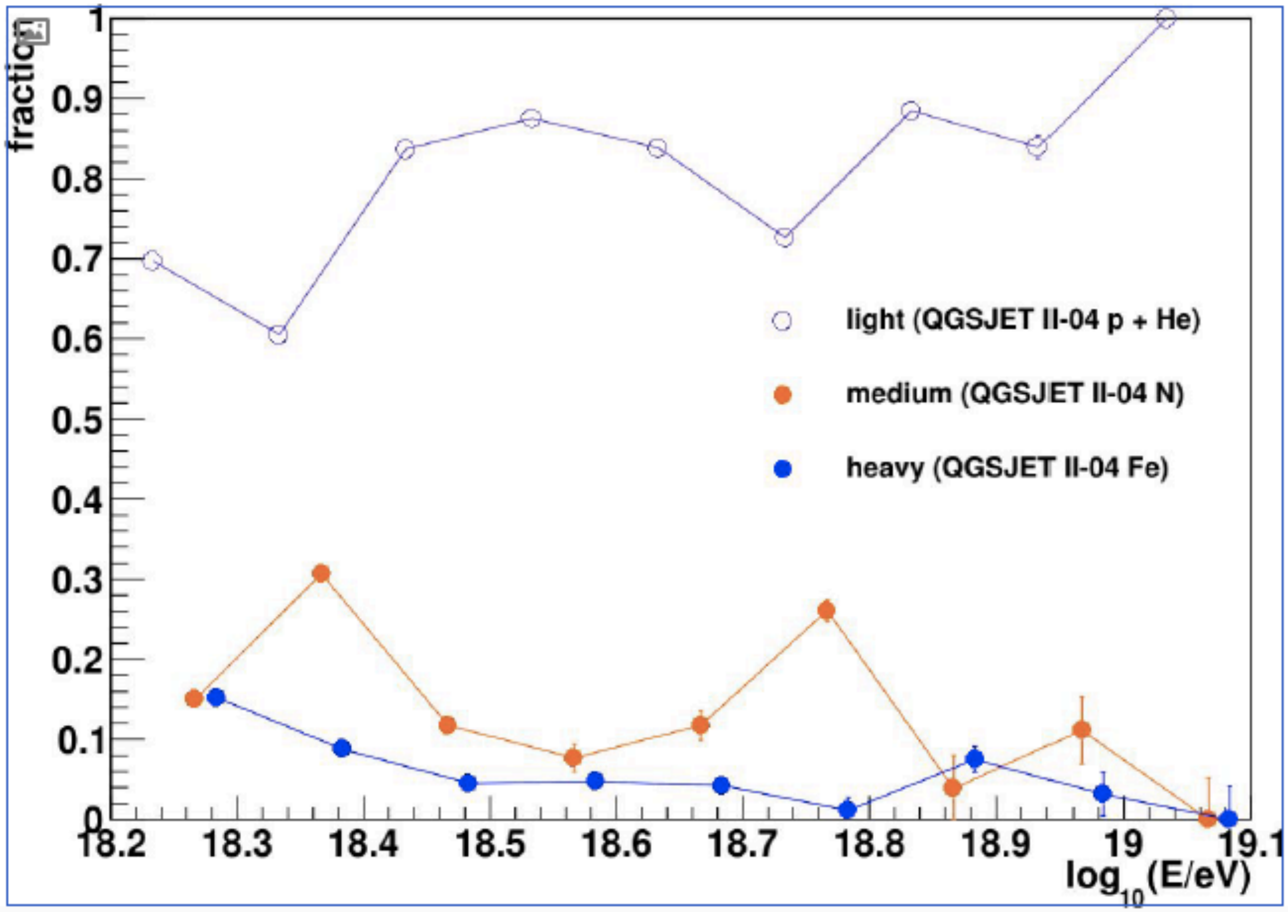

TA hybrid resolution, ~20 g/cm², which is about the difference in <X_{max}> of QGSJET II-04 proton and helium, is not sufficient to make accurate measurements of proton and helium individual fractions in a mixture.

Until resolutions are significantly improved, we should still think in terms of light. medium, and heavy composition.

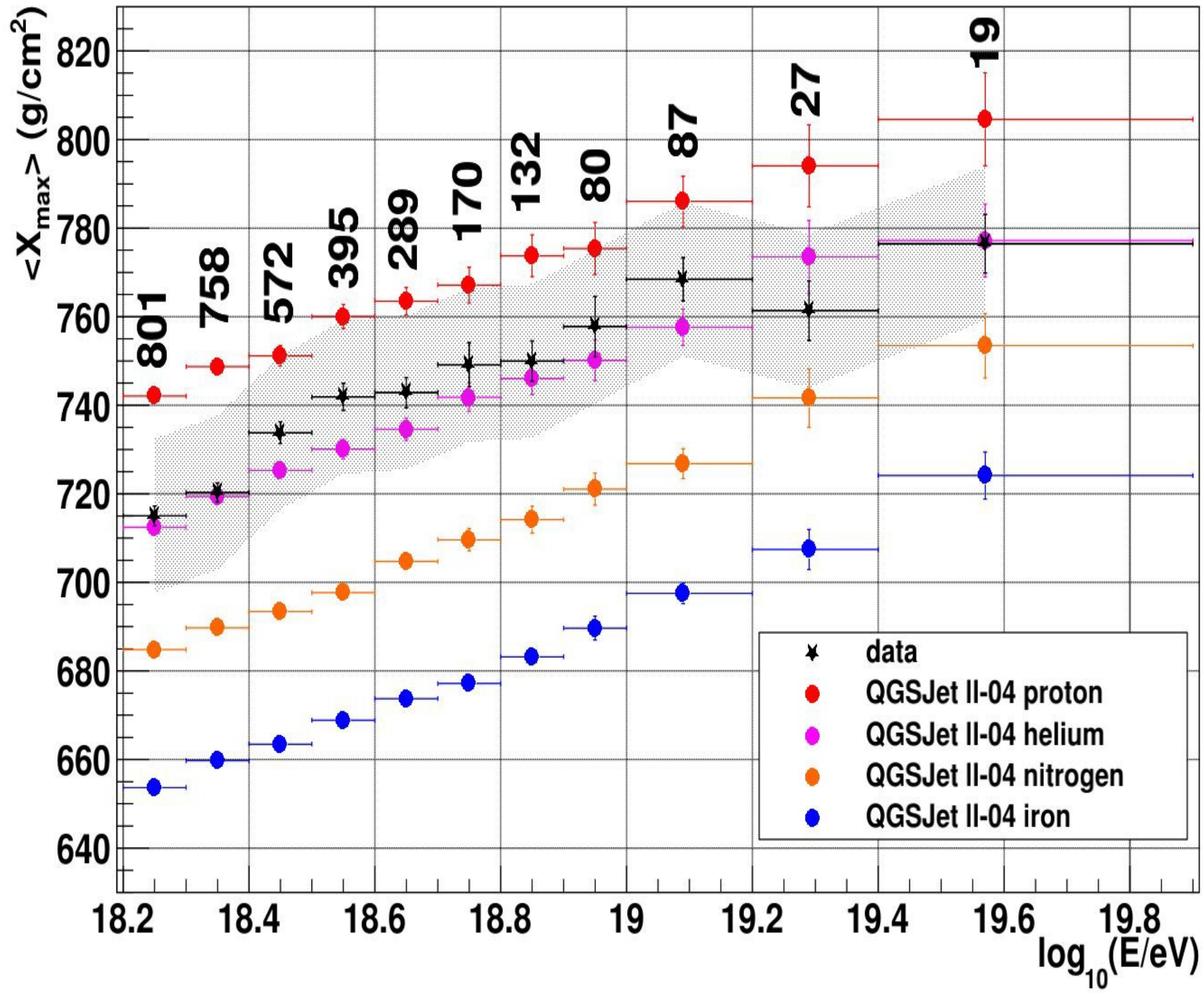

TA BR/LR hybrid 8.5 year $\langle X_{max} \rangle$, data and reconstructed QGSJet II-04 Monte Carlo

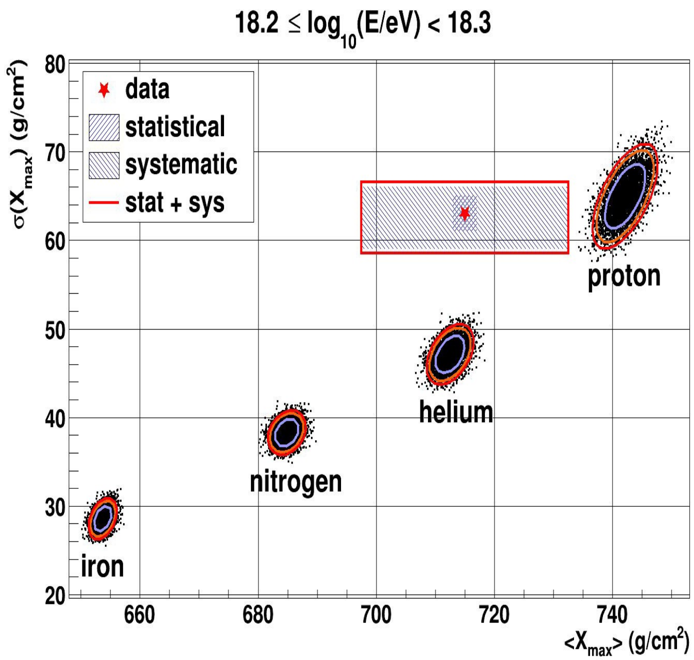

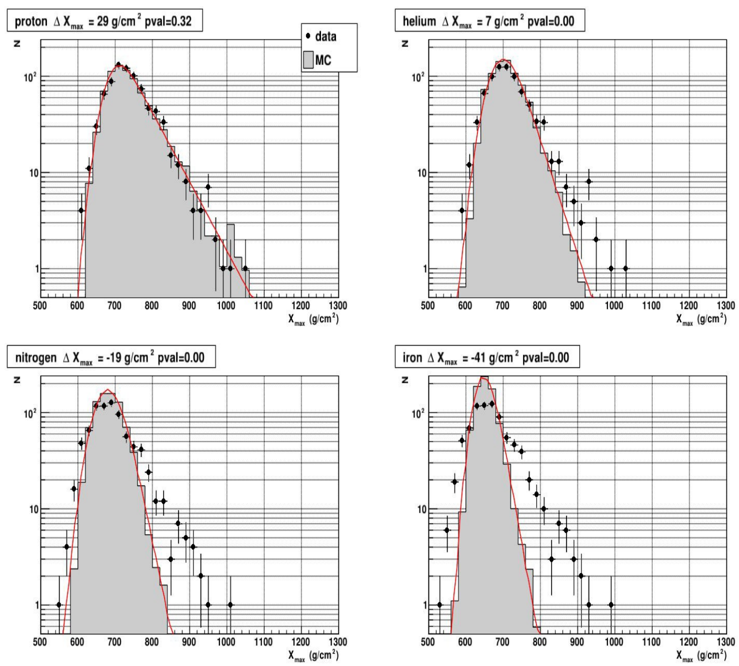

	$<X_{max}>$ (g/cm²)	a(X_{max}) (g/cm²)	Unbin ML L1X_{max} (g/cm²)	Unbin ML *p*-value
data	715 ± 2 [± 17.4]	63 ± 2 [+ 3 - 4]		
proton	742 ± 2	65 ± 2	29 ± 2	0.32 (0.5a)
helium	712 ± 2	47 ± 1	7 ± 2	10^{-25} (10.4a)
nitrogen	684 ± 1	38 ± 1	-19 ± 1	10^{-93} (21a)
iron	654 ± 1	28 ± 1	-41 ± 1	< 10^{-324} (>38a)

Unbin ML: Fail to reject H_0 for proton. Reject H_0 for helium, nitrogen, iron.

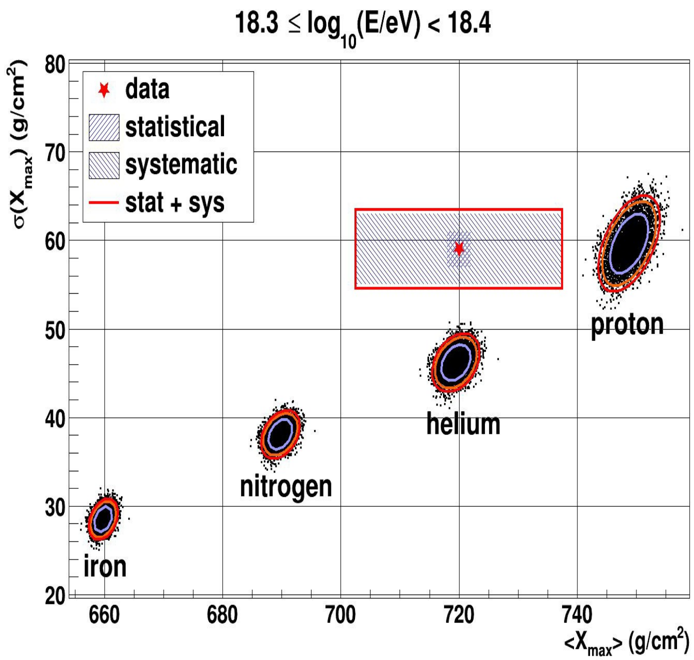

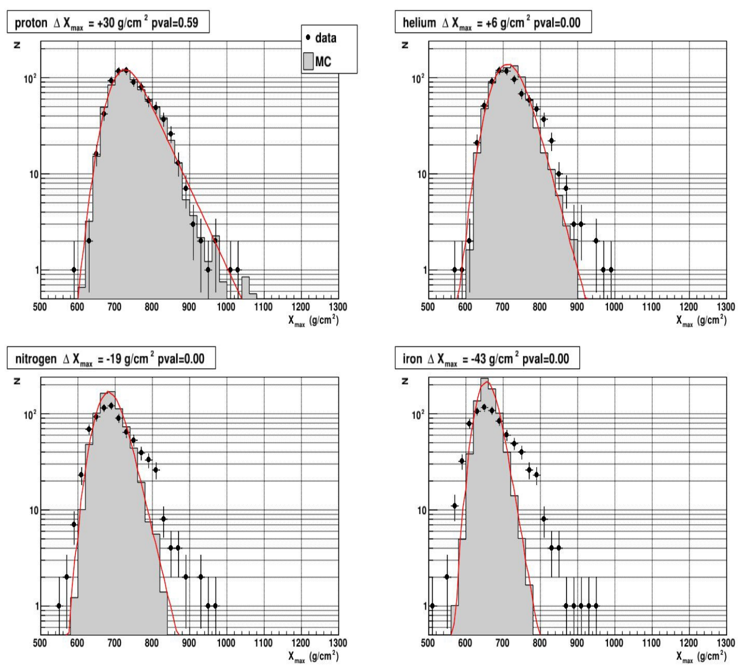

	$\langle X_{max} \rangle$ (g/cm^2)	a(X_{max}) (g/cm^2)	Unbin ML L1X_{max} (g/cm^2)	Unbin ML *p*-value
data	720 ± 2 [± 17.4]	59 ± 2 [+ 4 - 4]		
proton	748 ± 2	59 ± 2	30 ± 2	0.59
helium	719 ± 2	46 ± 1	6 ± 2	10^{-18} (8.8a)
nitrogen	689 ± 1	38 ± 1	-19 ± 1	10^{-80} (19a)
iron	660 ± 1	28 ± 1	-43 ± 1	< 10^{-324} (>38a)

Unbin ML: Fail to reject H_0 for proton. Reject H_0 for helium, nitrogen, iron.

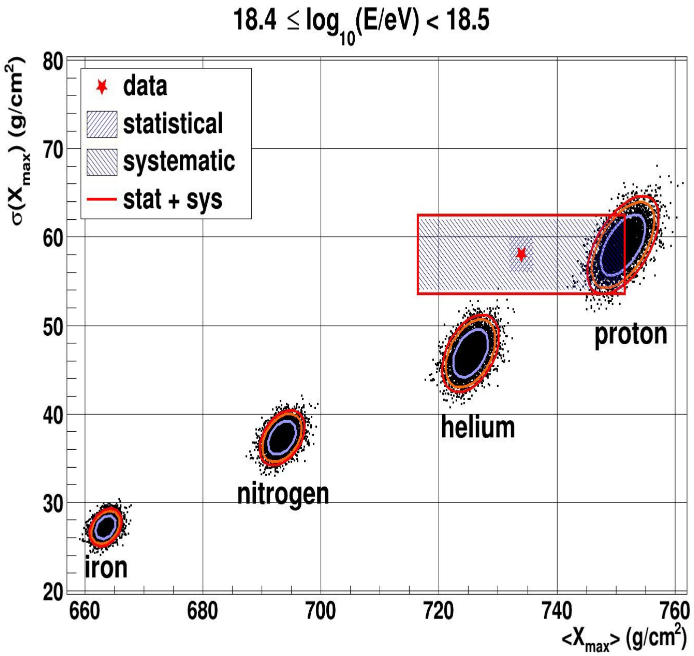

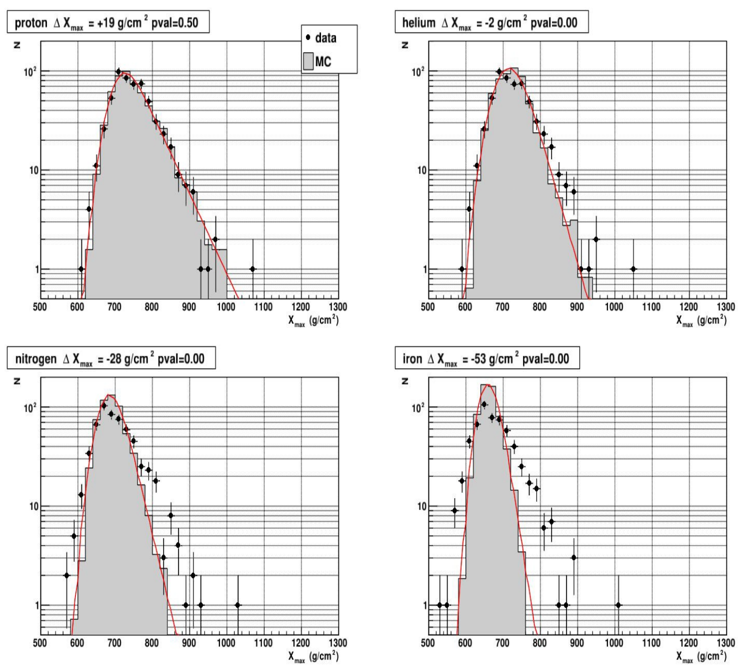

	$\langle X_{max} \rangle$ (g/cm^2)	a(X_{max}) (g/cm^2)	Unbin ML L1X_{max} (g/cm^2)	Unbin ML *p*-value
data	734 ± 2 [± 17.4]	58 ± 2 [+ 4 - 4]		
proton	751 ± 2	59 ± 2	19 ± 2	0.50
helium	725 ± 2	47 ± 2	-2 ± 2	10^{-11} (6.7a)
nitrogen	693 ± 1	37 ± 1	-28 ± 2	10^{-62} (17a)
iron	663 ± 1	27 ± 1	-53 ± 1	10^{-324} (>38a)

Unbin ML: Fail to reject H_0 for proton. Reject H_0 for helium, nitrogen, iron.

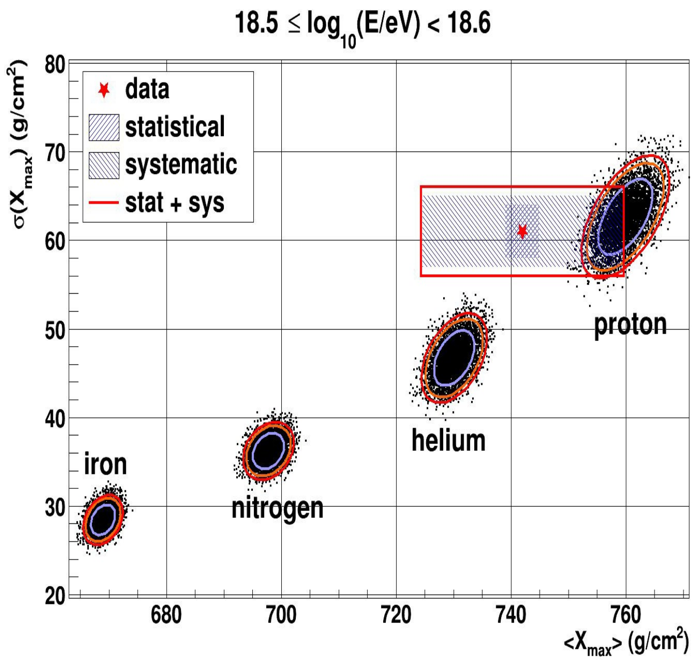

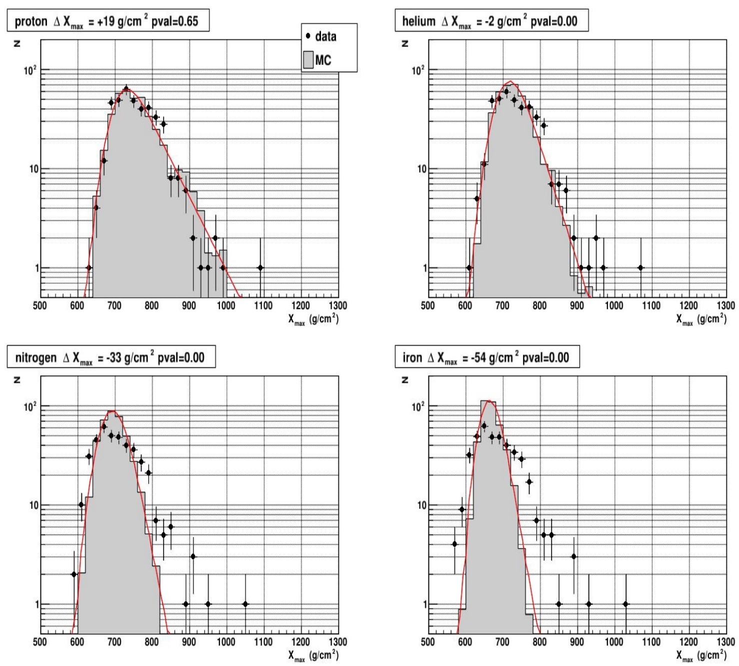

	$\langle X_{max} \rangle$ (g/cm^2)	a(X_{max}) (g/cm^2)	Unbin ML L1X_{max} (g/cm^2)	Unbin ML *p*-value
data	741 ± 3 [± 17.4]	61 ± 3 [+ 4 - 4]		
proton	760 ± 3	63 ± 2	19 ± 2	0.65
helium	730 ± 2	47 ± 2	-2 ± 2	10^{-11} (6.7a)
nitrogen	698 ± 2	36 ± 1	-33 ± 2	10^{-67} (17a)
iron	668 ± 1	28 ± 1	-54 ± 2	10^{-210} (31a)

Unbin ML: Fail to reject H_0 for proton. Reject H_0 for helium, nitrogen, iron.

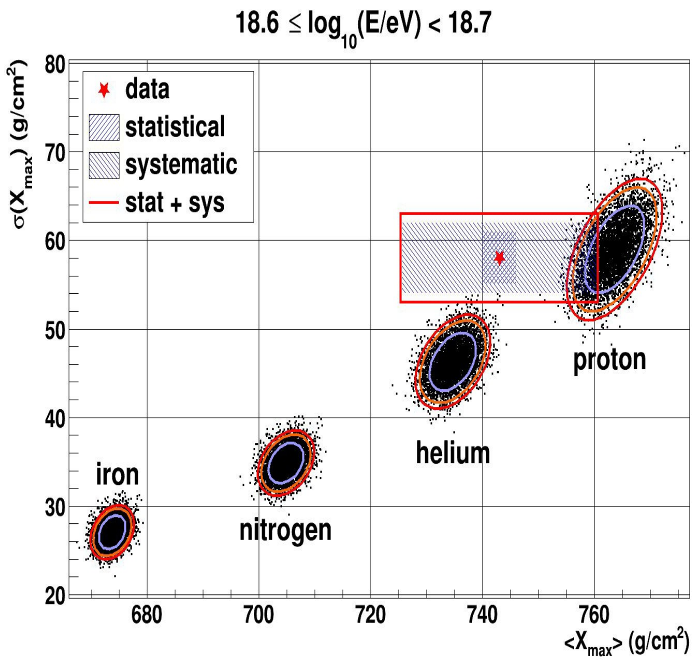

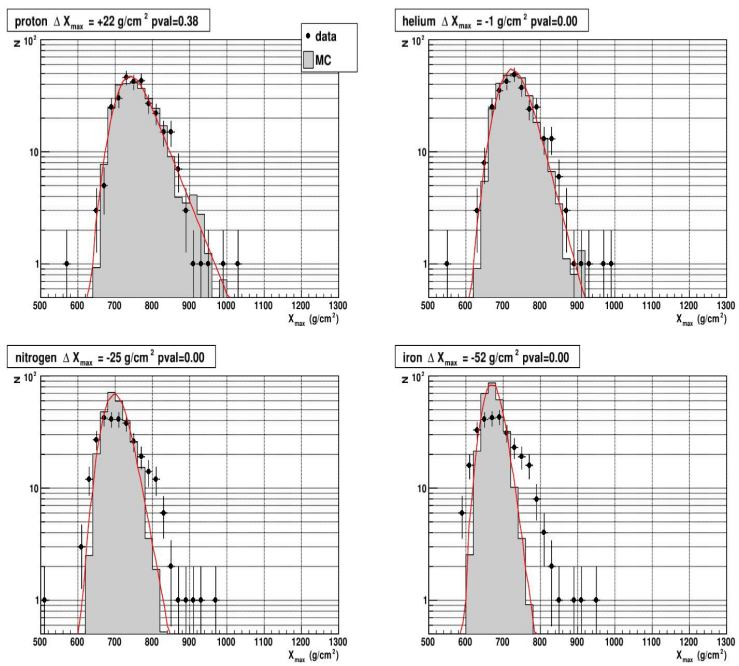

	$\langle X_{max} \rangle$ (g/cm^2)	a(X_{max}) (g/cm^2)	Unbin ML L1X_{max} (g/cm^2)	Unbin ML p-value
data	743 ± 3 [± 17.4]	58 ± 3 [+ 4 - 4]		
proton	764 ± 3	59 ± 3	22 ± 3	0.39 (0.3a)
helium	734 ± 3	46 ± 2	-1 ± 3	10^{-7} (5a)
nitrogen	704 ± 2	35 ± 1	-25 ± 2	10^{-53} (15a)
iron	674 ± 1	27 ± 1	-52 ± 2	10^{-188} (29a)

Unbin ML: Fail to reject H_0 for proton. Reject H_0 for helium, nitrogen, iron.

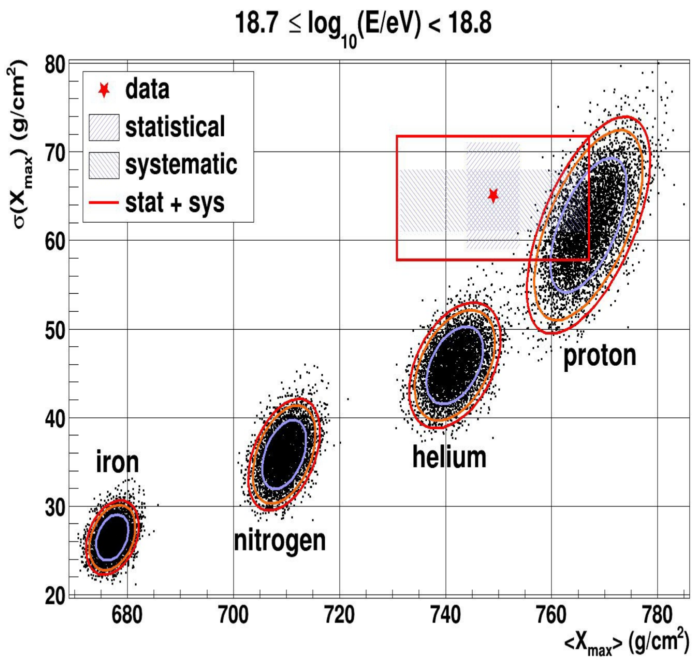

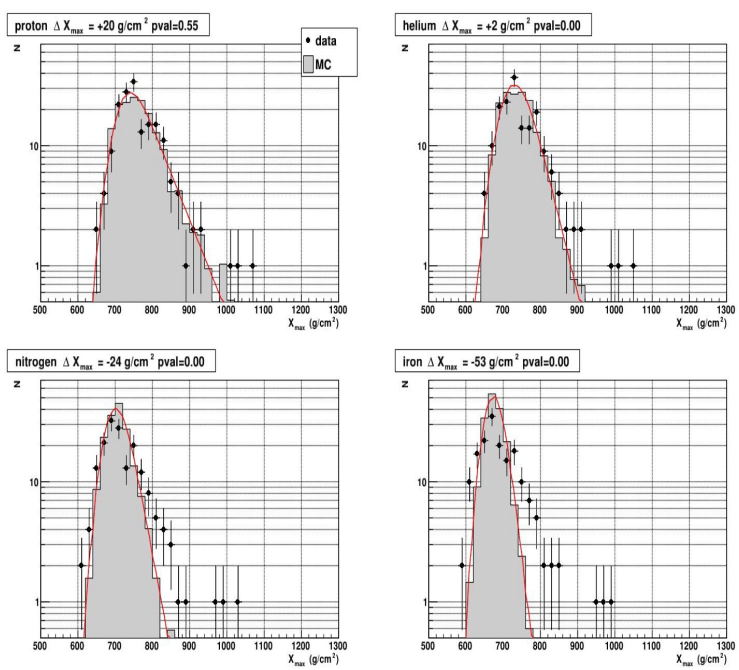

	$<X_{max}>$ (g/cm²)	$a(X_{max})$ (g/cm²)	Unbin ML L1X_{max} (g/cm²)	Unbin ML *p*-value
data	749 ± 5 [± 17.4]	65 ± 6 [+ 3 - 4]		
proton	767 ± 4	62 ± 4	20 ± 4	0.56
helium	742 ± 3	46 ± 3	2 ± 3	10^{-6} (5a)
nitrogen	710 ± 3	36 ± 2	-24 ± 3	10^{-29} (11a)
iron	677 ± 2	26 ± 1	-53 ± 2	10^{-131} (24a)

Unbin ML: Fail to reject H_0 for proton. Reject H_0 for helium, nitrogen, iron.

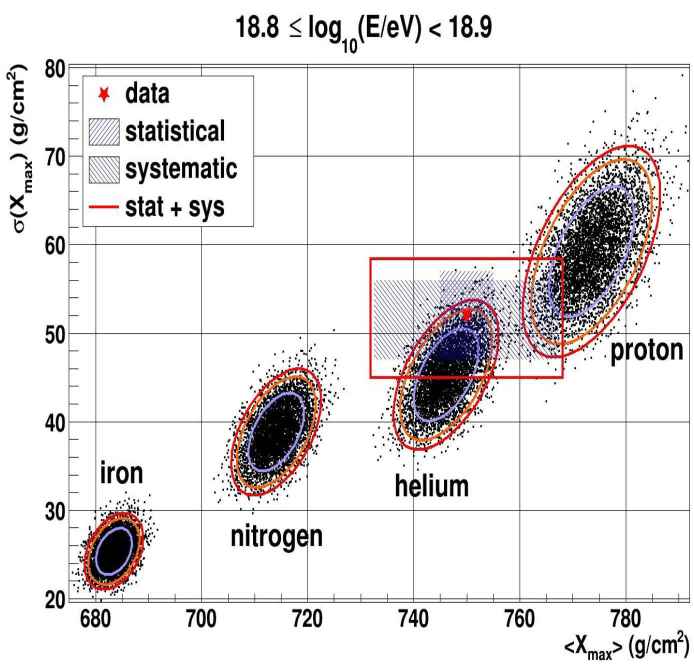

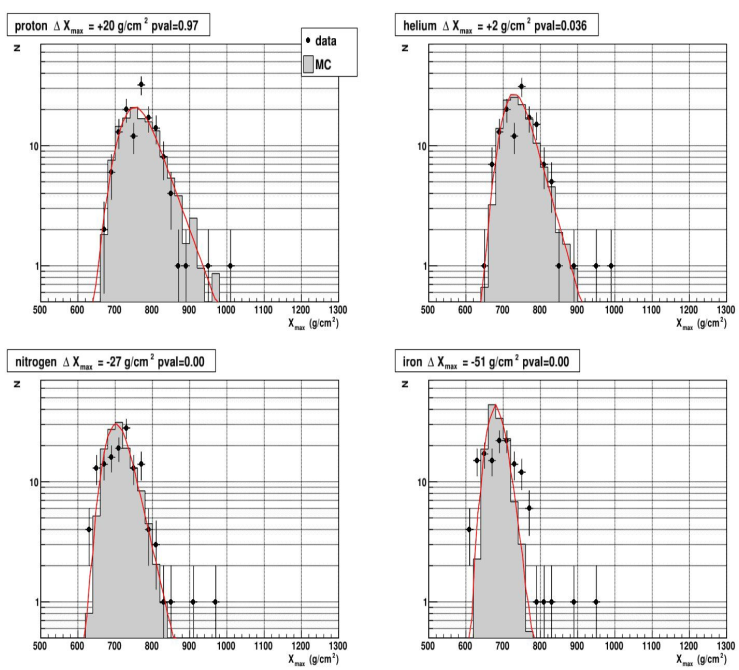

	$<X_{max}>$ (g/cm^2)	a(X_{max}) (g/cm^2)	Unbin ML L1X_{max} (g/cm^2)	Unbin ML *p*-value
data	750 ± 5 [± 17.4]	52 ± 5 [+ 4 - 4]		
proton	774 ± 5	60 ± 5	20 ± 4	0.97
helium	746 ± 4	45 ± 3	2 ± 3	0.027 (1.9a)
nitrogen	714 ± 3	39 ± 3	-27 ± 3	10^{-6} (4.7a)
iron	683 ± 2	25 ± 2	-51 ± 2	10^{-62} (17a)

Unbin ML: Fail to reject H_0 for proton. Reject H_0 for helium, nitrogen, iron.

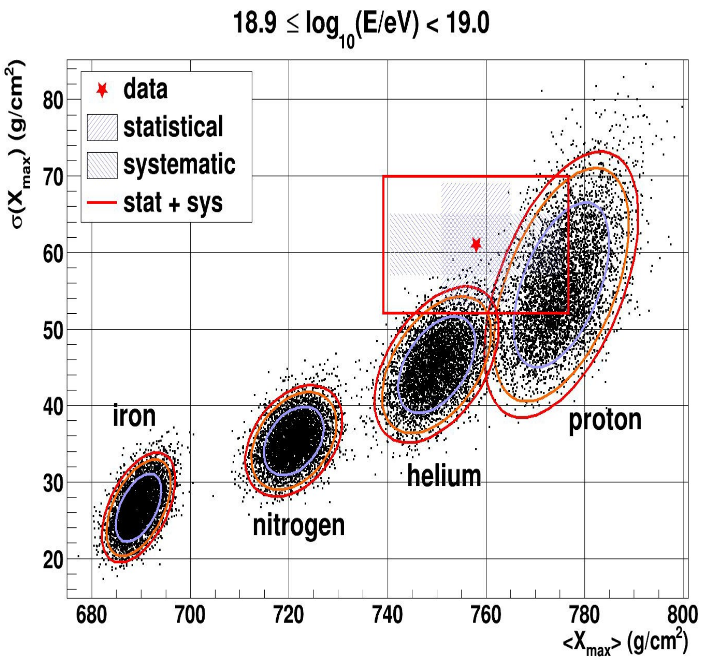

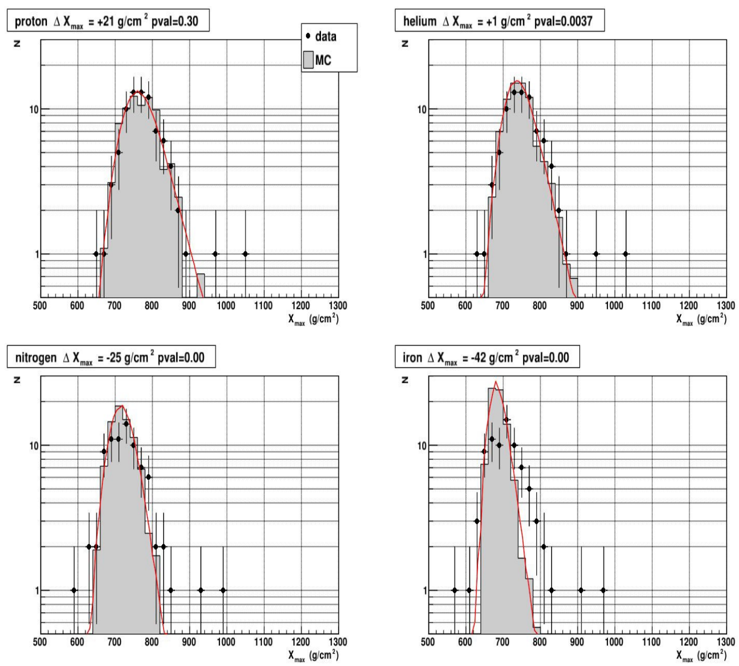

	$<X_{max}>$ (g/cm²)	$a(X_{max})$ (g/cm²)	Unbin ML L1X_{max} (g/cm²)	Unbin ML *p*-value
data	758 ± 7 [± 17.4]	61 ± 8 [+ 4 - 4]		
proton	775 ± 6	57 ± 5	21 ± 5	0.31 (0.5a)
helium	750 ± 5	46 ± 4	1 ± 5	0.0010 (3.1 a)
nitrogen	721 ± 4	35 ± 2	-25 ± 4	10^{-14} (7.7a)
iron	690 ± 3	27 ± 2	-42 ± 3	10^{-57} (16a)

Unbin ML: Fail to reject H_0 for proton. Reject H_0 for helium, nitrogen, iron.

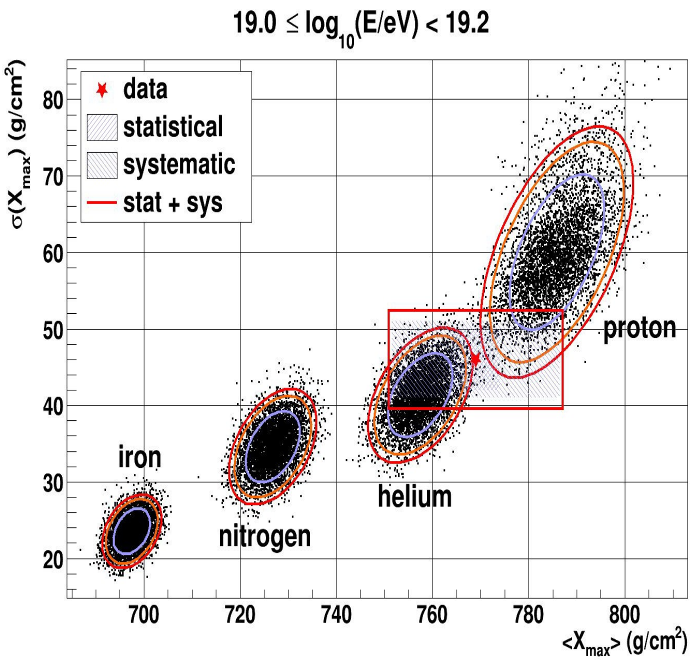

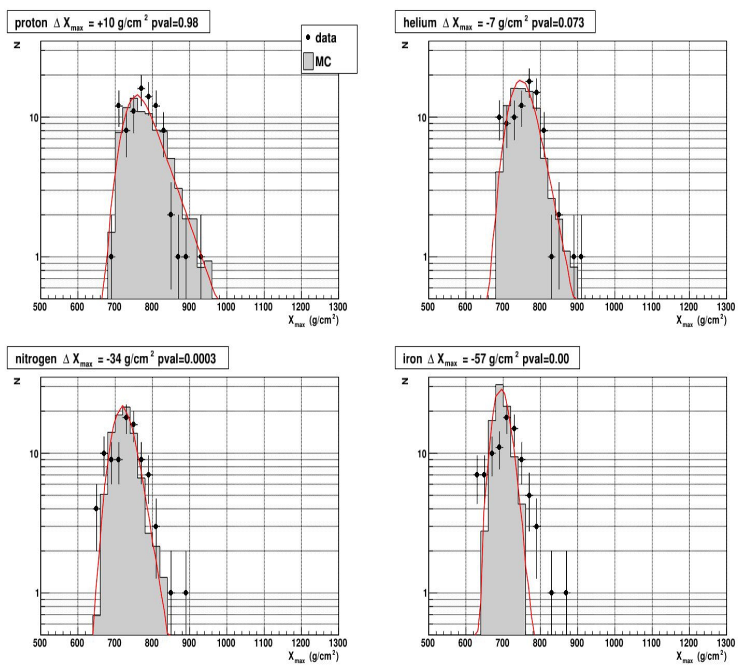

	<X_{max}> (g/cm^2)	a(X_{max}) (g/cm^2)	Unbin ML L1X_{max} (g/cm^2)	Unbin ML *p*-value
data	768 ± 5 [± 17.4]	46 ± 4 [+ 5 - 5]		
proton	786 ± 6	61 ± 5	10 ± 5	0.97
helium	758 ± 4	42 ± 3	-7 ± 4	0.059 (1.6a)
nitrogen	727 ± 3	35 ± 3	-34 ± 4	10^{-5} (4.3a)
iron	697 ± 2	24 ± 2	-57 ± 3	10^{-45} (14a)

Unbin ML: Fail to reject H_0 for proton, helium. Reject H_0 for nitrogen, iron.

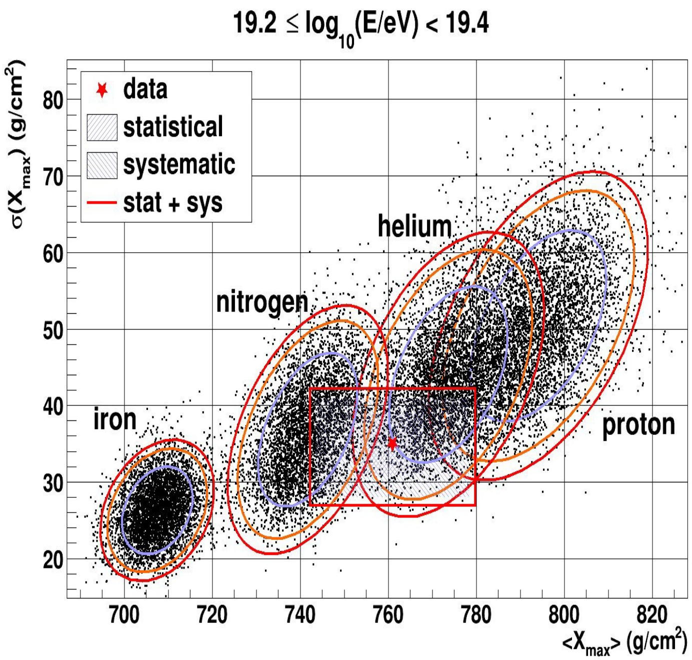

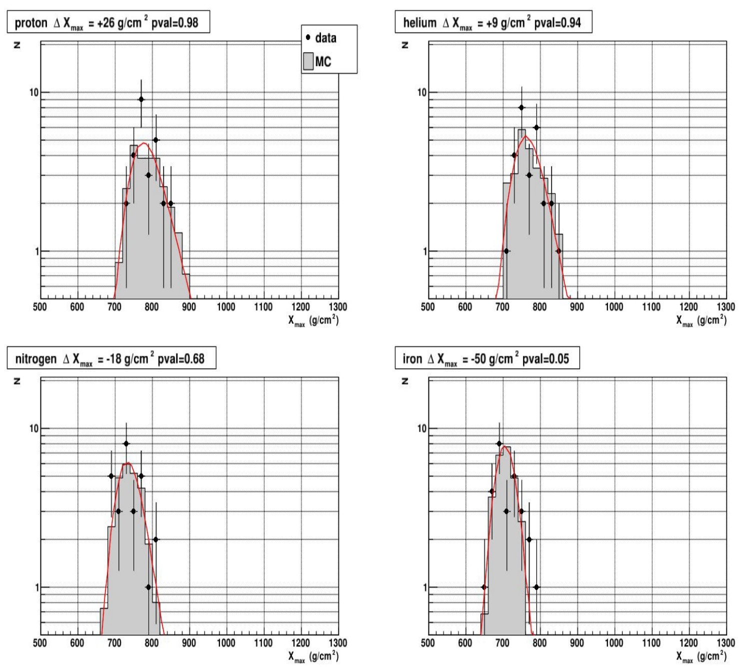

	$\langle X_{max} \rangle$ (g/cm^2)	$a(X_{max})$ (g/cm^2)	Unbin ML L1X_{max} (g/cm^2)	Unbin ML *p*-value
data	761 ± 7 [± 17.4]	35 ± 4 [+ 6 - 7]		
proton	794 ± 9	52 ± 7	26 ± 8	0.97
helium	773 ± 8	46 ± 7	9 ± 8	0.93
nitrogen	742 ± 7	38 ± 6	-18 ± 7	0.71
iron	707 ± 5	27 ± 3	-50 ± 5	0.027 (1.9a)

Unbin ML: Fail to reject H_0 for proton, helium, nitrogen. Reject H_0 for iron.

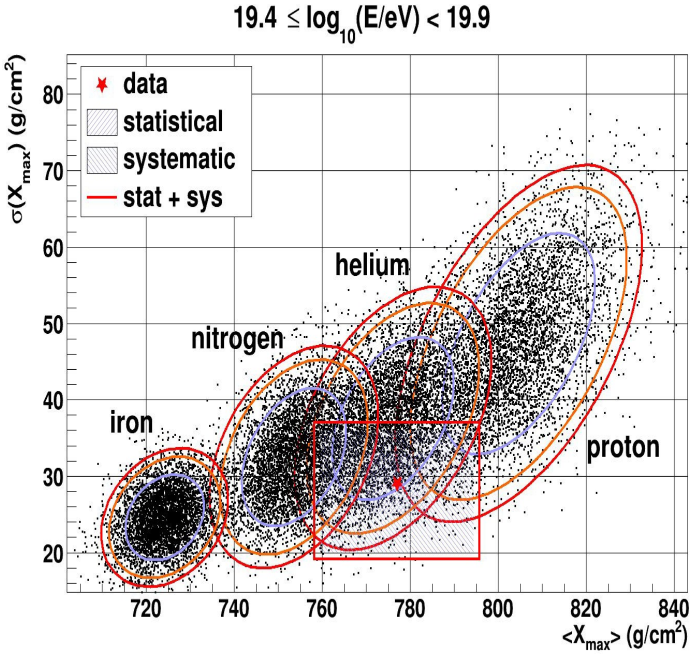

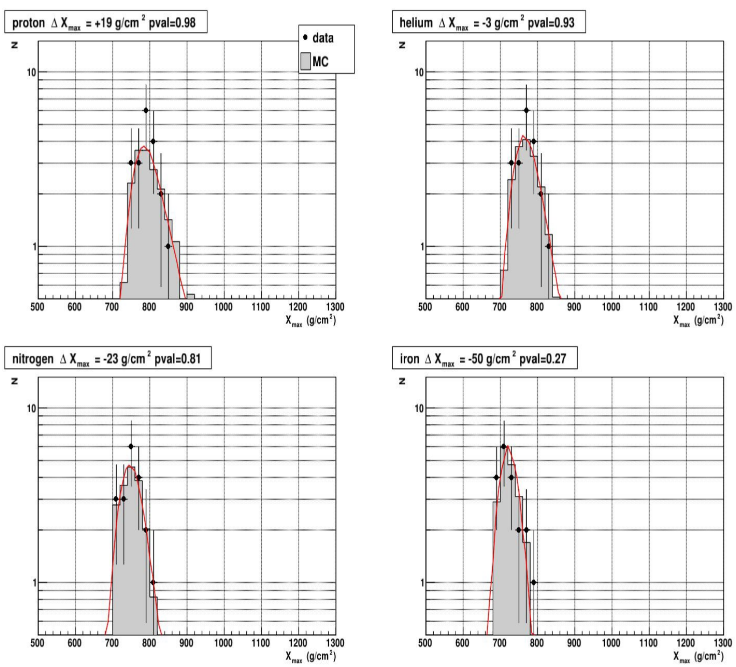

	$\langle X_{max} \rangle$ (g/cm^2)	$a(X_{max})$ (g/cm^2)	Unbin ML L1X_{max} (g/cm^2)	Unbin ML *p*-value
data	776 ± 7 [± 17.4]	29 ± 4 [+ 7 - 9]		
proton	805 ± 11	50 ± 9	19 ± 8	0.98
helium	777 ± 8	42 ± 7	-3 ± 8	0.92
nitrogen	753 ± 7	34 ± 5	-23 ± 7	0.81
iron	724 ± 5	25 ± 4	-50 ± 6	0.26 (0.6a)

Unbin ML: Fail to reject H_0 for proton, helium, nitrogen, iron.

Probabilities after best shift to account for systematics

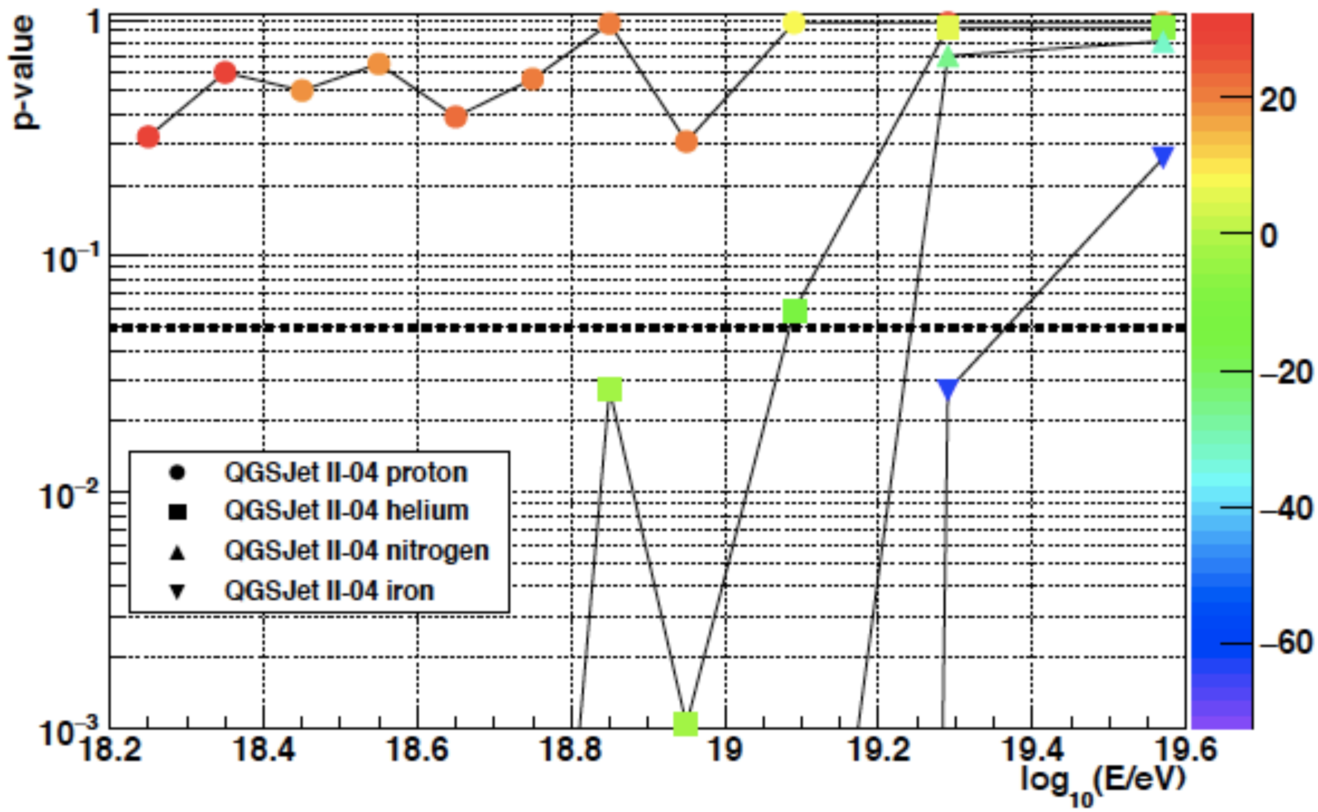

Figure 18. Unbinned maximum likelihood test on observed and simulated QGSJet II-04 X_{max} distributions after systematic shifting of the data to find the best log likelihood. Each point represents the probability of measuring a log likelihood more extreme than that observed in the data after it is shifted by the best ΔX_{max}. The color of the point indicates the ΔX_{max} measured in g/cm^2 required to find the maximum log likelihood value. The dashed line at p-value = 0.05 indicates the threshold below which the data is deemed incompatible with the Monte Carlo at the 95% confidence level.

P. Tinyakov, oral, 103

Correlations with LSS

E > 10 EeV: 2130 ev.

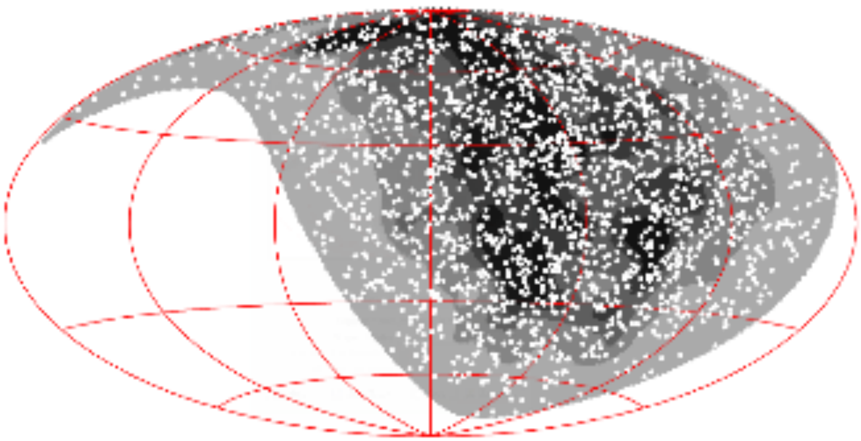

E > 40 EeV: 132 ev.

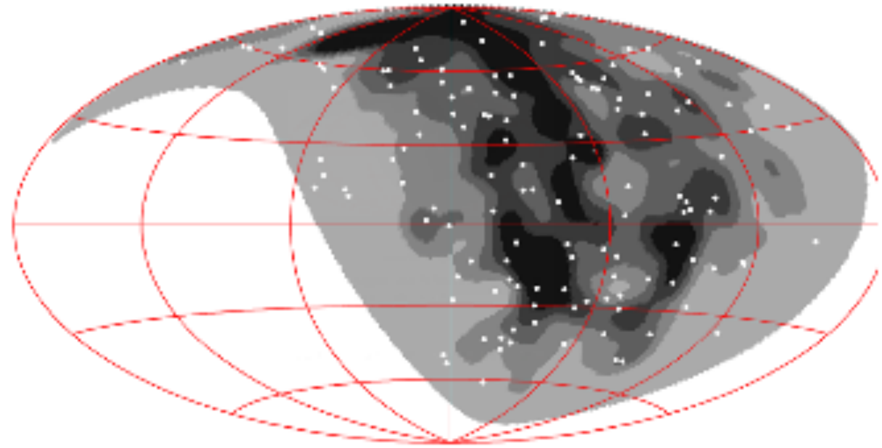

E > 57 EeV: 52 ev.

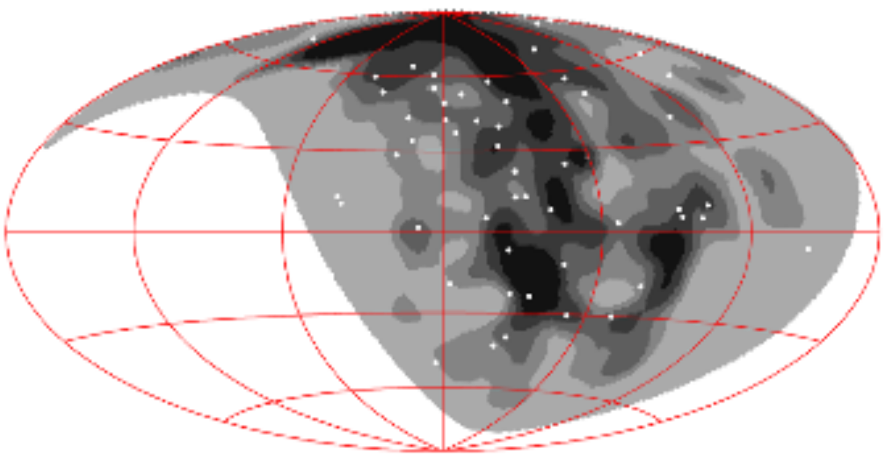

White dots: TA data with zenith angle < 55

Gray patterns:
  expected flux density from proton LSS
  2MASS Galaxy Redshift catalog (XSCz)

AUTOCORRELATION FUNCTIONS (10yr)

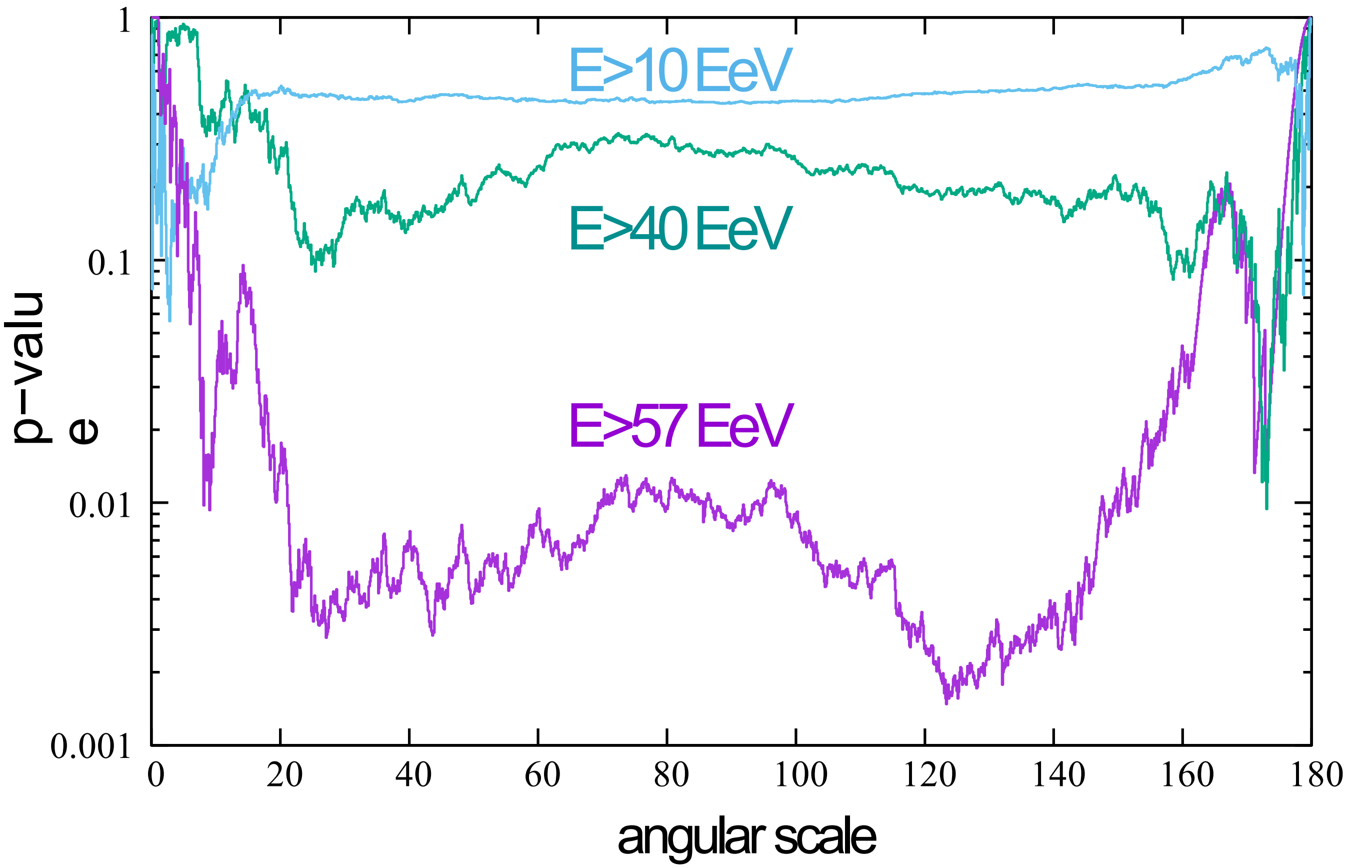

$\Longrightarrow$ compatible with isotropy (deviations at $E > 57$ EeV?)

CORRELATIONS WITH LSS

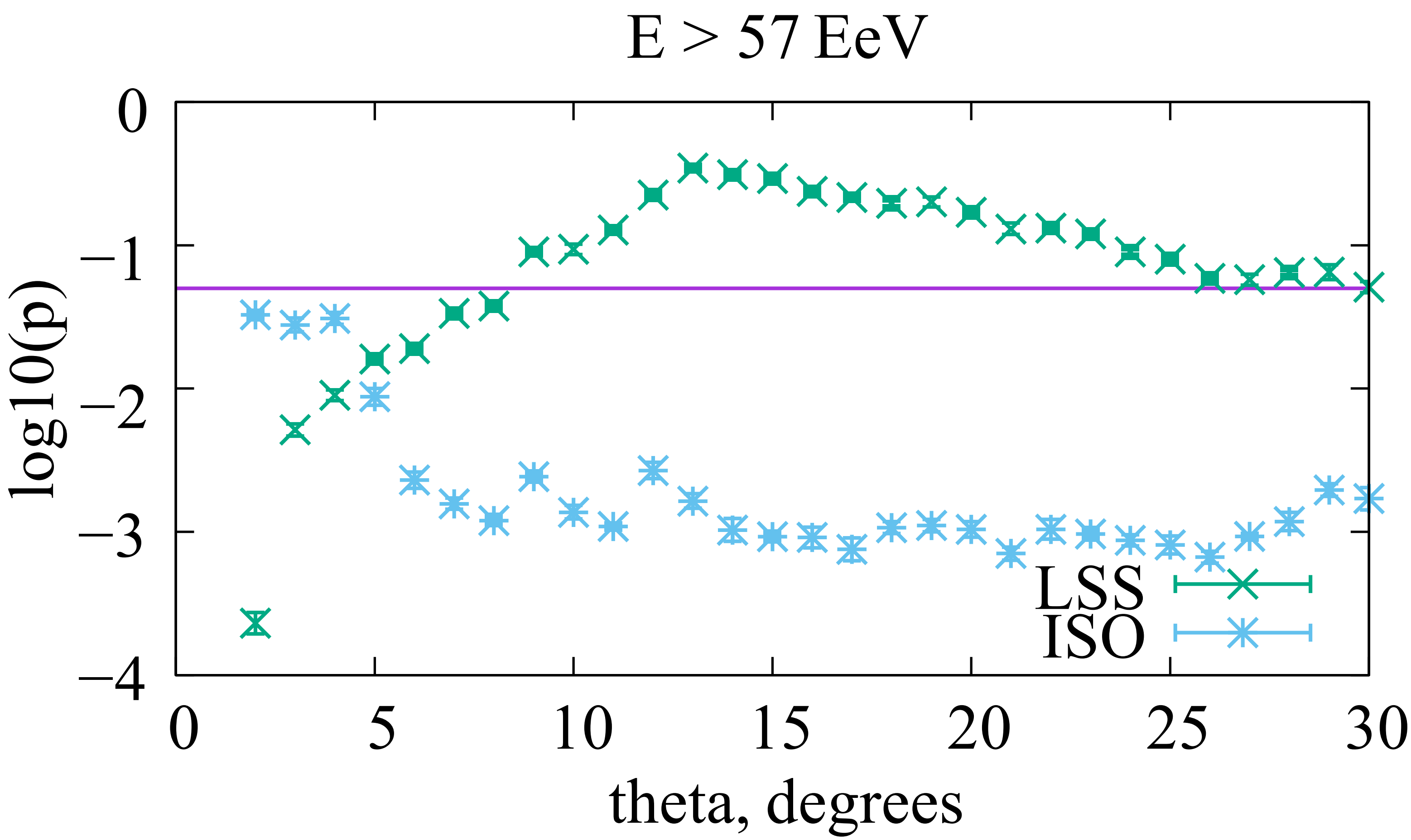

Model Dependence of TALE composition result

Fit results (QGSJetII-03)

- Lowest Energy bin starts at: $\log_{10}(E_{cal}) = 15.7$
- Mean log(A) calculated as a weighted sum of log(A) for each of 4 fit primaries.
- MC thrown with equal number of primaries: <ln (A)> = 2.01
- Reconstructed MC <ln (A)> blue squares.
- TALE data (corrected fractions) shown in red.

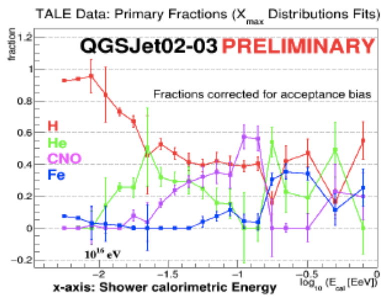

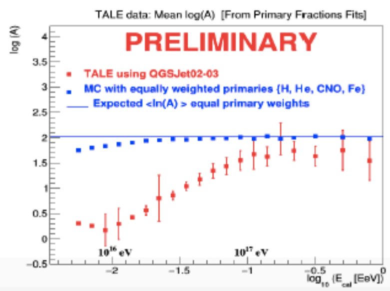

15

Fit results (EPOS-LHC)

- Lowest Energy bin starts at: $\log_{10}(E_{cal}) = 15.2$
- Mean log(A) calculated as a weighted sum of log(A) for each of 4 fit primaries.
- MC thrown with equal number of primaries: <ln (A)> = 2.01
- Reconstructed MC <ln (A)> blue squares.
- TALE data (corrected fractions) shown in red.

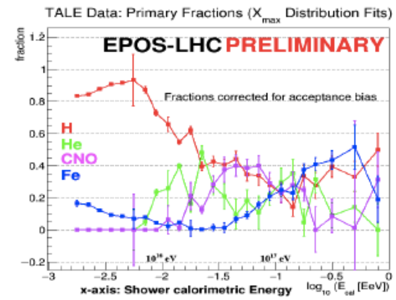

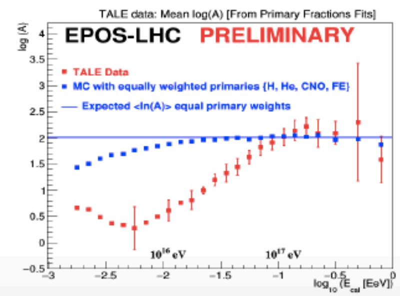

14